

**SYNTHESIS OF IRON MODIFIED SUGARCANE BAGASSE ACTIVATED  
CARBON FOR DEGRADATION OF ORGANIC DYE**

**CHEAM WAI CHONG**

**A project report submitted in partial fulfilment of the  
requirements for the award of Bachelor of Engineering  
(Hons.) Chemical Engineering**

**Lee Kong Chian Faculty of Engineering and Science  
Universiti Tunku Abdul Rahman**

**September 2018**

## DECLARATION

I hereby declare that this project report is based on my original work except for citations and quotations which have been duly acknowledged. I also declare that it has not been previously and concurrently submitted for any other degree or award at UTAR or other institutions.

Signature : \_\_\_\_\_

Name : Cheam Wai Chong

ID No. : 1400045

Date : 18 September 2018

**APPROVAL FOR SUBMISSION**

I certify that this project report entitled “**SYNTHESIS OF IRON MODIFIED SUGARCANE BAGASSE ACTIVATED CARBON FOR DEGRADATION OF ORGANIC DYE**” was prepared by **Cheam Wai Chong** has met the required standard for submission in partial fulfilment of the requirements for the award of Bachelor of Engineering (Hons) Chemical Engineering at Universiti Tunku Abdul Rahman.

Approved by,

Signature : \_\_\_\_\_

Supervisor : Dr. Pang Yean Ling

Date : 18 September 2018

Signature : \_\_\_\_\_

Co-Supervisor : Dr. Chua Kein Huat

Date : 18 September 2018

The copyright of this report belongs to the author under the terms of the copyright Act 1987 as qualified by Intellectual Property Policy of Universiti Tunku Abdul Rahman. Due acknowledgement shall always be made of the use of any material contained in, or derived from, this report.

© 2018, Cheam Wai Chong. All right reserved.

## ACKNOWLEDGEMENTS

I would like to thank everyone who had contributed to the successful completion of this project. I would like to express my gratitude to my research supervisor, Dr. Pang Yean Ling and co-supervisor, Dr. Chua Kein Huat for their invaluable advice, guidance and enormous patience throughout the development of the research.

In addition, I would also like to express my gratitude to my loving parents and friends who had helped and given me encouragement throughout the period in completing my final year project.

Last but not least, I am very thankful to UTAR for providing a comfortable environment and all the necessary equipment in completing this project.

## ABSTRACT

$\text{Fe}_3\text{O}_4$ , AC and  $\text{Fe}_3\text{O}_4/\text{AC}$  composites at various weight ratios were synthesised and analysed by using SEM-EDX, XRD and FTIR. SEM depicted that  $\text{Fe}_3\text{O}_4$  was irregular particles whilst the AC was pieces-like in structure.  $\text{Fe}_3\text{O}_4/\text{AC}$  composite sample at various weight ratios showed a combination of irregular particles and pieces-like structure. EDX results demonstrated that the amount of Fe and C elements increased upon raising the weight ratio of  $\text{Fe}_3\text{O}_4$  to AC in the composite sample. In addition,  $\text{Fe}_3\text{O}_4$  possess atomic ratio of Fe and O at approximately 3 to 4. On the other hand, FTIR analysis indicated the occurrence of AC due to the presence of O-H,  $\text{C}\equiv\text{C}$  and C-O-C bonding in the composite samples. Furthermore, Fe-O stretching which symbolised the functional group of  $\text{Fe}_3\text{O}_4$  was also being determined. Among the composite samples synthesised,  $\text{Fe}_3\text{O}_4/\text{AC} = 1:1$  (FeAC11) showed the highest degradation activity due to its adequate amount of  $\text{Fe}_3\text{O}_4$  in the composite structure and causing less blockage of active site on AC. The effect of several parameters such as organic dye concentration (30, 50, 70, 90 and 110 ppm), catalyst dosage (0, 0.2, 0.4, 0.6, 0.8, 1.0 and 1.2 g/L), solution pH (pH 1, 3, 5, 7 and 9) and  $\text{H}_2\text{O}_2$  dosage (0, 1, 2, 3, 4, 5 and 6 mM) were investigated in this study. The highest degradation efficiency of malachite green was achieved at initial dye concentration of 30 ppm, FeAC11 dosage of 0.8 g/L, pH 5, 4 mM of  $\text{H}_2\text{O}_2$  with the degradation efficiency of 89.22 % after 3 min. The composite sample showed high stability as only little amount of leached iron (about 4 mg/L) detected by ICP-OES. Pseudo second-order kinetics was best fitted to the reaction kinetics of heterogeneous photo Fenton and Fenton-like on the degradation of malachite green at different solution pH (pH 1, 3, 5, 7 and 9).

## TABLE OF CONTENTS

<b>DECLARATION</b>	<b>ii</b>
<b>APPROVAL FOR SUBMISSION</b>	<b>iii</b>
<b>ACKNOWLEDGEMENTS</b>	<b>v</b>
<b>ABSTRACT</b>	<b>vi</b>
<b>TABLE OF CONTENTS</b>	<b>vii</b>
<b>LIST OF TABLES</b>	<b>x</b>
<b>LIST OF FIGURES</b>	<b>xi</b>
<b>LIST OF SYMBOLS / ABBREVIATIONS</b>	<b>xiii</b>
<b>LIST OF APPENDICES</b>	<b>xvi</b>

### CHAPTER

<b>1</b>	<b>INTRODUCTION</b>	<b>1</b>
	1.1 Water Pollution in Malaysia	1
	1.2 Production of Dyes and its Environmental Impact	2
	1.3 Organic Dyes Removal Techniques	7
	1.4 Problem Statement	7
	1.5 Aims and Objectives	8
	1.6 Scope of Study	9
	1.7 Outline of the Report	9
<b>2</b>	<b>LITERATURE REVIEW</b>	<b>11</b>
	2.1 Background of Biomass	11
	2.2 Preparation and Activation of Biochar as Activated Carbon	13
	2.3 Functionalisation of Biochar as Activated Carbon	17
	2.3.1 Sulfonation	18
	2.3.2 Activated Carbon Based Composite	19
	2.4 Characterisation of Catalyst	20

2.4.1	X-Ray Diffraction (XRD)	20
2.4.2	Scanning Electron Microscope Coupled with Energy Dispersive X-Ray (SEM-EDX)	22
2.4.3	Fourier Transform Infrared Spectroscopy (FTIR)	22
2.5	Advance Oxidation Processes (AOPs)	25
2.5.1	Photocatalysis	26
2.5.2	Fenton and Fenton-like Processes	29
2.6	Parameter Study	33
2.6.1	Effect of Organic Dye Concentration	33
2.6.2	Effect of Catalyst Dosage	33
2.6.3	Effect of Solution pH	34
2.6.4	Effect of H <sub>2</sub> O <sub>2</sub> Dosage	35
2.7	Kinetic Study	36
<b>3</b>	<b>METHODOLOGY AND WORK PLAN</b>	<b>38</b>
3.1	Materials and Chemicals	38
3.2	Equipment	38
3.3	Overall Experiment Flowchart	38
3.4	Experiment Setup	41
3.5	Preparation of Fe <sub>3</sub> O <sub>4</sub> , AC and Fe <sub>3</sub> O <sub>4</sub> /AC at Various Weight Ratios	41
3.6	Characterisation of Fe <sub>3</sub> O <sub>4</sub> , AC and Fe <sub>3</sub> O <sub>4</sub> /AC at Various Weight Ratios	43
3.6.1	XRD	43
3.6.2	SEM-EDX	43
3.6.3	FTIR	44
3.7	Parameter Studies	44
3.7.1	Effect of Organic Dye Concentration	44
3.7.2	Effect of Catalyst Dosage	44
3.7.3	Effect of Solution pH	45
3.7.4	Effect of H <sub>2</sub> O <sub>2</sub> Dosage	45
3.8	Kinetic Study	46
3.9	Liquid Sample Analysis	47



<b>4</b>	<b>RESULTS AND DISCUSSIONS</b>	<b>48</b>
4.1	Characterisations of Fe <sub>3</sub> O <sub>4</sub> , AC and Fe <sub>3</sub> O <sub>4</sub> /AC at Various Weight Ratios	48
4.1.1	XRD Results	48
4.1.2	FTIR Results	49
4.1.3	SEM-EDX Results	50
4.2	Catalytic Activities for Fe <sub>3</sub> O <sub>4</sub> /AC at Various Weight Ratios	52
4.3	Parameter Studies	53
4.3.1	Effect of Organic Dye Concentration	53
4.3.2	Effect of Catalyst Dosage	55
4.3.3	Effect of Solution pH	56
4.3.4	Effect of H <sub>2</sub> O <sub>2</sub> Dosage	57
4.4	Kinetic Study	58
4.5	ICP-OES Results	61
<b>5</b>	<b>CONCLUSIONS AND RECOMMENDATIONS</b>	<b>64</b>
5.1	Conclusions	64
5.2	Recommendations for Future Study	65
	<b>REFERENCES</b>	<b>66</b>
	<b>APPENDICES</b>	<b>83</b>

**LIST OF TABLES**

Table 1.1:	Degree of Fixation and the Percentage Loss in Effluent for Various Types of Dyes (Kausar, et al., 2018)	3
Table 1.2:	Summary for Variant Groups of Dyes (Adegoke and Bello, 2015; Kausar, et al., 2018; Rangabhashiyam, Anu and Selvaraju, 2013)	4
Table 2.1:	Conversion of Biomass by Using Pyrolysis and Gasification (Mohan, et al., 2014)	15
Table 2.2:	Abbreviated Table of Group Frequencies for Various Organic Functional Groups (Skoog, Holler and Crouch, 2007)	23
Table 3.1:	Chemicals Used in the Experiment and Their Specifications	38
Table 3.2:	Chemical Properties of Model Pollutants	39
Table 3.3:	List of Models and Functions of Each Instrument Involved	40
Table 4.1:	Atomic Percent for Synthesised Fe <sub>3</sub> O <sub>4</sub> , AC and Fe <sub>3</sub> O <sub>4</sub> /AC at Various Weight Ratios	52
Table 4.2:	Rate Coefficients for Heterogeneous Photo Fenton and Fenton-like Degradation of Malachite Green by FeAC11 at Different Solution pH Values	61

## LIST OF FIGURES

Figure 1.1:	River Water Quality Trend in Malaysia from 2005-2014 (Afroz and Rahman, 2017)	1
Figure 2.1:	Some Common Functional Groups Attached to Biochar (Lee, Kim and Kwon, 2017)	18
Figure 2.2:	Two Pathways to Produce Iron Modified Activated Carbon (Tan, et al., 2016)	20
Figure 2.3:	Schematic Diagram of SEM (Joshi, Bhattacharyya and Ali, 2008)	23
Figure 2.4:	General Reactivity of •OH (Araujo, et al., 2011)	26
Figure 2.5:	Illustration of Mechanism for Degrading Organic Pollutants by Using TiO <sub>2</sub> Semiconductor as Photocatalyst (Ibhadon and Fitzpatrick, 2013)	28
Figure 2.6:	Mechanism of Photocatalysis by Using Iron Oxide Photocatalyst (Spasiano, et al., 2015)	29
Figure 3.1:	Flow Chart of Overall Research Activities	42
Figure 3.2:	Schematic Diagram of Experimental Setup for heterogeneous photo Fenton and Fenton-like processes	43
Figure 4.1:	XRD Patterns for (a) Fe <sub>3</sub> O <sub>4</sub> , (b) FeAC31, (c) FeAC11, (d) FeAC13, (e) AC	48
Figure 4.2:	FTIR Results for (a) Fe <sub>3</sub> O <sub>4</sub> , (b) FeAC31, (c) FeAC11, (d) FeAC13, (e) AC	49
Figure 4.3:	SEM Images of (a) Fe <sub>3</sub> O <sub>4</sub> , (b) FeAC31, (c) FeAC11, (d) FeAC13, (e) AC	51
Figure 4.4:	Heterogeneous Photo Fenton and Fenton-like Degradation Efficiency of Malachite Green in the Presence of Various Types of Catalysts (Catalyst Dosage = 1 g/L, Initial Dye Concentration = 30 mg/L, Room Temperature, neutral pH, Reaction Time = 30 min)	53
Figure 4.5:	Effect of Malachite Green Concentration on the Heterogeneous Photo Fenton and Fenton-like Degradation Efficiency of Malachite Green	

- (FeAC11 Dosage = 1 g/L, Solution Temperature = 25 °C, pH = 7, Reaction Time = 30 min) 54
- Figure 4.6: Effect of Catalyst Dosage on the Heterogeneous Photo Fenton and Fenton-like Degradation Efficiency of Malachite Green (Dyes Concentration = 30 ppm, Solution Temperature = 25 °C, pH = 7, Reaction Time = 30 min) 55
- Figure 4.7: Effect of pH Solution on the Heterogeneous Photo Fenton and Fenton-like Degradation Efficiency of Malachite Green (Dyes Concentration = 30 ppm, FeAC11 Dosage = 0.8 g/L, Solution Temperature = 25 °C, Reaction Time = 30 min) 56
- Figure 4.8: Effect of H<sub>2</sub>O<sub>2</sub> Dosage on the Heterogeneous Photo Fenton and Fenton-like Degradation Efficiency of Malachite Green (Dyes Concentration = 30 ppm, FeAC11 Dosage = 0.8 g/L, pH = 5, Solution Temperature = 25 °C, Reaction Time = 3 min) 58
- Figure 4.9: Pseudo Second-order Reaction Kinetics Plot for Heterogeneous Photo Fenton and Fenton-like Degradation of Malachite Green at Different Solution pH Values 60
- Figure 4.10: Leached Iron Concentration on the Heterogeneous Photo Fenton and Fenton-like Degradation of Malachite Green under Optimal Condition (Dyes Concentration = 30 ppm, FeAC11 Dosage = 0.8 g/L, pH = 5, Solution Temperature = 25 °C, Reaction Time = 3 min) 62

## LIST OF SYMBOLS / ABBREVIATIONS

$C_o$	initial concentration of organic dyes, ppm
$C_t$	concentration of organic dyes at certain time, ppm
$d$	interplanar spacing producing the diffraction
$E^\circ$	standard reduction potential
$e^-_{CB}$	electron in the conduction band
$h^+_{VB}$	electron vacancy or hole in the valence band
$h\nu$	UV radiation
$k_1$	first order rate constant, $\text{min}^{-1}$
$K_1$	shape factor of the crystalline, 0.9
$k_1$	first order rate constant, $\text{min}^{-1}$
$k_2$	second order rate constant, $\text{ppm}^{-1} \text{min}^{-1}$
$k_o$	zero order rate constant, $\text{ppm min}^{-1}$
$n$	an integer
$r$	rate of organic dyes concentration, $\text{ppm min}^{-1}$
$B_{1/2}$	full width at half maximum diffraction peak, rad
$\gamma$	gamma
$\lambda_x$	wavelength of the x-rays, nm
$\theta$	diffraction angle, $^\circ$
$\bullet\text{OH}$	hydroxyl radicals
AOPs	advance oxidation processes
As	arsenic atom
C	carbon atom
C(f)	carbon surface site
C(H)	surface hydrogen complexes
C(O)	surface oxide
-C=C-	carbon-carbon double bond
-CHO	aldehyde group
CO	carbon monoxide
COD	chemical oxygen demand
C-O	carbon single bond to oxygen
CO <sub>2</sub>	carbon dioxide

-COOH	carboxyl group
-COOH	carboxyl group
Cr	chromium atom
DMR	direct molecular reaction
$E^\circ$	standard reduction potential
$Fe^{2+}$	iron ions with two positive charges
$Fe_2O_3$	iron (III) oxide
$Fe^{3+}$	iron ions with three positive charges
$Fe_3O_4$	magnetite
$FeS_2$	pyrite
$FeSO_4$	iron sulphate
FTIR	fourier transform infrared spectroscopy
$H^+$	hydrogen ions
$H_2$	hydrogen molecules
$H_2O$	water molecules
$H_2O_2$	hydrogen peroxide
$H_2SO_4$	sulphuric acid
$H_3PO_3$	phosphoric acid
HCl	hydrochloric acid
$HO_2\bullet$	peroxyl radicals
HTC	hydrothermal carbonisation
ICP-OES	inductively coupled plasma optical emission spectrometry
IR	infrared spectroscopy
IRR	indirect radical reaction
K	potassium atom
KOH	potassium hydroxide
$N_2$	nitrogen molecules
NaOH	sodium hydroxide
$NH_3$	ammonia
$NO_x$	nitrogen oxides
$O_2$	oxygen molecules
$O_2\bullet^-$	superoxide radicals
$OH^-$	hydroxyl ions
S	sulphur atom

Se	selenium atom
SEM-EDX	scanning electron microscopy coupled with energy dispersive x-ray
SO <sub>3</sub>	sulfur trioxide
SO <sub>3</sub> H	sulfonate group
SO <sub>4</sub> <sup>2-</sup>	sulfate ion
TGA	thermogravimetric analysis
TiO <sub>2</sub>	titanium dioxide
UV	ultraviolet light
XRD	x-ray diffraction
α – FeOOH	goethite
α-Fe <sub>2</sub> O <sub>3</sub>	hematite
γ – FeOOH	lepidocrocite

**LIST OF APPENDICES**

APPENDIX A:	Preparation of Various Concentrations of Organic Dyes	83
APPENDIX B:	Preparation of 0.1 M HCl from a 37 % HCl Solution	85
APPENDIX C:	Preparation of 0.1 M NaOH from a 97 % NaOH	87
APPENDIX D:	Preparation of 0.1 M H <sub>2</sub> O <sub>2</sub> from 30 % H <sub>2</sub> O <sub>2</sub>	88
APPENDIX E:	Preparation of Standard Solution for ICP-OES Analysis	90
APPENDIX F:	Calibration Curve of Organic Dye	92
APPENDIX G:	Calibration Curve of Standard Solution for ICP-OES Analysis and Curve for Extended Reaction Time for Leached Iron Concentration Detection	93
APPENDIX H:	Reaction Kinetics Plot	94
APPENDIX I:	Safety Data Sheet (SDS)	96



## CHAPTER 1

### INTRODUCTION

#### 1.1 Water Pollution in Malaysia

Water is an essential component in supporting and maintaining the health of human, as well as developing a sustainable ecosystem (Sun, et al., 2016). However, the amount of polluted water generated has been shot up as a result of rapid growth in population (Rezania, et al., 2016; Udaiyappan, et al., 2017).

There are generally two types of polluted water sources, namely point and non-point sources. The former is mostly originated from sewage treatment plants, agro-based industries, manufacturing and farms whereas the latter is mainly for diffused sources such as run-off from farmland, grassland and forest (Yan, et al., 2011; Pang and Abdullah, 2013). In Malaysia, poor river quality will cause serious impact on water supply due to about 97 % of water supply is from river (Chan, 2012). Figure 1.1 illustrates the number of clean, slighted polluted, as well as polluted rivers from 2005 to 2014. The number of clean river was reduced from 338 clean river in 2005 to 244 clean river in 2014 (Afroz and Rahman, 2017).

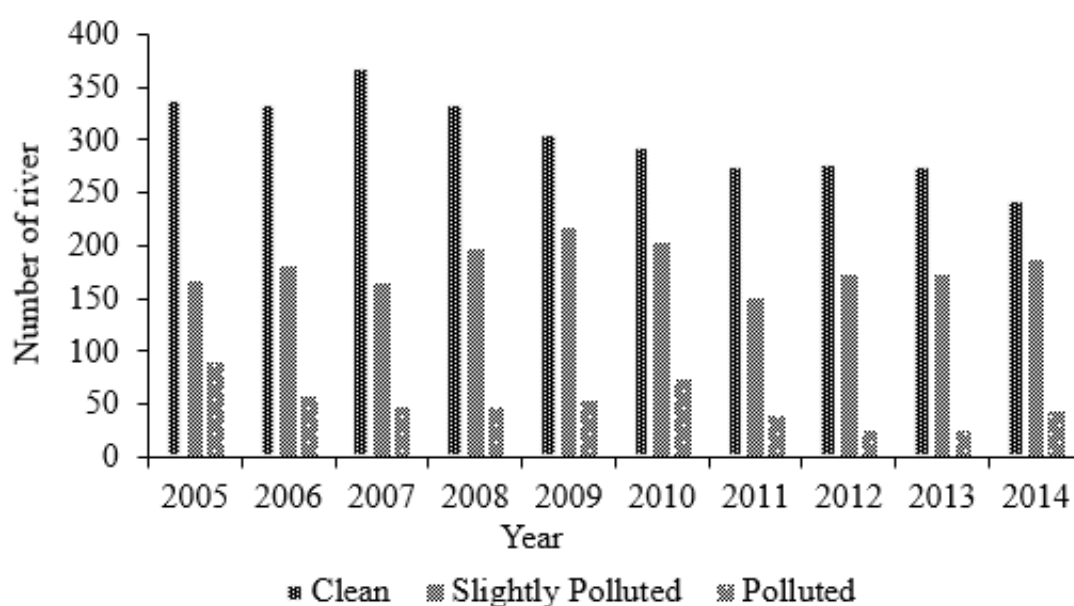


Figure 1.1: River Water Quality Trend in Malaysia from 2005-2014 (Afroz and Rahman, 2017)

## 1.2 Production of Dyes and its Environmental Impact

In industry, there are more than ten thousand dyes and about  $7 \times 10^5$  tons of synthetic dyes are generated every year globally (Rajoriya, et al., 2018). Dyes have been used widely in a wide range of industries as colourants such as paint, textiles, cosmetic, leather, paper making and plastic industry (Huang, et al., 2017; Sham and Notley, 2018; Zhang, Li and Sun, 2018). Textile industry produces the highest amount of wastewater containing dyes, which is about two-third of total amount among all industries (Rangabhashiyam, Anu and Selvaraju, 2013).

Dyes can be differentiated into natural or synthetic. Synthetic dyes are preferable in industry due to its low cost and provide various new colours to the dyeing materials. The specific wavelength absorbed by dyes could be varied from one type to another (Rangabhashiyam, Anu and Selvaraju, 2013). There are basically two functional groups which contribute to the colouring effect of dyes, namely chromophore and auxochrome. The chromophore is an electron-withdrawing group like  $-C=C-$ ,  $-C=N-$ ,  $-C=O$ ,  $-N=N-$ ,  $-NO_2$  and  $-NO$  which normally control the colour of the dyes whereas the auxochrome group such as  $-NH_2$ ,  $-NR_2$ ,  $-OH$  and  $-COOH$ , is an electron-donating group serves to intensify the colour of the chromophore by making the system more soluble, as well as enhancing dyes adherence to the fibres (Rangabhashiyam, Anu and Selvaraju, 2013).

Specifically, dyes can be grouped into several types based on their applications to textiles such as acid, basic, disperse, direct, reactive and vat dyes (Adegoke and Bello, 2015; Truskewycz, Shukla and Ball, 2016). Table 1.2 summarises the variant groups of dyes. Acid dyes are water soluble and anionic compounds which normally applicable for various materials, including silk, wool, nylon, paper, food and leather. Methyl orange, acid blue 25, acid red 57 are few examples of acid dyes. On the other hand, basic dyes are water soluble and very bright, which are suitable for modified polyesters and nylons, polyacrylonitrile, medicine and paper industry. The examples of basic dyes include malachite green, basic yellow 28 and crystal violet. Besides, the dyes which suitable for cellulose acetate, cellulose fibres, as well as nylon and acrylic fibres are termed as disperse dyes. Disperse dyes are normally water insoluble. For instance, disperse yellow, disperse blue and disperse orange. Another type of dyes appropriate for leather, cotton and rayon is known as direct dyes. Direct dyes are also water soluble and anionic compounds which can be used directly to cellulosic without the aid of

mordants such as chromium and copper which serve to improve the fastness of dyes on the fibres. For example, direct orange 34, direct black and direct blue. Reactive dyes are the next group of dyes to be highlighted which are accessible on wool, nylon and cotton fibres. These dyes are water soluble, anionic compounds and belongs to the largest among all types of dyes. The common dyes under this group are reactive red, reactive yellow 2, and reactive black 5. Lastly, vat dyes, which are water insoluble, oldest dyes and more complex in chemical structure could be the option for wool, rayon fibres, cotton and flax wool. Indigo, Vat green 6 and vat blue are the few examples of this group.

It was proven that there will be a portion of dyes lost in wastewater during the dyeing stage due to incomplete dye-fibres fixation. Table 1.1 shows the degree of fixation and the percentage of loss in effluent for various dyes. The dyes lost to the water source is difficult to be decolourized (Hamid, Shahadat and Ismail, 2017).

Table 1.1: Degree of Fixation and the Percentage Loss in Effluent for Various Types of Dyes (Kausar, et al., 2018)

<b>Type of Dyes</b>	<b>Fibre Type</b>	<b>Degree of Fixation (%)</b>	<b>Loss in Effluent (%)</b>
<b>Acid</b>	Cellulose	70-95	5-30
<b>Basic</b>	Polyamide	80-95	5-20
<b>Disperse</b>	Acrylic	95-100	0-5
<b>Direct</b>	Cellulose	50-90	10-50
<b>Reactive</b>	Polyester	90-100	0-10

Discharge of effluents containing dyes has caused both healthy and environmental effect (Adegoke and Bello, 2015; Zhang, Li and Sun, 2018). Detriment on health of aquatic and humans could be happened with even just 1 mg/L of dyes concentration due to the carcinogenic and mutagenic properties of dyes (Adegoke and Bello, 2015). Malfunction of kidneys, reproductive system, liver and brain are several symptoms that could be incurred (Hamid, Shahadat and Ismail, 2017). In terms of environment, the presence of dyes in the solution will cause the reduction of photosynthetic activity as the result of light penetration is inhibited (Ariyanti, Maillot and Gao, 2018; Ramírez-Montoya, Hernández-Montoya and Montes-Morán, 2014).

Table 1.2: Summary for Variant Groups of Dyes (Adegoke and Bello, 2015; Kausar, et al., 2018; Rangabhashiyam, Anu and Selvaraju, 2013)

<b>Types of Dyes</b>	<b>Properties</b>	<b>Principle Substrates</b>	<b>Method of Application</b>	<b>Chemical Types</b>	<b>Example</b>
<b>Acid</b>	Water insoluble and anionic compounds	Silk, wool, nylon, paper, food and leather, ink,	Normally from neutral to acidic dyes baths	Azo (including premetalized, anthraquinone, triphenylmethane, azine, xanthene, nitro and nitroso azo	Methyl orange, congo red, acid blue 25, acid red 57
<b>Basic</b>	Water soluble and very bright	Modified polyesters and nylons, polyacrylonitrile, medicine, ink and paper	Applied from acidic dyes bath	Cyanine, xanthene, hemicyanine, diazahemicyanine, diphenylmethane, acridine, oxazine, anthraquinone, azo and azine	Malachite green, basic yellow 28, basic red 46, methylene blue, basic red 9, basic brown and crystal violet

Table 1.2 (Continued)

<b>Types of Dyes</b>	<b>Properties</b>	<b>Principle Substrates</b>	<b>Method of Application</b>	<b>Chemical Types</b>	<b>Example</b>
<b>Disperse</b>	Water insoluble	Polyester, nylon, polyamide, cellulose acetate, cellulose fibers and acrylic fibers	Fine aqueous dispersion always used by high temperature or pressure, or lower temperature carrier methods; dyes could be padded on cloth and baked on or thermofixed	Azo, benzodifuranone, anthraquinone, styryl and nitro	Disperse yellow, disperse red, disperse blue, and disperse orange
<b>Direct</b>	Water soluble, anionic compounds and absence of mordant	Leather, rayon and cotton	Applied from neutral or slightly alkaline baths containing additional electrolyte	Azo, oxazine, phthalocyanine, and stilbene	Direct orange 34, direct violet, direct black and direct blue

Table 1.2 (Continued)

<b>Types of Dyes</b>	<b>Properties</b>	<b>Principle Substrates</b>	<b>Method of Application</b>	<b>Chemical Types</b>	<b>Example</b>
<b>Reactive</b>	Water soluble, anionic compounds and largest in size among all type of dyes	Wool, cotton fibres and nylon	Reactive site on dyes reacts with functional group on fiber to bind dyes covalently under influence of heat and pH (alkaline)	Azo, anthraquinone, phthalocyanine, formazan, oxazine and basic	Reactive yellow 2, reactive red, remazol and reactive black 5
<b>Vat</b>	Water insoluble, oldest and more complex in chemical structure	Wool, cotton, rayon fibres and flax wool	Water insoluble dyes solubilized by reducing with sodium hydrogensulphite, then exhausted on fibre and reoxidised	Anthraquinone (including polycyclic quinines) and indigoids	Vat green 6, indigo and vat blue

### 1.3 Organic Dyes Removal Techniques

In industry, there are several conventional techniques in removing the organic dyes, namely physical, chemical and biological methods. Nonetheless, each group has its respective advantages and drawbacks that need to be addressed. Physical methods are deemed to be a non-destructive method which only separate instead of destroying the dyes from the effluents, causing an additional post-treatment step on the disposal of solid waste is needed. Few examples of physical methods are adsorption, ion exchange and filtration. On the other hand, chemical means like coagulation or flocculation are generating gargantuan amount of sludge due to utilising high dosage of chemicals during the treatment process, leading to the needs of further disposal process (Ariyanti, Maillot and Gao, 2018). Biological ways include aerobic and anaerobic treatment are better than both physical and chemical methods in terms of its destructive properties, generating less sludge and less costly. However, biological methods are rather limited to be applied in industry due to the requirement of a huge land, sensitive to the toxicity of particular chemicals and the lengthy operation time (Garcia-Segura and Brillas, 2017; Ariyanti, Maillot and Gao, 2018).

Hence, removal of dyes from wastewater through advance oxidation processes (AOPs) which involves the use of hydroxyl radicals ( $\bullet\text{OH}$ ) for complete degradation of dyes with least amount of sludge produced, have received much attention recently (Guin, Bhardwaj and Varshney, 2017). Several ubiquitous AOPs are Fenton type reaction (Mirzaei, et al., 2017), photocatalysis (Inyang and Dickenson, 2015), ozonation (Moreira, et al., 2016), ultrasound, microwaves,  $\gamma$  irradiation (Trojanowicz, et al., 2018), electrochemical processes and wet oxidation processes (Dewil, et al., 2017).

### 1.4 Problem Statement

Biochar, as one of the products yielded after the pyrolysis process on carbon-rich biomass such as agricultural biomass, is similar to activated carbon and suitable to be applied as the supporter for the metallic catalyst (Xiong, et al., 2017). There are various agriculture by products generated enormously in Malaysia, particularly in oil palm, paddy, cocoa, pineapple and sugarcane production (Kadir and Maasom, 2013). The latter is the largest agriculture crop over the globe (Varma and Mondal, 2017). While doing the harvesting of sugarcane, the tops and leaves are left in the field and

the stalks will be transported to the mill, followed by crushing process to extract the sugar juice for the sugar production process. As the result, there will be two residues generated, which are bagasse (the fibrous fraction following juice extraction) and straw (the harvest residue) (Río, et al., 2015). In general, about 280 kg of bagasse will be produced upon utilising 1 ton of sugarcane to produce sugar and there are about 54 million dry tonnes of bagasse yielded every year globally (Kadir and Maasom, 2013). As one of the environmental friendly means to handle such amount of bagasse, it can be transformed into higher value products such as biochar by pyrolysis process. Then, biochar can be turned into activated biochar, which serves as adsorbent for various organic pollutants in wastewater or act as catalyst support (Gonçalves, Pereira and Veit, 2016).

In general, the advent of organic dyes in the effluents are hard to be removed due to its recalcitrant organic compounds, ability to withstand aerobic digestion, stable under light, heat and oxidising agents (Rangabhashiyam, Anu and Selvaraju, 2013). Hence, it is essential to develop an environmental friendly and energy efficient technique to treat the effluents consisting of organic dyes before discharging (Rajoriya, et al., 2018). Fenton and Fenton-like reactions involve the use of iron ions ( $\text{Fe}^{2+}/\text{Fe}^{3+}$ ), are considered as one of the most cost-effective AOPs to degrade the organic dyes (Munoz, et al., 2015). To overcome few issues such as undesired sludge and narrow range of pH accessible (Pouran, Raman and Daud, 2014), heterogeneous instead of homogeneous Fenton and Fenton-like processes are selected for this study. Sugarcane bagasse with rich carbon content are suitable to be used as the supporter for metallic catalyst particles in a stable and active manner (Duarte, Maldonado-hódar and Madeira, 2013).

## **1.5 Aims and Objectives**

The aim of this study is to study the heterogeneous photo Fenton and Fenton-like processes to degrade the organic dye. The sub-objectives include:

- i. To synthesise and characterise iron modified sugarcane bagasse activated carbon for heterogeneous photo Fenton and Fenton-like degradation of organic dyes.
- ii. To investigate the process behaviour of iron modified sugarcane bagasse activated carbon under various operating conditions such as the concentration



of dye, catalyst dosage, hydrogen peroxide ( $\text{H}_2\text{O}_2$ ) dosage and solution pH in order to determine the optimum conditions.

- iii. To study the reaction kinetic order for the oxidation degradation of organic dye.

## **1.6 Scope of Study**

The scope of this study involves the preparation, characterisation of the iron modified sugarcane bagasse activated carbon. The catalysts will be prepared through chemical impregnation method. The amount of iron precursor and activated carbon will be varied to determine the optimum ratio for better catalytic activity. Next, the synthesised catalysts will be characterised by using scanning electron microscopy coupled with energy dispersive X-ray (SEM-EDX), X-Ray diffraction (XRD) and fourier transform infrared spectroscopy (FTIR).

A series of experiments will be carried out to identify the effect of variant parameters on heterogeneous photo Fenton and Fenton-like degradation of malachite green such as organic dye concentration (30, 50, 70, 90 and 110 ppm), catalyst dosage (0, 0.2, 0.4, 0.6, 0.8, 1.0 and 1.2 g/L), solution pH (pH 1, 3, 5, 7 and 9) and  $\text{H}_2\text{O}_2$  dosage (0, 1, 2, 3, 4, 5 and 6 mM) in order to determine the optimum condition. Lastly, the amount of catalyst leaching during the degradation reaction will be measured to determine the stability of the catalyst.

## **1.7 Outline of the Report**

Basically, this report comprises of five chapters. Chapter 1 introduces the water pollution in Malaysia, classification of dyes, environmental impact caused by effluents containing dyes from textile industry and dyes removal techniques. The problem statement which summarises the issues to be addressed, as well as the aims and objectives which target to solve the problem statements are also included. Also, the scope of study which elaborates the details in aims and objectives are mentioned.

Chapter 2 covers the literature review, including the background of biomass, preparation and activation of biochar to become activated carbon from biomass, functionalisation of biochar such as sulfonation and biochar based composite. Besides, the principle of photocatalysis, Fenton and Fenton-like processes are presented.

In chapter 3, the details of the materials, chemicals and research methodology employed are presented. The preparation steps and type of catalysts to be synthesised are listed. Besides, experimental setup and characterisation pathways are also covered in details.

On the other hand, chapter 4 mainly present the results and discuss about the catalyst characterisation and the effect of various operating parameters. In addition, reaction kinetic used to predict the catalytic activity is present. The outcome of leaching study are also included in this chapter.

Last but not least, chapter 5 summarises the results obtained from this study. It also concludes the present study and list down recommendations for future study based on the current result.

## CHAPTER 2

### LITERATURE REVIEW

#### 2.1 Background of Biomass

In general, biomass can be explained as the biodegradable fraction of products, wastes and residues from various origin such as agriculture (Barbieri, et al., 2013). Biomass has a complicated combination of carbon (C), oxygen (O<sub>2</sub>), sulphur (S), nitrogen (N<sub>2</sub>), hydrogen (H<sub>2</sub>) and small portion of other substances such as alkali and heavy metals. The C element usually has the highest portion within biomass, followed by O<sub>2</sub> and H<sub>2</sub> elements (Tripathi, Sahu and Ganesan, 2016). The constituent will be different depending on the feedstock and reaction condition (Godlewska, et al., 2017; Yu, et al., 2017; Tan, et al., 2017). Broadly, biomass is ample in nature and can be grouped under natural or anthropogenic based on their origin. The former is the biomass found in nature whereas the latter can be obtained via miscellaneous processing technologies on natural biomass. Specifically, biomass can be further categorised into five small groups based on the location of source, including woody, aquatic, human and animal, industrial as well as agricultural biomass (Barbieri, et al., 2013; Tripathi, Sahu and Ganesan, 2016).

The biomass is termed as woody biomass due to the involvement of various parts of trees such as stems, branches, leaves and lumps. Few examples of woody biomass are oaks, pines, redwoods and maples which are mainly from forest area. Aquatic biomass covers the species of microalgae, plants and microbes present in water. For example, blue algae, fungus and variant water seeds. Meanwhile, the animal and human biomass comprises of animals manure, cooked or uncooked food, fruits and others. On the other hand, industrial biomass includes the waste generated from different industries. For instance, paper sludge from paper industry, food wastes from food processing industry, as well as sugar cane residues from sugar mill industry. Industrial biomass is distinguished from animal and human biomass due to the containment of various toxic chemicals and additives in industrial biomass (Tripathi, Sahu and Ganesan, 2016). Last but not least, agricultural waste consists of the waste yielded as the result of agricultural operation (Urbaniec and Bakker, 2015). Agricultural biomass are able to be obtained from coconut, cocoa, coffee, sugarcane and others (Shafie, et al., 2012; Ozturk, et al., 2017).

The product generated under thermal decomposition process such as pyrolysis using carbon-rich biomass at relatively low temperature (less than 700 °C) is termed as biochar (Ahmad, Buang and Bhat, 2016; Tan, et al., 2017; Yu, et al., 2017). There are three variant pore sizes formed after the pyrolysis process by using biomass, namely nano-pores (less than 0.9 nm), micro-pores (less than 2 nm) and macro-pores (larger than 50 nm) (Li, et al., 2017). Pore formation is the result of liberating the volatiles from the backbone of carbonaceous feedstock (You, et al., 2017). Adsorption capacity of biochar is better within the small pore size. On the other hand, large pore size is good to promote soil breathability, raise the amount of water of soil and also keep spacing for microbial growth and reproduction (Tan, et al., 2017). With the favourable properties of biochar, it can be used as adsorbent and catalyst (Wang, et al., 2017). Xu, et al. (2016) reports that the removing capacity of mercury by using biochar such as bagasse and hickory chips is higher than conventional activated carbon. Sugarcane bagasse comprises of 3 major components, including cellulose, hemi-cellulose and lignin. Formation of higher microporous activated carbon is achievable with the presence of ample cellulose within the structure. In addition, the presence of lignin in the sugarcane bagasse allowing it to be a suitable precursor for producing activated carbon due to its high carbon content (Noor, et al., 2017). Sugarcane bagasse is effective to be used as the precursor of activated carbon for various organic compounds adsorption in polluted water such as organic dyes (Zhou, Zhang and Cheng, 2015).

The interaction of biochar and pollutants is greatly affected by the surface area, surface polarity, aromaticity and porosity of biochar (Ahmad, et al., 2014; Li, et al., 2017; Yuan, et al., 2017). The mentioned properties can be governed by the operating conditions such as temperature, gas flow and the availability of air, carbon dioxide (CO<sub>2</sub>) or N<sub>2</sub> (Yuan, et al., 2017). During the adsorption mechanisms, cationic organic substances are attracted by the negatively charged surface of biochar through electrostatic attraction (Ahmad, et al., 2014). Biochar has better properties for organic contaminants adsorption when undergoing pyrolysis at higher temperature (more than 500 °C). This is because at temperature above 500 °C, polarity on the surface of biochar reduces whereas the aromaticity increases due to the losing of O and H containing functional group. Hence, the adsorption capacity of organic matter will be increased as the result of enhancing the aromaticity (Ahmad, et al., 2014). By increasing the pore sizes and density of functional groups, the ability of biochar as

adsorbent can be improved (You, et al., 2017). Biochar is an appropriate selection to adsorb various contaminants such as phosphorus (Wang, et al., 2018), organic dyes (Vyavahare, et al., 2018), phenolic and pesticides (Mohan, et al., 2014).

## **2.2 Preparation and Activation of Biochar as Activated Carbon**

Dry biomass is more preferable than wet biomass as the feedstock in producing biochar due to tar will be produced as the side product with the presence of moisture, leading to a decrease in the amount of biochar yielded (Tripathi, Sahu and Ganesan, 2016). The most common technique used to produce biochar from biomass is through thermochemical processes such as pyrolysis, gasification and hydrothermal carbonisation (HTC) (Qian, et al., 2015; Cheng, Zeng and Jiang, 2017).

Pyrolysis process is defined as the thermal degradation of biomass in its chemical contents with limited O<sub>2</sub> environment (Tripathi, Sahu and Ganesan, 2016). Primary constituents of biomass such as cellulose and hemi-cellulose will go through their respective reaction pathways to yield solid, liquid and gaseous products upon thermal decomposition. The solid product obtained is generally biochar, liquid product yielded will be bio-oil and the gaseous product formed is syngas (Cheng, Zeng and Jiang, 2017). The reason of pyrolysis in an O<sub>2</sub> free environment is to avoid combustion process and the products will be more stable under such condition (Tripathi, Sahu and Ganesan, 2016). Pyrolysis is regarded as an environmental friendly reaction since the products consist of limited amount of S and nitrogen oxides (NO<sub>x</sub>) (Tripathi, Sahu and Ganesan, 2016). It is worth noting that the amount of biochar produced will be reduced by 10 % for every increment of 100 °C due to the loss of volatile material (Sizmur, et al., 2017).

Pyrolysis process involves few chemical pathways. As the starting point (temperature less than 100 °C), moisture will be vaporised. Upon reaching 220 to 315 °C, hemi-cellulose degenerates easily. With temperature increase up to 315 to 400 °C, cellulose is burnt off (Deng, Li and Wang, 2016). The pore size of solid will be enlarged during pyrolysis process. Heat transfer in the pores involves three mechanisms, including conduction inside the biomass' particle, convection within the pores of the biomass materials and lastly, radiation from the surface of the end product (Thines, et al., 2017).

Basically, pyrolysis can be categorised into slow and fast pyrolysis (Mohan, et al., 2014). Slow pyrolysis requires long retention time (up to days) at the

temperature about 350 to 550 °C in O<sub>2</sub> limited environment (Oliveira, et al., 2017). This condition favours the biochar production (Ahmad, et al., 2014). Additionally, slow pyrolysis is also known as conventional carbonisation (Qian, et al., 2015). Elements such as H<sub>2</sub> and O<sub>2</sub> are being removed from the carbonisation process, leaving the biochar as the carbonaceous residue. On the other hand, fast pyrolysis is favourable in producing bio-oil instead of biochar due to the short residence time (less than 2 seconds) (Ahmad, et al., 2014). In this process, moisture content of the feedstock with or less than 10 wt% is used. The particle size of biomass is controlled in between 1-2 mm (Mohan, et al., 2014). The temperature range used in heating the biomass is 850 to 1250 °C. Liquid product instead of biochar is formed due to the insufficient time of the biomass to react and convert into biochar in fast pyrolysis process (Tripathi, Sahu and Ganesan, 2016). Thus, the major product for fast pyrolysis is bio-oil whereas the main products for slow pyrolysis is biochar (Qian, et al., 2015).

Gasification is defined as the process of heating the biomass at temperature higher than 700 °C in the environment where the O<sub>2</sub> amount is monitored (Ahmad, et al., 2014). Biomass undergoes partial thermochemical oxidation process to produce the mixture of gaseous products such as CO<sub>2</sub>, carbon monoxide (CO) and some other higher hydrocarbon product (Cheng, Zeng and Jiang, 2017). The produced gaseous product is able to be used for direct heat or electricity generation purpose. Table 2.1 illustrates the fraction of each products formed by using pyrolysis and gasification process. Few important parameters such as temperature, holding period, particle size and pressure can be varied in order to obtain the desired fractions of solid, liquid and gaseous products (Mohan, et al., 2014).

HTC is another suitable thermochemical process to transform the biomass feedstocks into carbon rich solids (Nizamuddin, et al., 2017). The process takes place in a closed reactor where the biomass is dissolved in water (Cheng, Zeng and Jiang, 2017). Operating temperature of HTC is lower (about 160 °C) as compare with other techniques such as pyrolysis and gasification (Cheng, Zeng and Jiang, 2017; Nakason, Panyapinyopol and Kanokkantung, 2017). In this process, water serves as the solvent or catalyst for the conversion of biomass, avoiding the needs of pre-drying stage for wet biomass feedstock (Nakason, Panyapinyopol and Kanokkantung, 2017).

Table 2.1: Conversion of Biomass by Using Pyrolysis and Gasification (Mohan, et al., 2014)

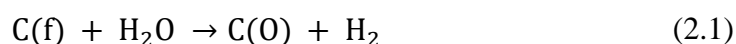
Name of the Process	Product Distribution (wt%)		
	Solid (Biochar)	Liquid (Bio-oil)	Gas (Mixture of Gaseous Product)
Slow Pyrolysis (Carbonisation)	35	30	35
Fast Pyrolysis	10	70	20
Gasification	10	5	85

The product yielded by HTC is termed as hydrochar instead of biochar due to it is a water slurry product (Mohan, et al., 2014; Yu, et al., 2017). Hydrochar is uniform spherical particles and its porosity and functional surfaces such as hydroxyl ions (OH<sup>-</sup>) can be controlled. The chemical structure of biochar produced by pyrolysis or gasification is quite similar to hydrochar. However, biochar has lower H<sub>2</sub> to C ratio (more aromatisation) as compare to hydrochar (Cha, et al., 2016; Tan, et al., 2017; Yuan, et al., 2017). The presence of dense aromatic structure will lead to difficulty in oxidation and microbial degradation (Yuan, et al., 2017). Furthermore, hydrochar can be treated as an alternative as precursors for producing highly porous activated carbons due to rich in carbon, low ash content, limited aromatisation as well as plenty of oxygenated functional groups (Islam, et al., 2017).

The limitations of biochar in its application include insufficient surface area and porosity, as well as poor functional groups (Mendonça, et al., 2017; Chen, et al., 2017). Besides, the formation of tar might occur as the result of producing biochar through gasification process, leading to the blockage of active site on biochar (Feng, et al., 2018). Biochar has lesser surface area as compare to activated carbon before any treatment or modification (Gupta, et al., 2015). To overcome these issues, biochar can be activated. Common activation method used is either by physical or chemical activation process (Chen, et al., 2017). In addition, pore structure, specific surface area, functionality, sorption capacity are able to be enhanced by activating the biochar (Gupta, et al., 2015; Ahmad, Buang and Bhat, 2016; Cha, et al., 2016; Lam, et al., 2017).

For physical activation, biochar can be activated by using variant oxidising gases such as steam at temperature of more than 700 °C (Cha, et al., 2016;

Mohamed, Mohammadi and Darzi, 2010). Another term to be used for physical activation is called gas activation (Cha, et al., 2016). This process is simple and economic viable despite it is less effectual than the chemical activation process (Rajapaksha, et al., 2016). For steam activation process, the reaction begins with the transfer of O<sub>2</sub> from water molecules to the carbon surface site (C(f)) of the biochar so that a surface oxide (C(O)) and H<sub>2</sub> are generated as shown in Equation (2.1). H<sub>2</sub> formed is likely to react with the C(f) to produce surface hydrogen complexes (C(H)) as illustrated in Equation (2.2). Subsequently, steam oxidises the produced surface sites to form H<sub>2</sub> and CO<sub>2</sub>, leading to the surface of biochar to be activated. The release of excess syngas such as H<sub>2</sub> would increase the surface area and pore volume. Among the parameters, activation time and the amount of steam applied are the important parameters to control the physical and sorption capacity of biochar (Rajapaksha, et al., 2016). Supply of the additional energy is necessary to maintain the mentioned reactions due to their endothermic properties. This process is termed as burn-off, where the weight percent of activated carbon reduces due to the removal of C atom. The development of porosity can be achieved through burn-off process (Mohamed, Mohammadi and Darzi, 2010).



Other than the physical activation processes, the porosity of biochar is able to be enhanced by impregnating chemical agents onto the biochar, followed by thermal activation in inert atmosphere. This process is termed as chemical activation (Tzvetkov, et al., 2016). The required temperature for chemical activation is lower (about 450 °C) as compared to physical activation (>700 °C) (Lam, et al., 2017). Activation of biochar is possible to be conducted by using acid or alkali activator. Several examples of acid activator are phosphoric acid (H<sub>3</sub>PO<sub>3</sub>), sulphuric acid (H<sub>2</sub>SO<sub>4</sub>) and hydrochloric acid (HCl), whereas the alkali activator could be sodium hydroxide (NaOH), potassium hydroxide (KOH) and ammonia (NH<sub>3</sub>) (Cha, et al., 2016; Lam, et al., 2017). Among the chemical agents, KOH is applied extensively because of its ability to produce activated carbon with high specific surface area and pore volume (Huang, Ma and Zhao, 2015). As the initiating step, surface carbon will react with KOH to form metallic potassium atom (K) as the consequence of KOH



reduction. Subsequently, high temperature is applied to transform the K atom from solid to vapour state. This enables the K atom to travel through the interior part of the biochar matrix, enlarging the existing pores and generating new pores (Mao, et al., 2015; Li, et al., 2017).

Thermal treatment is a crucial step to be carried out in chemical activation process (Nair and Vinu, 2016). Conventionally, electrical oven or furnace are the options to be used. Heat transfer to the material is performed through conduction and convection mechanisms. The drawbacks of the conventional methods include long duration for heat transfer due to numerous mediums to pass through and large amount of energy loss. To avoid the mentioned problems in the conventional pyrolysis, microwave pyrolysis has been used as an alternative heating method (Lam, et al., 2017).

Microwave pyrolysis has few outstanding properties such as its ability to provide prompt and energy-efficient heating as compare to the conventional methods. In addition, chemical reactions can be enhanced through microwave pyrolysis due to the thermal heating is specified to microwave receptive materials only, making the temperature profile to be consistent and subsequently, raising the yield of desired products (Lam, et al., 2015). Although there are many advantages for microwave pyrolysis, there are still some limitations to be overcome such as limited understanding of the system, effect of crucial process parameters on the desired outcome and less material selection for manufacturing the reactor (Lam, et al., 2017).

The type and amount of activating agent, as well as the operating temperature are the important variables that have impact on the activation rate of biochar. Chemical activation is proven to have higher efficiency than physical activation (Cha, et al., 2016). It is identified that higher C yield, larger surface area and better microporosity during chemical activation (Chen, et al., 2017). Although many advantages in chemical activation process, there are few disadvantages to be considered such as the occurrence of corrosion on equipment, intricate of chemical recovery and high cost of chemical (Cha, et al., 2016).

### **2.3 Functionalisation of Biochar as Activated Carbon**

Biochar consists of various functional groups, including OH<sup>-</sup>, carboxyl (-COOH) and phenolic group. This properties has favour the preparation of higher performance composites by using biochar. Biochar is inherited with numerous surface

functionalities such as carbon single bond to O<sub>2</sub> (C-O) and carbon double bond to O<sub>2</sub> (C=O). Figure 2.1 depicts some common functional groups attached to the biochar in different pore location. However, the desired functionality of biochar is arduous to be controlled by merely heat treatment process, leading to the needs of functionalisation process (Cao, Sun and Sun, 2017; Cheng, Zeng and Jiang, 2017).

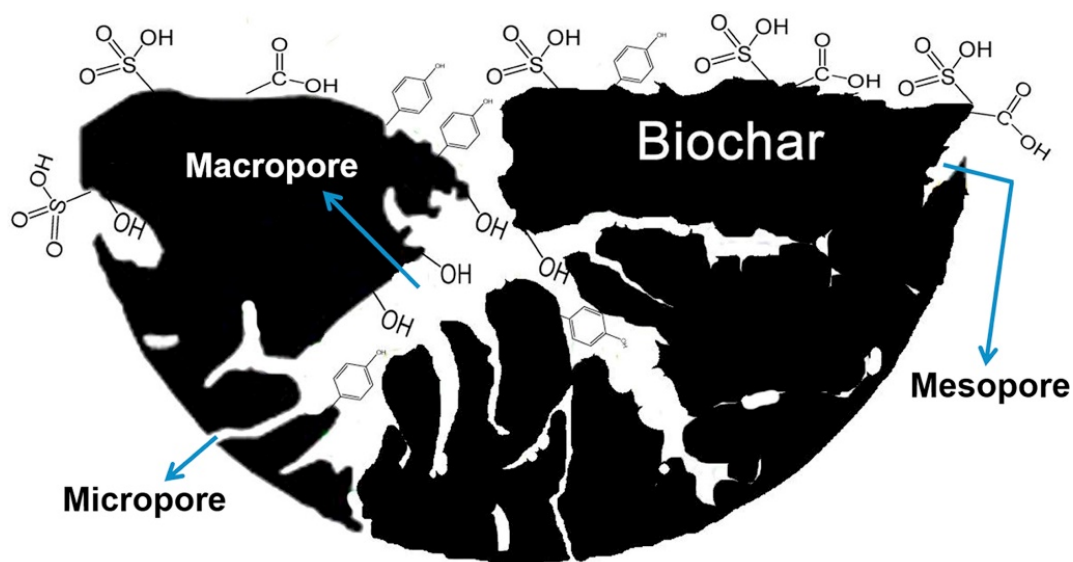


Figure 2.1: Some Common Functional Groups Attached to Biochar (Lee, Kim and Kwon, 2017)

Particular functionality is achievable through surface modification and doping process. Surface oxidation, surface amination and surface sulfonation are the examples of surface modification. The latter is most widely applied for biochar modification (Cheng, Zeng and Jiang, 2017).

### 2.3.1 Sulfonation

Sulfonation process can be differentiated into liquid sulfonation and gaseous sulfonation. Liquid sulfonation includes the stirring of biochar with concentrated sulphuric acid (more than 95 % H<sub>2</sub>SO<sub>4</sub>) at the temperature range in between 90 to 150 °C, followed by washing step until the solution is neutral without sulfate ion (-SO<sub>4</sub><sup>2-</sup>). Lastly, drying process takes place. On the other hand, gaseous sulfonation involves the introduction of sulfur trioxide (SO<sub>3</sub>) to biochar at temperature range of 25 to 150 °C, followed by the washing step to make sure that SO<sub>4</sub><sup>2-</sup> is undetectable before subjected to drying process (Lee, Kim and Kwon, 2017). Sulfonate group (-

SO<sub>3</sub>H) and some weak acid groups such as -COOH are introduced into the biochar by undergoing sulfonation process (Cao, Sun and Sun, 2017). Gaseous sulfonation produces biochar with higher density of -SO<sub>3</sub>H. Besides, activation temperature plays an important role on the functionality of biochar. For instance, biochar that undergoing treatment at 450 °C will consist larger amount of aromatic groups after sulfonation as compare to the treatment at 650 and 850 °C (Lee, Kim and Kwon, 2017). The sulfonated biochar has higher reaction activity and is better for recycle, making it an appropriate options to supersede mineral acid catalyst (Cao, Sun and Sun, 2017).

### 2.3.2 Activated Carbon Based Composite

Production of activated carbon based composite is one of the means in modifying the surface properties of activated carbon. Activated carbon serves as the base or catalyst support to the material being deposited. Upon depositing composite materials on the surface of activated carbon, new functional groups will be formed. The surface area available is reduced due to the deposition of new functional group on the surface of activated carbon. For instance, the ability of activated carbon in eliminating negatively charged oxyanions from aqueous solutions can be improved by impregnating a positively charged metal oxide on the surface of activated carbon (Sizmur, et al., 2017).

The magnetic activated carbon such as ferrous ions (Fe<sup>2+</sup>) deposited activated carbon is more feasible for recycle during the separation process by using magnetic field. In addition, the sorption capacity of Fe based activated carbon on several undesired elements such as arsenic (As), chromium (Cr), selenium (Se) is strengthened (Park, et al., 2018). The deposition of ferromagnetic materials on activated carbon is able to be induced at two different stages, either before or after the pyrolysis process in producing activated carbon. For the former way, before the pyrolysis process, chemical impregnation of Fe<sup>2+</sup> and Fe<sup>3+</sup> is performed, followed by pyrolysis process (Tan, et al., 2016). Chemical impregnation is a convenient way to produce iron-oxide deposited on activated carbon from aqueous Fe<sup>2+</sup>/Fe<sup>3+</sup> salt solution. This method starts with impregnating the activated carbon with aqueous Fe<sup>2+</sup>/Fe<sup>3+</sup> solution, thereafter, adding a base under inert environment. Few characteristics such as shape, size, and the composition of magnetic activated carbon depend on the type of salts applied (Tan, et al., 2016; Noor, et al., 2017). On the

other hand, deposition of magnetic properties materials on activated carbon after the pyrolysis process can be conducted by mixing the activated carbon produced with aqueous  $\text{Fe}^{2+}/\text{Fe}^{3+}$  solution, followed by sodium hydroxide (NaOH) treatment. Figure 2.2 illustrates the two pathways to produce iron modified activated carbon. It has been reported that introducing the magnetic properties materials onto the surface of activated carbon before the pyrolysis process is superior in terms of saturation magnetization, thermal stability, and higher iron (III) oxide ( $\text{Fe}_2\text{O}_3$ ) loading content (Tan, et al., 2016).

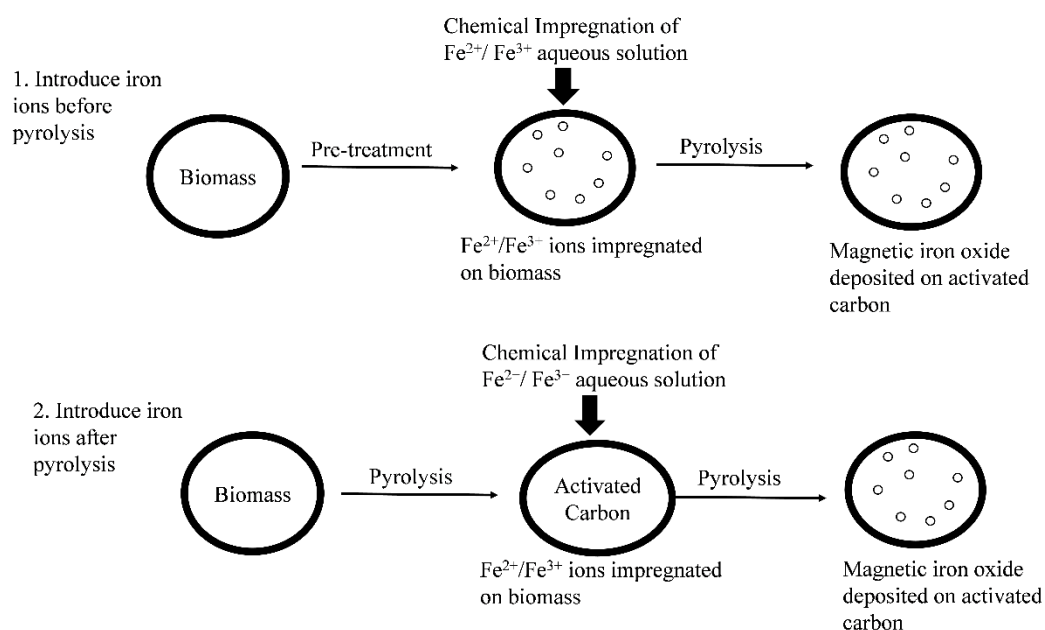


Figure 2.2: Two Pathways to Produce Iron Modified Activated Carbon (Tan, et al., 2016)

## 2.4 Characterisation of Catalyst

### 2.4.1 X-Ray Diffraction (XRD)

The diffraction of X-rays is practical to be employed in analysing the crystalline material producing the diffraction due to no component can have the identical crystals with same spacing of planets in all analogous directions. Hence, the X-rays diffracted by different substances will be in their own unique diffraction pattern, showing the fingerprint or their atomic and molecular structure (Khandpur, 2015). A constructive interference and a diffracted ray will be generated when Bragg's law is satisfied upon the interaction of incident rays and the sample. The law links the wavelength of electromagnetic radiation and the diffraction angle, as well as the

lattice spacing of the crystalline sample as shown in Equation (2.3). By applying a range of  $2\theta$  angles scanning on the sample, all probable generated diffraction directions of the lattice are obtainable due to the orientation of the powdered material is random. Subsequently, the diffraction peaks detected are converted to  $d$ -spacings. The comparison of the  $d$ -spacings and the standard reference patterns allows the identity of the substances to be determined due to each substance has different set of unique  $d$ -spacings (Bunaciu, Udriștioiu and Aboul-Enein, 2015).

$$n\lambda_x = 2d \sin \theta \quad (2.3)$$

where

$n$  = an integer

$\lambda_x$  = wavelength of the X-rays, nm

$d$  = interplanar spacing producing the diffraction

$\theta$  = diffraction angle

In order to determine the average size of the crystalline, Scherrer formula is applicable as demonstrated in Equation (2.4) (Ma, Zhou and Chen, 2017). As reported by Yu, et al. (2014), the increase in doping amount of Fe into mesoporous titanium dioxide ( $\text{TiO}_2$ ) resulted the peak intensity of anatase at 25.4 °C to be reduced slightly. It was deduced that the more Fe present in the structure, the poorer the crystalline structure of the sample.

$$D = \frac{K_1 \lambda}{\beta_{1/2} \cos \theta} \quad (2.4)$$

where

$D$  = average crystalline size, nm

$K_1$  = shape factor of the crystalline, 0.9

$\lambda_x$  = wavelength of X-Ray, 0.154 nm

$\beta_{1/2}$  = full width at half maximum diffraction peak, rad

$\theta$  = diffraction angle, °

#### **2.4.2 Scanning Electron Microscope Coupled with Energy Dispersive X-Ray (SEM-EDX)**

A scanning electron microscope (SEM) is an equipment most widely applied in material research laboratories due to its excellent capabilities in providing various crucial information such as topographical features, morphology, phase distribution, variance in composition, orientation of crystal, crystal structure, as well as the location of electrical defects. Figure 2.3 illustrates the schematic diagram of SEM. With the supplement of another equipment called energy dispersive X-rays (EDX), the near surface elements and their proportion at various location is detectable (Joshi, Bhattacharyya and Ali, 2008). All mentioned details are attainable by utilising finely focused beam of energetic electrons. An electron-optical system is applied to form the electron probe which aids in scanning the sample's surface in a raster pattern. Miscellaneous signals such as secondary electrons, auger electrons and backscattered electrons are yielded through the interaction of the beam with the sample for analysis (Khandpur, 2015). Conventionally, a light microscope uses a sequence of glass lenses to bend the light waves and generate a magnified image. However, SEM utilising electrons instead of light waves which can generate a more superior magnified images (Joshi, Bhattacharyya and Ali, 2008). Electrons are very light (about 1/1836 the mass of proton) and will be scattered or absorbed in air, hence, a vacuum system is required for the sample chamber and restricting the sample size to a few centimetres on edge (Khandpur, 2015).

Karunanayake, et al. (2018) mentioned that iron loading on the biochar is identifiable with the intense peak present in elemental composition graphs by using SEM-EDX. Magnetic activated carbon had shown higher percentage of iron peak (11.35 %) as compare to non-magnetic activated carbon (0.11 %).

#### **2.4.3 Fourier Transform Infrared Spectroscopy (FTIR)**

Infrared (IR) spectroscopy is one of the oldest and broadly applied analysis equipment in analysing solid sample. Nonetheless, other than solid samples, liquids, gases and soft matters are able to be analysed by using IR spectroscopy as well. The absorption of light from the spectrum is the underlying principle of IR spectroscopy. Progressively, fourier transform technique has been integrated into the IR measurement and the system is called FTIR. The system allows prompt and precise measurement of whole spectra. The vibration of molecules which will alter their

dipole moment are IR active and could lead to absorption of light at a specific wavelength. The specific wavelength where the light is absorbed enables the identification of specific bonds of a molecule (Wang and Zhou, 2017).

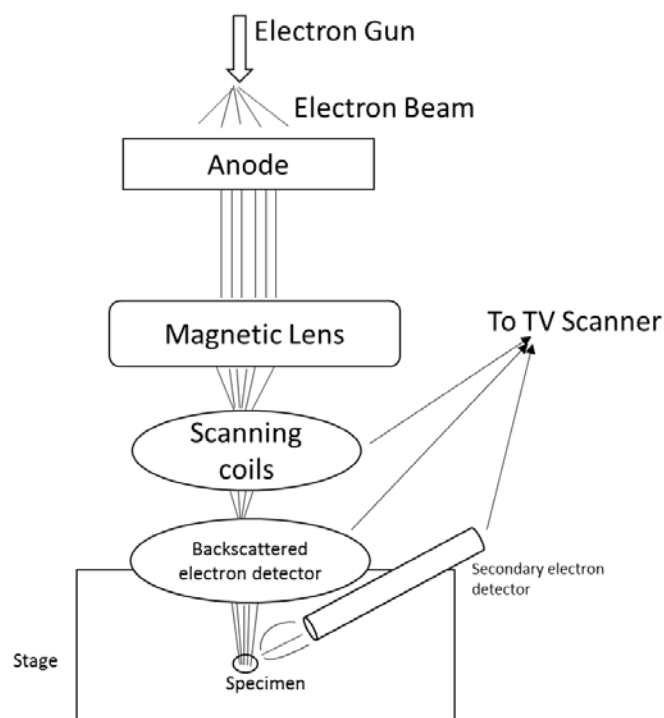


Figure 2.3: Schematic Diagram of SEM (Joshi, Bhattacharyya and Ali, 2008)

As discussed by Lin, et al. (2017), a detection of peak at  $3400\text{ cm}^{-1}$  in the FTIR spectra indicated the  $\text{-OH}$  stretching and bending vibration modes. Besides, Szczepanik, et al. (2015) mentioned that a C-O stretching peak was occurred at the peak of  $1510\text{ cm}^{-1}$ . The peaks at approximately  $2650$  and  $2530\text{ cm}^{-1}$  in FTIR spectra was deduced to be aldehyde group ( $\text{-CHO}$ ) (Taherymoosavi, et al., 2017). A more detailed abbreviated table of group frequencies for various organic function groups is summarised in Table 2.2.

Table 2.2: Abbreviated Table of Group Frequencies for Various Organic Functional Groups (Skoog, Holler and Crouch, 2007)

Bond	Type of Compound	Frequency	Intensity
		Range, $\text{cm}^{-1}$	
C-H	Alkanes	2850-2970	Strong
		1340-1470	Strong

Table 2.2 (Continued)

<b>Bond</b>	<b>Type of Compound</b>	<b>Frequency Range, cm<sup>-1</sup></b>	<b>Intensity</b>
<b>C-H</b>	Alkenes (H <sub>2</sub> C=CH <sub>2</sub> )	3010-3095	Medium
		675-995	Strong
<b>C-H</b>	Alkynes (HC≡CH)	3300	Strong
<b>C-H</b>	Aromatic rings	3010-3100	Medium
		690-900	Strong
<b>O-H</b>	Monomeric alcohols, phenols	3590-3650	Variable
	Hydrogen-bonded alcohols, phenols	3200-3600	Variable, sometimes broad
	Monomeric carboxylic acids	3500-3650	Medium
	Hydrogen-bonded carboxylic acids	2500-2700	Broad
<b>C=C</b>	Alkenes	1610-1680	Variable
<b>C=C</b>	Aromatic rings	1500-1600	Variable
<b>C≡C</b>	Alkynes	2100-2260	Variable
<b>C-N</b>	Amines, amide	1180-1360	Strong
<b>C≡N</b>	Nitriles	2210-2280	Strong
<b>C-O</b>	Alcohols, ethers, carboxylic acids, esters	1050-1300	Strong



Table 2.2 (Continued)

Bond	Type of Compound	Frequency Range, $\text{cm}^{-1}$	Intensity
C=O	Aldehydes, ketones, carboxylic acids, esters	1690-1760	Strong
NO <sub>2</sub>	Nitro compounds	1500-1570	Strong

## 2.5 Advance Oxidation Processes (AOPs)

Advance oxidation processes (AOPs) utilises the in situ formation of highly reactive hydroxyl radical ( $\bullet\text{OH}$ ) to degrade majority of the organic pollutants (Garcia-Segura and Brillas, 2017; Meng, Zhang and Li, 2015). Figure 2.4 shows the possible routes of  $\bullet\text{OH}$  in degrading organic compounds.  $\bullet\text{OH}$  tends to abstract one electron from organic compounds which are rich in electron or any other species occurred in the medium to form hydroxide anion. Moreover,  $\bullet\text{OH}$  can serve to extract one hydrogen atom from hydrocarbon or other organic compounds if the bond energy of the hydrogen bond within the compounds are below  $109 \text{ kcal mol}^{-1}$  (the energy for the formation of O-H bond in the process). Generally, -OH bond energy is greater than majority of C-H bond. Hence, extraction of hydrogen atom from any organic compound is thermodynamically feasible. Besides, the attack to multiple bonds by  $\bullet\text{OH}$ , especially  $\Pi$  clouds of aromatic substances, alkenes and other unsaturated organic compounds is another probable reaction route due to the  $\bullet\text{OH}$  is able to act as strong electrophile (Araujo, et al., 2011).

The lifetime of  $\bullet\text{OH}$  is only a few nanoseconds in water, enabling it to be self-removing from the treatment system in a jiffy (Garcia-Segura and Brillas, 2017). Besides, the produced  $\bullet\text{OH}$  is known as the most powerful oxidants after fluorine with the standard reduction potential,  $E^\circ = 2.8\text{V}$  to degrade the organic contaminants (Almazán-Sánchez, et al., 2014). AOPs are versatile as there are various alternative routes to generate  $\bullet\text{OH}$  (Bethi, et al., 2016). The beneficial characteristics of AOPs include the generation of less harmful species in the product stream (Dewil, et al., 2017) and utilisation of natural light source (Ultraviolet (UV) light) (Bethi, et al., 2016). Degradation efficiency of AOPs is affected by a few parameters such as the ability of the AOPs method to generate  $\bullet\text{OH}$  (Klančar, et al., 2016), complexity of

water matrix as well as the concentration and the type of pollutants (Dewil, et al., 2017). AOPs are applicable in removing organic pollutants such as methyl methacrylate (Almazán-Sánchez, et al., 2014), pesticides (Singh, Philip and Ramanujam, 2017) and organic dyes (Guin, Bhardwaj and Varshney, 2017).

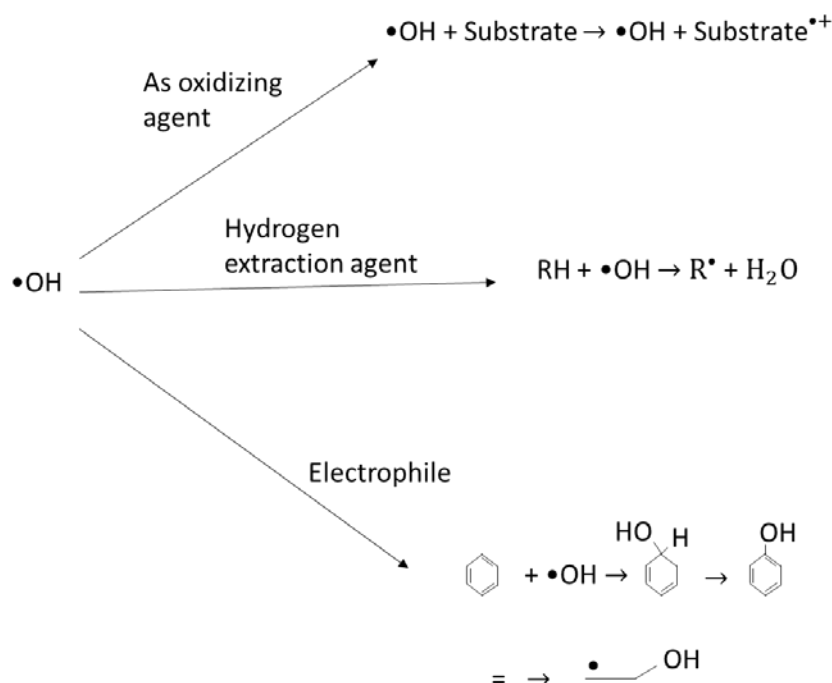


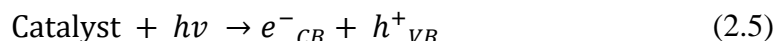
Figure 2.4: General Reactivity of  $\bullet\text{OH}$  (Araujo, et al., 2011)

### 2.5.1 Photocatalysis

The word photocatalysis is the combination of two words, which are photo (light source) and catalysis (enhancement of chemical reaction rate by additional substance without being changed ultimately) (Nahar, et al., 2017). As a whole, photocatalysis is defined as the expedition of photoreaction due to the occurrence of catalyst. It is regarded as one of the practical techniques to eliminate pollutants in wastewater due to low cost, ability to mineralise the pollutants and low toxicity (Kumar, et al., 2017; Chen, et al., 2017). Besides, milder operating conditions such as temperature and pressure is used (Meng, et al., 2018).

Photocatalysis involves the illumination of UV light on the surface of photocatalyst (Khataee, Zarei and Ordikhani-Seyedlar, 2011). Upon the exposure to the UV light, promotion of electrons from the valence band to the conduction band happens, leading to the formation of an electron-hole pair as shown in Equation (2.5).

Valence band is the band with the highest energy located by electrons whereas the conduction band is the band with least energy in which no electron occupation at the ground state (Nahar, et al., 2017).



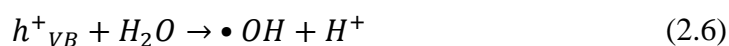
where

$h\nu$  = UV radiation

$e^{-}_{CB}$  = electron in the conduction band

$h^{+}_{VB}$  = electron vacancy or hole in the valence band

Generally, both  $e^{-}_{CB}$  and  $h^{+}_{VB}$  formed can transfer to the surface of catalyst, undergoing a redox reaction with other compounds on the surface.  $h^{+}_{VB}$  will normally react with surface bound water ( $H_2O$ ) to produce  $\bullet OH$  and  $H^{+}$ , whereas  $e^{-}_{CB}$  may react with  $O_2$  to yield  $O_2\bullet^{-}$ . The reactions are illustrated in Equations (2.6) – (2.7). The products,  $\bullet OH$  and  $O_2\bullet^{-}$  then oxidise the organic pollutants such as organic dyes to produce other smaller organic substances in the water (Rauf and Ashraf, 2009).



Semiconductor has gained much attention as the photocatalyst to degrade both organic and inorganic pollutants from aqueous or vapour state system (Ibhadon and Fitzpatrick, 2013). At present, titanium dioxide ( $TiO_2$ ) is one of the surpassing semiconductors as photocatalyst because of its non-toxicity, chemical inert properties, low cost (Zuo, et al., 2014) and longstanding photostability. The semiconductor remains unchanged during the reaction and the needs of consumable chemicals is not required. The photocatalytic characteristic of  $TiO_2$  is modifiable with proper monitoring of the surface treatment and process condition (Ibhadon and Fitzpatrick, 2013). The promotion of electrons from the valence band to the conduction band occurs when  $TiO_2$  is irradiated by using the light source with wavelength of more than 390 nm to generate electron-hole pairs for degradation of organic pollutants.  $\bullet OH$  and  $O_2\bullet^{-}$  are subsequently formed as the desired products to remove the contaminants nearby the surface of  $TiO_2$ . Toxic and bioresistant compounds are

eventually degraded into more environmental friendly species such as  $\text{CO}_2$  and water (Khataee, Zarei and Ordikhani-Seyedlar, 2011). Sludge disposal to landfill is not required as the result of complete degradation of organic pollutants (Ibhadon and Fitzpatrick, 2013). Figure 2.5 demonstrates the mechanism for degrading organic pollutants by using  $\text{TiO}_2$  as photocatalyst.

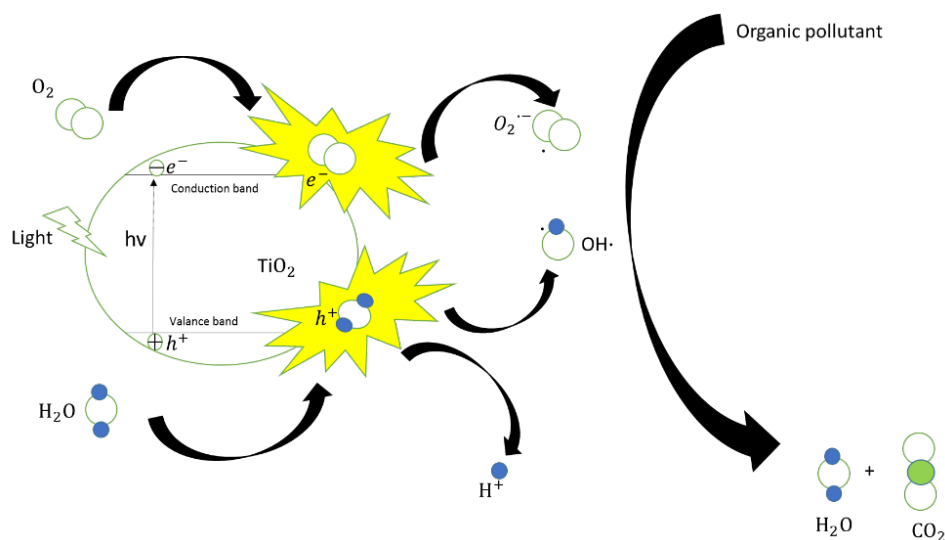


Figure 2.5: Illustration of Mechanism for Degrading Organic Pollutants by Using  $\text{TiO}_2$  Semiconductor as Photocatalyst (Ibhadon and Fitzpatrick, 2013)

Despite the excellent properties in degrading organic pollutants,  $\text{TiO}_2$  has few shortcomings to be considered. One of the weaknesses from using  $\text{TiO}_2$  is its poor ability to absorb sunlight due to the wide band gap (about 3.2 eV). The photocatalytic reaction takes place upon irradiating by UV light of wavelength below 387 nm which only account for 4 to 5 % of the energy from sunlight (Sugrañez, et al., 2015). This technique is not so practical at the areas where exposure of UV radiation is limited. In addition, the cost of production for pure  $\text{TiO}_2$  is relatively high (Balbuena, et al., 2018).

Besides  $\text{TiO}_2$ , iron oxide has been proposed as another excellent photocatalyst (Pang, et al., 2016). Among various phases of iron oxide,  $\alpha\text{-Fe}_2\text{O}_3$  is widely used due to its an n-type semiconductor with a favourable optical band gap of 1.8 to 2.2 eV, ample in environment, low cost (Cao, et al., 2016) and the most thermodynamically stable iron oxides. The conduction band edge of hematite is located at the position where single-electron reduction of  $\text{O}_2$  is unfavourable, affecting the degradation efficiency in the presence of  $\text{O}_2$  molecules. Hence, the

addition of  $\text{H}_2\text{O}_2$  into aqueous suspension with iron oxide could serve as an electron scavenger (Sajjadi and Goharshadi, 2017). By irradiating sunlight on surface of the iron oxide photocatalyst with wavelength below 580 nm, hydrated ferric ions  $(\text{Fe}(\text{OH}))^{2+}$  are photo-reduced to produce  $\text{Fe}^{2+}$  ions and  $\bullet\text{OH}$ . Subsequently,  $\text{Fe}^{2+}$  ions will be reoxidised to ferric ions by  $\text{H}_2\text{O}_2$  or molecular oxygen and form additional reactive radicals such as  $\bullet\text{OH}$  and  $\text{HO}_2\bullet$ . The produced radicals work to oxidise the organic compounds to form carbon dioxide and water. The initial concentration of  $\text{H}_2\text{O}_2$  and  $\text{Fe}^{2+}$  ions are crucial to affect the degradation efficiency. The higher dosage of both substances raises the degradation efficiency. Nonetheless, the surplus amount of  $\text{Fe}^{2+}$  and  $\text{H}_2\text{O}_2$  will reduce the performance of the reaction as they tend to be hydroxyl radical scavengers (Spasiano, et al., 2015). The mechanism of the reaction is illustrated in Figure 2.6.

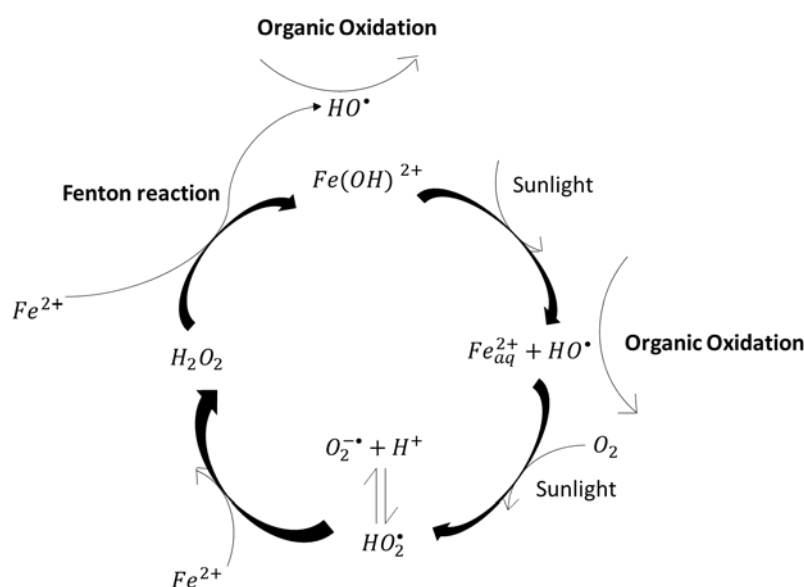


Figure 2.6: Mechanism of Photocatalysis by Using Iron Oxide Photocatalyst (Spasiano, et al., 2015)

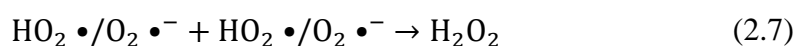
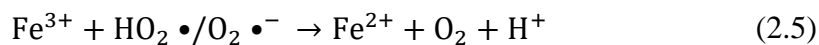
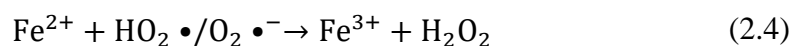
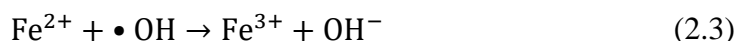
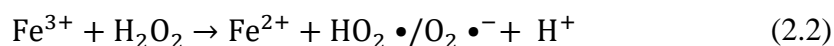
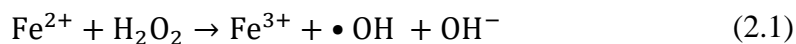
### 2.5.2 Fenton and Fenton-like Processes

Fenton reaction involves the generation of  $\bullet\text{OH}$  due to the reaction between  $\text{Fe}^{2+}$  from the iron salts and  $\text{H}_2\text{O}_2$  (Shen, et al., 2017). Similarly,  $\bullet\text{OH}$  will be produced in Fenton-like reaction where  $\text{Fe}^{3+}$  initiates the reaction with  $\text{H}_2\text{O}_2$  instead of  $\text{Fe}^{2+}$  in Fenton reaction. Both Fenton and Fenton like process are found to have an inherent relationship, where Fe (II) catalyses the Fenton reaction and Fe (III) as the product of Fenton reaction catalyses the Fenton like reaction. The involvement of Fenton-like

will inevitably relates to Fenton reaction due to the interconversion between  $\text{Fe}^{3+}$  and  $\text{Fe}^{2+}$  ions (Jiang, et al., 2013).

The Fenton reaction was introduced by Henry J. H. Fenton in 1894 and is most widely applied in wastewater treatment industry among the AOPs due to its lower capital cost and higher efficiency properties (Hermosilla, Cortijo and Pao, 2009; Fischbacher, Sonntag and Schmidt, 2017). Fenton and Fenton-like processes have been recognised as an effectual method to generate  $\bullet\text{OH}$  by the reaction between  $\text{H}_2\text{O}_2$  and iron salts (Mirzaei, et al., 2017). The Fenton and Fenton-like processes which uses iron salts as catalyst is defined as homogeneous Fenton and Fenton-like processes (Pouran, Raman and Daud, 2014). The amount of oxidant is necessary to be adjusted based on the stoichiometric ratio for a complete mineralisation (Munoz, et al., 2015). It is also highlighted that the solution pH should be set in the optimal range of pH 2.5 to 3 in common homogeneous Fenton reaction (Park, et al., 2018). A rigorous control of solution pH in optimal range is to ensure the maximum quantum yield of  $\bullet\text{OH}$  (Pouran, Raman and Daud, 2014) and avoid any precipitation of inactive iron oxyhydroxides (Clarizia, et al., 2017).

Homogeneous Fenton and Fenton-like processes involves the transfer of electron between  $\text{H}_2\text{O}_2$  and iron salts such as iron sulphate ( $\text{FeSO}_4$ ) (Hermosilla, Cortijo and Pao, 2009; Araujo, et al., 2011).  $\text{Fe}^{3+}$  and  $\bullet\text{OH}$  are yielded upon reacting  $\text{Fe}^{2+}$  and  $\text{H}_2\text{O}_2$  as shown in Equation (2.1). At this stage,  $\text{Fe}^{3+}$  converts back to  $\text{Fe}^{2+}$  and forming peroxy ( $\text{HO}_2\bullet$ ) or superoxide radicals ( $\text{O}_2\bullet$ ) and hydrogen ions ( $\text{H}^+$ ) with the presence of  $\text{H}_2\text{O}_2$  as depicted in Equation (2.2). In the advent of an organic substrate (R-H), abstraction of hydrogen atom from R-H will occur as the result of  $\bullet\text{OH}$  present in the solution, forming  $\text{R}\bullet$  which will be transformed to different oxidation products at later stage. Theoretically, the excess amount  $\text{Fe}^{2+}$  and  $\text{H}_2\text{O}_2$  in the solution should lead to complete mineralisation of organic compounds into  $\text{CO}_2$  and water. Nevertheless, this is unachievable due to the non-specific and enhanced reactivity of  $\bullet\text{OH}$  on both organic and inorganic substrates (Bokare and Choi, 2014). Numerous other reactions that might affect the organic oxidation process occur such as the redox equilibria of Fe ions (interchange between  $\text{Fe}^{2+}$  and  $\text{Fe}^{3+}$ ) as demonstrated in Equations (2.3) – (2.5) and regeneration of  $\text{H}_2\text{O}_2$  as illustrated in Equations (2.4), (2.6) – (2.7). The reaction will halt at the moment where  $\text{H}_2\text{O}_2$  is exhausted (Shen, et al., 2017).



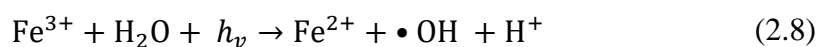
However, there are a few disadvantages to be concerned in homogeneous Fenton and Fenton-like processes such as the pH reliance of the system, additional cost on removing the iron sludge and recovery of catalyst is difficult (Pouran, Raman and Daud, 2014; Munoz, et al., 2015). In addition, another main drawback of homogeneous photo-Fenton and Fenton-like processes is the needs of transparent solution for better removal efficiency. The occurrence of organic compounds with strong absorption bands in UV zone tends to inhibit the photon absorption by  $\text{Fe}^{3+}$  (Araujo, et al., 2011).

In order to overcome the mentioned issues, heterogeneous Fenton and Fenton-like processes which utilises additional solid supported catalyst is a promising alternative to be applied (Pouran, Raman and Daud, 2014; Munoz, et al., 2015). Supported catalyst provides a matrix that allows the metal species to be dispersed as very tiny particles and enlarge the surface area of the species. Furthermore, thermal and chemical stability of the catalyst can be enhanced and sintering effect on the active site of the catalyst is reducible (Munoz, et al., 2015). Few important parameters to be considered in selecting an efficient Fenton and Fenton-like processes catalyst are the stability, selectivity of the catalyst on utilising  $\text{H}_2\text{O}_2$  and operating condition for the catalyst to perform catalytic activity (Araujo, et al., 2011). Numerous heterogeneous catalysts are widely applied, including clays (Araujo, et al., 2011), magnetic carbon (Zhou, et al., 2015), alginate (Cruz, et al., 2017), zeolites (Arimi, 2017) and iron containing minerals. The latter material has received great attention due to its plentiful available in the earth crust (Pouran, Raman and Daud, 2014). Magnetite ( $\text{Fe}_3\text{O}_4$ ) (Liang, et al., 2013), goethite ( $\alpha - \text{FeOOH}$ ) (Lin, et al., 2014), pyrite ( $\text{FeS}_2$ ) (Labiadh, et al., 2015), hematite ( $\text{Fe}_2\text{O}_3$ ) and lepidocrocite ( $\gamma - \text{FeOOH}$ ) are the common iron oxides used in removing

emerging contaminants (Mirzaei, et al., 2017). Magnetite exhibits the highest Fenton activity among the iron oxides (Liang, et al., 2013).

Fe<sub>3</sub>O<sub>4</sub> is cubic inverse spinel in structure with chemical formula of (Fe<sup>3+</sup>)<sub>Tet</sub>[Fe<sup>2+</sup> Fe<sup>3+</sup>]<sub>Oct</sub>O<sub>4</sub> where Fe<sup>2+</sup> occupies in octahedral sites and Fe<sup>3+</sup> locates in both octahedral and tetrahedral sites (Liang, et al., 2013; Munoz, et al., 2015). In the presence of both Fe<sup>2+</sup> and Fe<sup>3+</sup> in octahedral sites, the structure of Fe<sub>3</sub>O<sub>4</sub> allows the Fe species to be reversibly oxidised and reduced while maintaining the same structure (Liang, et al., 2013). Munoz, et al. (2015) reported that Fe<sub>3</sub>O<sub>4</sub> supported catalyst could enhance the oxidation performance on various non-biodegradable organic contaminants. Additional outstanding properties of Fe<sub>3</sub>O<sub>4</sub> are the ease of separation from the solution due to the excellent magnetic property and better electron mobility within its spinel structure as the result of higher dissolution rate among the iron oxide (Pouran, Raman and Daud, 2014). Heterogeneous Fenton and Fenton-like processes widen the application solution pH value thorough the process and eases the issues related to the separation of large amount of Fe ions after the reaction (Mirzaei, et al., 2017).

The production of •OH in Fenton and Fenton-like processes is able to be improved with the presence of UV light. The process is termed as photo Fenton and Fenton-like processes. In photo Fenton and Fenton-like processes, the Fe<sup>3+</sup> ions generated behave as light-absorbing elements to produce additional •OH as demonstrated in Equations (2.8) - (2.9) (Mirzaei, et al., 2017). In addition, disinfection effect is achievable due to the inactivation of microorganism by applying UV irradiation technique in photo-Fenton and Fenton-like processes (Mirzaei, et al., 2017). In homogeneous photo Fenton and Fenton like processes, the catalyst leaching occurs and the recovery process is arduous. Hence, several heterogeneous iron catalysts such as Fe/TiO<sub>2</sub>, Fe/clays and γ-Al<sub>2</sub>O<sub>3</sub> are suitable to be used. The process is called as heterogeneous photo Fenton and Fenton-like processes (Dias, et al., 2016; Li, et al., 2015).





## **2.6 Parameter Study**

### **2.6.1 Effect of Organic Dye Concentration**

An increase on the organic dye concentration was proven to reduce the removal rate of the dye due to the hindering of light adsorption by the catalyst might occur as the result of excessive dye molecules adsorbed on the surface of catalyst (Hassani, et al., 2018). Moreover, the presence of excessive amount of dye molecules might cause a retrenchment on the probability of effective collision between the catalyst and organic dye, impeding the degradation process (Hu, et al., 2018).

Based on the study conducted by Khataee, Gholami and Sheydaei (2016), it was reported that a raise of the initial amount of reactive orange 29 had caused negative effect on the degradation efficiency while maintaining the constant catalyst dosage and H<sub>2</sub>O<sub>2</sub> amount in heterogeneous Fenton and Fenton-like processes due to the insufficient supply of reactive radicals to degrade the dyes. As reported by Liu, et al. (2017a), the decolourisation efficiency of methylene blue was in a downward trend with the increase in the amount of methylene blue. It was justified that the catalyst surface might reach saturation promptly due to the excessive dyes presence, hence, slowing down the degradation efficiency.

### **2.6.2 Effect of Catalyst Dosage**

Generally, the amount of catalyst used has an impact in heterogeneous Fenton and Fenton-like processes as it affects the decomposition rate of H<sub>2</sub>O<sub>2</sub> (Liu, et al., 2017a). It was shown that the degradation reaction rate of acid orange 7 was raised from 0.014 to 0.0265 min<sup>-1</sup> upon adding the dosage of heterogeneous Fenton and Fenton-like processes catalyst from 0.2 to 0.6 g/L. However, further increase the amount of catalyst to 0.8 g/L has resulted the reaction rate to drop to 0.0265 min<sup>-1</sup>. This phenomena was due to the decomposition rate of H<sub>2</sub>O<sub>2</sub> to produce •OH was in an upwards trend upon adding more catalyst into the system up to a certain level. Excessive amount of catalyst could reduce the degradation rate due to more frequent collision between nanoparticles in the solution, causing the agglomeration to take place and blocking some available active sites. Besides, the limitation of mass transfer rate between H<sub>2</sub>O<sub>2</sub> and the organic dyes might be another factor of reducing the degradation rate in excessive catalyst environment (Fang, et al., 2017).

Khataee, Gholami and Sheydaei (2016) reported that the decolourisation efficiency of reactive orange 29 increased by adding the dosage of catalyst up to 3

g/L before a slight drop for further increasing the amount of catalyst. It might be due to the scavenging effect of Fe ions on generated  $\bullet\text{OH}$ . Liu, et al. (2017b) also stated that there was an optimal catalyst dosage (around 0.4 g/L) for degrading methyl orange, further increasing the dosage will lead to the decrement of degradation efficiency due to the insufficient reactive sites to cater the degradation reaction. As reported by Xiao, Xie and Cao (2015), the increase in catalyst concentration might lead to the enhancement of degradation efficiency. However, excessive amount of catalyst could cause light transmission obstacles in photocatalytic ozonation.

### 2.6.3 Effect of Solution pH

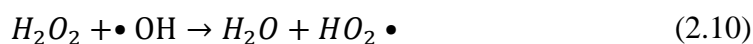
In Fenton and Fenton-like processes, pH plays a crucial role in controlling the degradation efficiency of organic dyes. In homogeneous Fenton and Fenton-like processes, the optimal pH value is around 3 (Fida, et al., 2017). As reported by Mark, et al. (2017), the highest degradation efficiency was achieved at pH 3 for both everzol red 239 and brilliant blue 19 dyes. Upon increasing the pH value to more than 3, the activity of Fenton reagent was dropped due to the occurrence of inactive iron oxohydroxides and ferric hydroxide precipitate as undesired products, reducing the amount of available Fe ions to generate  $\bullet\text{OH}$  radicals. On the other hand, reducing the pH value to lower than 3 would also lead to a decrease in the efficiency of Fenton reagent. This is because of the formation of iron complex species  $(\text{Fe}(\text{H}_2\text{O})_6)^{2+}$  has slower reactivity rate with  $\text{H}_2\text{O}_2$  than other species. Besides, higher concentration of  $\text{H}^+$  in very low pH condition could cause the peroxide to get solvated and produce stable oxonium ion  $(\text{H}_3\text{O}_2)^+$ . The produced ions tend to stabilise the  $\text{H}_2\text{O}_2$  and decrease the reactivity between  $\text{Fe}^{2+}$  and  $\text{H}_2\text{O}_2$ . Hence, proper control of pH at the optimal value is desired (Babuponnusami and Muthukumar, 2014).

In heterogeneous Fenton and Fenton-like processes, pH value applicable in a wider range (Wang, et al., 2014). Roonasi and Nezhad (2015) reported that a maximum degradation efficiency for organic pollutant such as phenol was achievable at neutral pH (close to pH 6) by using copper ferrites as catalyst. Wang, et al. (2014) presented that removal rate of reactive brilliant red X-3B at pH 5 and 7 were 97.3 and 98.8 % respectively. It was claimed that the distinctive properties of heterogeneous Fenton and Fenton-like processes catalyst such as well adsorption capacity and various oxygen containing groups ease or retard the generation of  $\text{Fe}^{2+}$ /

$\text{Fe}^{3+}$  hydroxide complexes. This was due to the interaction between  $\text{Fe}^{3+}$  and the catalyst after the  $\text{Fe}^{3+}$  has been attached onto the catalyst. In another study conducted by Chen, et al. (2014), the optimal pH value for few dyes was close to neutral, which was pH 6.5 for rhodamine 6, pH 5.6 for methyl blue and pH 6.7 for methyl orange by using Fe-titanate as the heterogeneous Fenton and Fenton-like processes catalysts.

#### 2.6.4 Effect of $\text{H}_2\text{O}_2$ Dosage

$\text{H}_2\text{O}_2$  serves as the main source in Fenton and Fenton-like processes to produce  $\bullet\text{OH}$  radicals in treating the organic dyes (Wang, et al., 2016). It was proven that the degradation efficiency of organic dyes such as acid red 66 and direct blue 71 increased upon raising the amount of  $\text{H}_2\text{O}_2$  used up to an optimum concentration. Further adding the  $\text{H}_2\text{O}_2$  after the optimum concentration led to the reduction of degradation efficiency. This observation was mainly because of escalating the amount of  $\text{H}_2\text{O}_2$  would lead to higher decomposition rate of  $\text{H}_2\text{O}_2$ , hence, more reactive radicals would be generated. Nonetheless, abundant dosage of  $\text{H}_2\text{O}_2$  tends to cause scavenging effect on  $\bullet\text{OH}$  radicals, resulting the decrement in degradation efficiency (Khataee, Gholami and Sheydaei, 2016). Equation (2.10) illustrates the scavenging effect of excess  $\text{H}_2\text{O}_2$  on  $\bullet\text{OH}$  radicals. Besides, as another backlash to be considered, an increase of chemical oxygen demand (COD) will be detected in the presence of excessive  $\text{H}_2\text{O}_2$  dosage in the solution, causing the possibility of treated water deviates from the COD discharge standard (Wang, et al., 2016).



In contrast, the decrease in the concentration of  $\text{H}_2\text{O}_2$  in the solution causes a lower degradation efficiency due to insufficient amount of  $\bullet\text{OH}$  are generated via decomposition of  $\text{H}_2\text{O}_2$  (Wang, et al., 2016). In a study conducted by He, et al. (2017), the reaction time needed to degrade the organic dyes had been shortened from 150 min to 60 min when the dosage of  $\text{H}_2\text{O}_2$  raised from 1.25 mM to 10 mM. Subsequently, the reaction time remained stagnant despite the continuous increase of  $\text{H}_2\text{O}_2$  amount after 12.5 mM. The optimal concentration was estimated in between 10 to 12.5 mM. According to Lin, et al. (2014), the removal efficiency of 2,4,40-trichlorobiphenyl by using heterogeneous Fenton and Fenton-like processes was in a

raising trend upon increasing the amount of H<sub>2</sub>O<sub>2</sub> from 0.17 to 17 g/L and achieved up to 99 % of elimination at the concentration of 17 g/L of H<sub>2</sub>O<sub>2</sub>.

## 2.7 Kinetic Study

In order to understand the reaction mechanism (Chai, et al., 2017) and perform the quantitative analysis and on the parameters, reaction kinetics of degradation of organic dyes are crucial to be identified by plotting the experimental data acquired into pseudo zero, first and second order reactions model. Based on the reaction order, the parameters which has larger and smaller effect can be identified (Chai, et al., 2017). The models are listed in Equations (2.11) – (2.13) and can be transformed into graphical form of equation as depicted in Equations (2.14) – (2.16). The experimental data obtained will be used in plotting graphs based on Equations (2.14) – (2.16) to generate linear plotting and determine the reaction order for the process (Zhang, et al., 2017).

$$r = -\frac{dC}{dt} = k_0 \quad (2.11)$$

$$r = -\frac{dC}{dt} = k_1 C \quad (2.12)$$

$$r = -\frac{dC}{dt} = k_2 C^2 \quad (2.13)$$

$$C_t = C_o - k_0 t \quad (2.14)$$

$$C_t = C_o e^{-k_1 t} \quad (2.15)$$

$$C_t = \frac{C_o}{1 + k_2 t C_o} \quad (2.16)$$

where

$r$  = rate of organic dyes concentration, ppm min<sup>-1</sup>

$C_o$  = initial concentration of organic dyes, ppm

$C_t$  = concentration of organic dyes at certain time, ppm

$k_0$  = zero order rate constant, ppm min<sup>-1</sup>

$k_1$  = first order rate constant, min<sup>-1</sup>

$k_2$  = second order rate constant, ppm<sup>-1</sup> min<sup>-1</sup>

Khataee, et al. (2015) reported that pseudo-first order was best fitted to the heterogeneous photo-Fenton-like degradation of acid red 17. It was also found that the degradation of orange g dyes by applying Fe-impregnated sugarcane residue biochar based catalyst in heterogeneous Fenton and Fenton-like processes was best fitted to first order kinetic equation (Park, et al., 2018).

## CHAPTER 3

### METHODOLOGY AND WORK PLAN

#### 3.1 Materials and Chemicals

The list of chemical reagents used throughout the experiment and their respective specifications are shown in Table 3.1. Hydrogen chloride (HCl) and sodium hydroxide (NaOH) were the main chemicals used in controlling pH in the experiment.

Table 3.1: Chemicals Used in the Experiment and Their Specifications

Chemical Reagents	Purity (%)	Brand	Usage
Malachite Green	99	Fisher Scientific	Model pollutant
Iron (III) Nitrate Nonahydrate	97	Merck	Iron precursor
H <sub>2</sub> O <sub>2</sub>	30	Sigma-Aldrich	Oxidant
Potassium Iodide (KI)	99	Sigma-Aldrich	Reducing agent
HCl	37	Sigma-Aldrich	pH adjustment
NaOH Powder	97	Sigma-Aldrich	pH adjustment
Potassium Hydroxide (KOH)	85	Sigma-Aldrich	Chemical activating reagent

The model pollutants used in this study was malachite green. The chemical properties of model pollutants are illustrated in Table 3.2.

#### 3.2 Equipment

The instruments involved along with their respective models and functions have been summarised in Table 3.3.

#### 3.3 Overall Experiment Flowchart

The flow chart for overall research activities are illustrated in Figure 3.1. Firstly, the synthesis process for various catalysts was carried out, followed by the characterisation process of the synthesised catalysts. Subsequently, parameter studies were conducted to determine the optimum condition.

Table 3.2: Chemical Properties of Model Pollutants

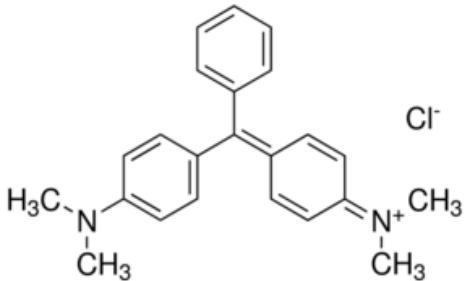
Model Pollutants	Chemical Structure	Classification	Molecular Weight (g/mol)	Maximum Wavelength Absorption, $\lambda$ (nm)
Malachite Green	 <p>The chemical structure of Malachite Green is shown. It consists of a central carbon atom double-bonded to a nitrogen atom (N+) which is bonded to two methyl groups (CH3). This central carbon is also single-bonded to a phenyl ring and a para-substituted benzene ring. The para-substituted benzene ring has a dimethylamino group (N(CH3)2) at the other end.</p>	Cationic basic triaryl methane	364.911	619

Table 3.3: List of Models and Functions of Each Instrument Involved

<b>Instrument</b>	<b>Model</b>	<b>Function</b>
<b>Carbolite Furnace</b>	Carbolite RHF 1500	Performing the heat treatment in catalyst synthesis process
<b>pH Meter</b>	Eutech PC 300	pH measurement
<b>Tube Furnace</b>	Lenton LTF12/100/940/3216 CC	Performing the heat treatment in catalyst synthesis process under inert environment
<b>Fourier Transform Infrared Spectroscopy (FTIR)</b>	Nicolet IS10	Identifying the functional groups present in the sample
<b>Inductively Coupled Plasma Optical Emission Spectrometry (ICP-OES)</b>	Optima 7000 DV	Identifying the iron ion in liquid sample
<b>Hot Plate</b>	IKA	Ensuring a well mixing of iron modified sugarcane bagasse activated carbon catalyst and organic dyes
<b>Halogen Lamp</b>	Philip	Acting as solar energy source (UV intensity: $30 \mu\text{W}/\text{cm}^2$ )
<b>SEM-EDX</b>	Hitachi SEM Model S-3400N	Catalyst characterisation



Table 3.3 (Continued)

<b>Instrument</b>	<b>Model</b>	<b>Function</b>
<b>XRD</b>	Shimadzu XRD-6000	Catalyst characterisation
<b>UV-vis Spectrophotometer</b>	Jenway 6320D	Analysing liquid sample

Besides, kinetic study was performed to identify the reaction order of the degradation process and the liquid sample was analysed to identify the stability of the synthesised catalysts.

### 3.4 Experiment Setup

The experiment setup for heterogeneous photo Fenton and Fenton-like degradation of malachite green is demonstrated in Figure 3.2. To ensure proper mixing of solution and catalyst, a magnetic hot plate stirrer was used.

### 3.5 Preparation of Fe<sub>3</sub>O<sub>4</sub>, AC and Fe<sub>3</sub>O<sub>4</sub>/AC at Various Weight Ratios

At the beginning, sugarcane bagasse was collected in huge amount and used as the activated carbon source. The bagasse was first cut into smaller pieces and washed with distilled water to remove dust particles on the surface. Next, the bagasse was undergone calcination process at 550 °C for about 2 hours to produce activated carbon. The iron precursor aqueous solution was prepared by mixing the iron (III) nitrate nanohydrate aqueous solution with diluted KI solution in the weight ratio of 3 to 1 in order to obtain Fe<sup>2+</sup>/Fe<sup>3+</sup> aqueous solution. Subsequently, chemical impregnation was performed where the produced activated carbon was immersed in the produced Fe<sup>2+</sup>/Fe<sup>3+</sup> aqueous solution for an hour, followed by adding diluted KOH solution in the same amount as KI to enhance the porosity on activated carbon (Huang, Ma and Zhao, 2015; Rattanachueskul, et al., 2017).

The impregnated solid portion was undergone pyrolysis process in a tube furnace under inert environment at 550 °C for 2 hours. The mixing weight ratio for Fe<sup>2+</sup>/Fe<sup>3+</sup> ions to activated carbon was varied from 1:1, 1:3 and 3:1 to compare the efficiency in degrading dye. The different ratio catalysts are denoted as FeAC11,

FeAC13 and FeAC31 where the Fe represents the iron precursor, AC stands for activated carbon, the alphabets indicates the ratio of Fe precursor to activated carbon.

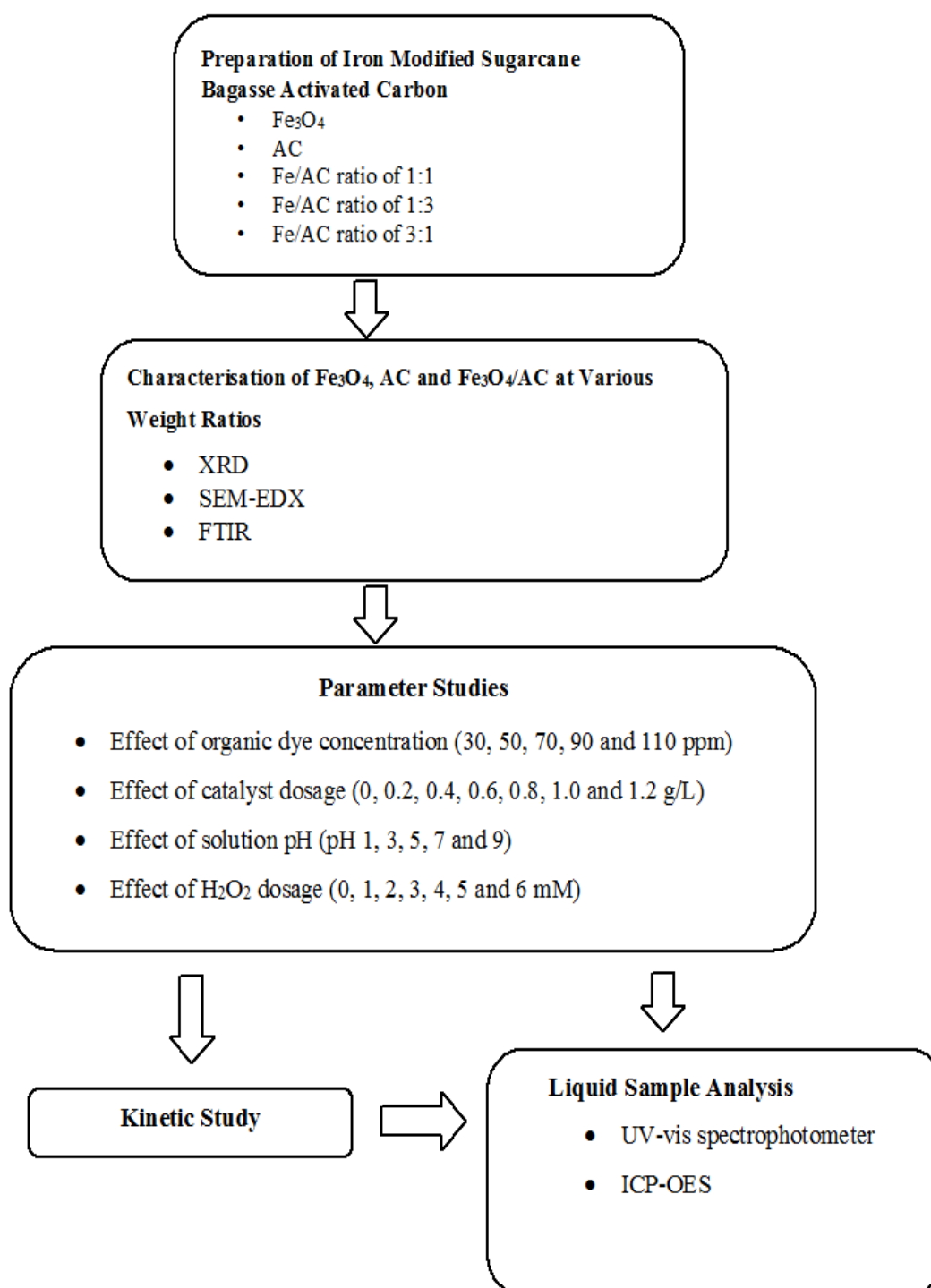


Figure 3.1: Flow Chart of Overall Research Activities

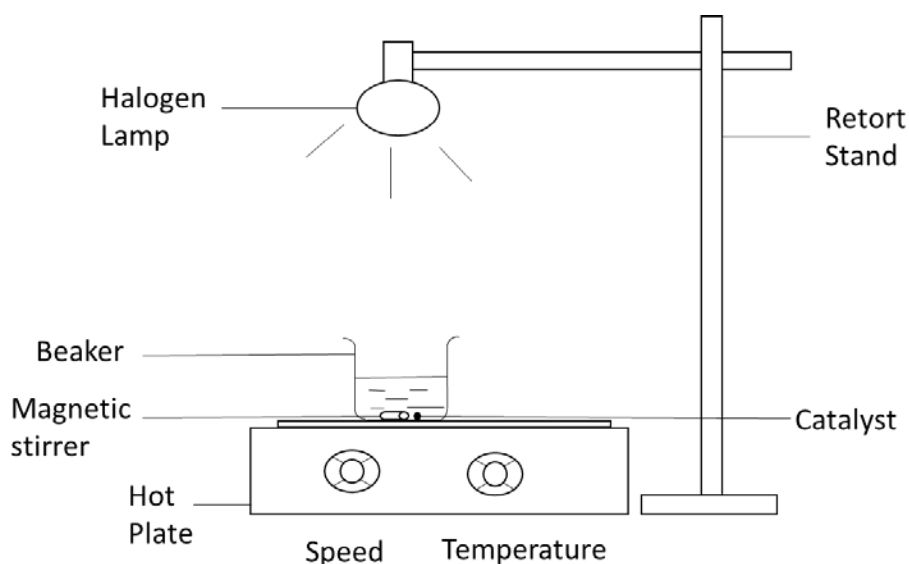


Figure 3.2: Schematic Diagram of Experimental Setup for Heterogeneous Photo Fenton and Fenton-like Processes

### 3.6 Characterisation of $\text{Fe}_3\text{O}_4$ , AC and $\text{Fe}_3\text{O}_4/\text{AC}$ at Various Weight Ratios

Catalyst characterisation is a crucial step in the process to provide insights of the structure, compositions, as well as chemical properties of the developed catalyst. Hence, the synthesised catalysts were characterised by XRD, SEM-EDX and FTIR.

#### 3.6.1 XRD

The crystalline phase structure of produced solid catalyst was identified by using X-ray diffractometer model XRD-6000 supplied by Shimadzu. The  $\text{Cu-K}\alpha$  ( $\lambda = 1.5405 \text{ \AA}$ ) radiation course was monitored at 40 kW/3 mA. All interference peaks were eliminated by using K-beta filter. Both divergence slit and scattering slit were applied at  $1^\circ$  and 0.3 mm, respectively. The sample was then smeared onto glass slide and placed into a sample holder. The intensity of diffracted X-rays was recorded continuously by controlling the diffraction pattern occurring in the  $2\theta$  ranging from  $10^\circ$  to  $70^\circ$ . The scan rate and scan step was set at  $2^\circ/\text{min}$  and  $0.02^\circ$  respectively. An intense peak occurred when the mineral had lattice planes with  $d$ -spacing suitable to diffract X-rays at value of  $\theta$  (Ma, Zhou and Chen, 2017).

#### 3.6.2 SEM-EDX

Analysis of scanning electron microscopy was performed to determine the morphological structure of prepared catalysts. Double-sided adhesive tape was used

to ensure proper adherent of catalyst on specimen holder before undergoing analysis by SEM model S-3400N supplied by Hitachi. Gloves were essentially to be worn throughout the preparation and transferring of sample to avoid contamination to SEM system. The scanning electron images were obtained by using the acceleration voltage of 20 kV and magnification of 10, 20 and 40 kX. The elemental composition of catalyst was identified by coupling SEM with EDX technique (Joshi, Bhattacharyya and Ali, 2008).

### **3.6.3 FTIR**

The samples were compared in terms of active surface functional groups by using the FTIR spectrometer model Nicolet IS10 supplied by ThermoFisher Scientific. The method used was attenuated total reflectance (ATR). The FTIR spectra for different samples were recorded in the spectral range of 400 to 4000  $\text{cm}^{-1}$  at a resolution of 4  $\text{cm}^{-1}$  and 254 scans. The spectra obtained was compared with the established database in literature review (Wang and Zhou, 2017).

## **3.7 Parameter Studies**

### **3.7.1 Effect of Organic Dye Concentration**

The effect of malachite green concentration on the heterogeneous photo Fenton and Fenton-like degradation of malachite green was analysed by varying the concentration of dyes to 30, 50, 70, 90 and 110 ppm. Firstly, 100 mL of malachite green solution with concentration of 30 ppm was transferred into the beaker. 1 g/L of catalyst was then added into the beaker. The temperature was at 25 °C and the pH was at pH 7. Next, the sample solution was collected every 5 min for 30 min and performed centrifugation to separate out the catalyst before further analysis. The experiment was repeated with 50, 70, 90 and 110 ppm of dyes while keeping other parameters constant. The optimal concentration was used for further parameter studies.

### **3.7.2 Effect of Catalyst Dosage**

The effect of iron modified sugarcane bagasse activated carbon dosage on heterogeneous photo Fenton and Fenton-like degradation of malachite green was determined by manipulating the loading between 0, 0.2, 0.4, 0.6, 0.8, 1.0 and 1.2 g/L.

At the beginning, 100 mL of malachite green solution with concentration of 30 ppm was filled into a beaker along with 1 g/L of catalyst. The beaker was then placed on the hot plate for magnetic stirring. The temperature was remained at 25 °C and pH was set at pH 7. The sample solution was collected every 5 min for 30 min, followed by centrifugation to separate the catalyst for subsequent analysis. The process was repeated by changing the catalyst dosage to 0, 0.2, 0.4, 0.6, 0.8 and 1.2 g/L while maintaining the other parameter conditions. The optimal dosage for catalyst was identified and used for the subsequent parameter study.

### **3.7.3 Effect of Solution pH**

The effect of solution pH value on the heterogeneous photo Fenton and Fenton-like degradation of malachite green was identified by varying the pH value between pH 1, 3, 5, 7 and 9. The adjustment of pH was done by adding 0.1 M NaOH or 0.1 M HCl, 100 mL of 30 ppm of dyes was transferred into the beaker with the optimal amount of catalyst under magnetic stirring. The pH was then adjusted to pH 1 for the first run. The temperature was at 25 °C. The sample was collected every 5 min for 30 min for further analysis. The collected samples were undergone centrifugation to separate out the catalyst before further analysis. The experiment was repeated by changing the pH value to pH 3, 5, 7 and 9 while fixing other parameters to determine the optimal pH for subsequent parameter study.

### **3.7.4 Effect of H<sub>2</sub>O<sub>2</sub> Dosage**

The effect of H<sub>2</sub>O<sub>2</sub> dosage on the heterogeneous photo Fenton and Fenton-like degradation of malachite green was studied by changing the dosage from 0, 1, 2, 3, 4, 5 and 6 mM. Similarly, 100 mL of dyes with concentration of 30 ppm was poured into the beaker together with optimal amount of catalyst and 1 mM of H<sub>2</sub>O<sub>2</sub>. The pH was adjusted to optimal pH value and the temperature was at 25 °C. The sample solution was taken every 5 min for 30 min and centrifugation was performed before proceeding to further analysis. The experiment was run again by setting the dosage of H<sub>2</sub>O<sub>2</sub> at 0, 2, 3, 4, 5 and 6 mM while maintaining constant for other parameters.

### 3.8 Kinetic Study

Kinetic study was analysed in this experiment to identify the reaction order. Pseudo zero order, pseudo first order and pseudo second order reaction kinetics were applied to study the degradation kinetics of dyes by using heterogeneous photo Fenton and Fenton-like processes in the presence of iron modified sugarcane bagasse activated carbon catalyst. The respective expression of different reaction order can be identified by Equations (3.1) - (3.3).

Pseudo zero order reaction kinetics:

$$C_t = C_o - k_0 t \quad (3.1)$$

Pseudo first order reaction kinetics:

$$\ln C_t = \ln C_o - k_1 t \quad (3.2)$$

Pseudo second order reaction kinetics:

$$\frac{1}{C_t} = \frac{1}{C_o} + k_2 t \quad (3.3)$$

where

$C_o$  = initial concentration of organic dyes, ppm

$C_t$  = concentration of organic dyes after certain time, ppm

$k_0$  = zero order rate constant, ppm min<sup>-1</sup>

$k_1$  = first order rate constant, min<sup>-1</sup>

$k_2$  = second order rate constant, ppm<sup>-1</sup> min<sup>-1</sup>

The regression analysis was performed based on pseudo zero order, pseudo first order and pseudo second order reaction kinetics for degrading the dyes. A linear plot was obtained under the correct order of reaction kinetic (Chai, et al., 2017).

### 3.9 Liquid Sample Analysis

The concentration of dyes for every 5 min interval from the sample solution after undergoing the oxidation method under various conditions was analysed in order to identify the degradation efficiency of the reactions. The absorbance of organic dyes were measured with the aid of UV-vis spectrophotometer at the wavelength with highest absorbance,  $\lambda_{\max}$  for the respective dyes. The  $\lambda_{\max}$  value was listed in Table 3.2 for malachite green. The degradation efficiency was then computed by using Equation (3.4) (Khataee, et al., 2017).

$$\text{Degradation efficiency (\%)} = \frac{C_o - C_t}{C_o} \times 100 \% \quad (3.4)$$

where

$C_o$  = initial concentration of organic dyes, ppm

$C_t$  = concentration of organic dyes after certain time, ppm

Besides, ICP-OES, a powerful and popular analytical tool to determine the composition of trace elements within the unknown sample solution was also used. The analytical tool involves the continuous discharge of radio frequency to stimulate the emission of photon from the atoms or ions present in the unknown sample. The trace element in the sample was determined based on this principle (Khandpur, 2015). In addition, the stability of iron modified sugarcane bagasse activated carbon catalyst in the degradation process was determined based on its leaching effect of iron from the catalyst and the concentration of leached iron. In this study, iron (III) nitrate nonahydrate was used as iron source to prepare the standard solution for analysis.

## CHAPTER 4

### RESULTS AND DISCUSSIONS

#### 4.1 Characterisations of $\text{Fe}_3\text{O}_4$ , AC and $\text{Fe}_3\text{O}_4/\text{AC}$ at Various Weight Ratios

##### 4.1.1 XRD Results

The crystal structure of  $\text{Fe}_3\text{O}_4$ , AC and  $\text{Fe}_3\text{O}_4/\text{AC}$  at various weight ratios were analysed by using XRD analysis. Figure 4.1 demonstrates the XRD pattern of various particles. Based on Figure 4.1, a broad peak around  $22^\circ$  was observed for the sample AC. The peak might represent the presence of cellulose crystal in the activated carbon (Qiao, et al., 2017; Zhang, et al., 2018). A small and broad peak was observed could be explained by the cellulose structure was partially or completely burnt off at temperature as high as 315 to 400  $^\circ\text{C}$  while performing the calcination process under inert environment (Deng, Li and Wang, 2016; Varma and Mondal, 2017). Similarly, FeAC13, FeAC11 and FeAC31 which involved the activated carbon as the support material showed a small peak at around  $22^\circ$ , signifying the presence of activated carbon.

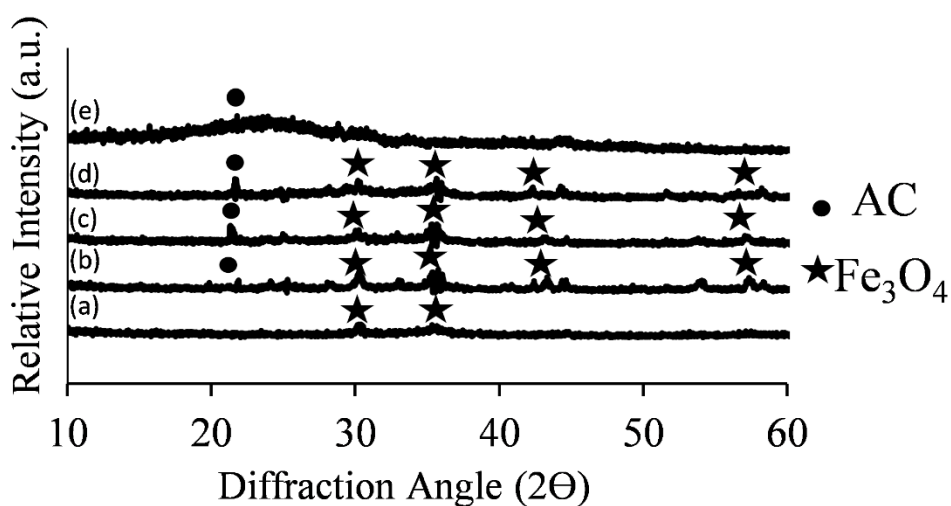


Figure 4.1: XRD Patterns for (a)  $\text{Fe}_3\text{O}_4$ , (b) FeAC31, (c) FeAC11, (d) FeAC13, (e) AC



It was reported that the peaks appeared at 30.3, 35.7, 43.4, 57.4, and 63 ° indicated the face-centred cubic structure of Fe<sub>3</sub>O<sub>4</sub> (Yu, et al., 2012; Rattanachueskul, et al., 2017). Besides, Noraini, et al. (2016) identified that the diffraction peaks detected at 35.48, 57.72 and 63.22 ° symbolised the presence of Fe<sub>3</sub>O<sub>4</sub> as the major crystalline phase. The appearance of these peaks for Fe<sub>3</sub>O<sub>4</sub>/AC composite samples implied that the Fe<sub>3</sub>O<sub>4</sub> were precipitated on AC. From Figure 4.1, it could be concluded that Fe<sub>3</sub>O<sub>4</sub> was present in the sample (a) - (d) as the main diffraction peaks were occurred at around 30, 35, 43 and 57 ° which were tally with the literatures.

#### 4.1.2 FTIR Results

The functional group of Fe<sub>3</sub>O<sub>4</sub>, AC and Fe<sub>3</sub>O<sub>4</sub>/AC at different weight ratios were analysed by using FTIR analysis. Figure 4.2 illustrates the spectra of different samples from the range of 500 to 4000 cm<sup>-1</sup>. The broad peak appeared at 3400 cm<sup>-1</sup> for all samples synthesised accounted by the stretching vibration of -OH groups. Similar peak was reported by Rattanachueskul, et al. (2017), where the stretching vibration of -OH groups occurred at the peak of 3427 cm<sup>-1</sup>. Another peak at around 2350 cm<sup>-1</sup> was observed for FeAC13 and FeAC01 samples which possess huge amount of activated carbon. The peak indicated the alkynes groups formed as the result of liberating light volatile matters such as hydrogen group during calcination process (Azmi, et al., 2015).

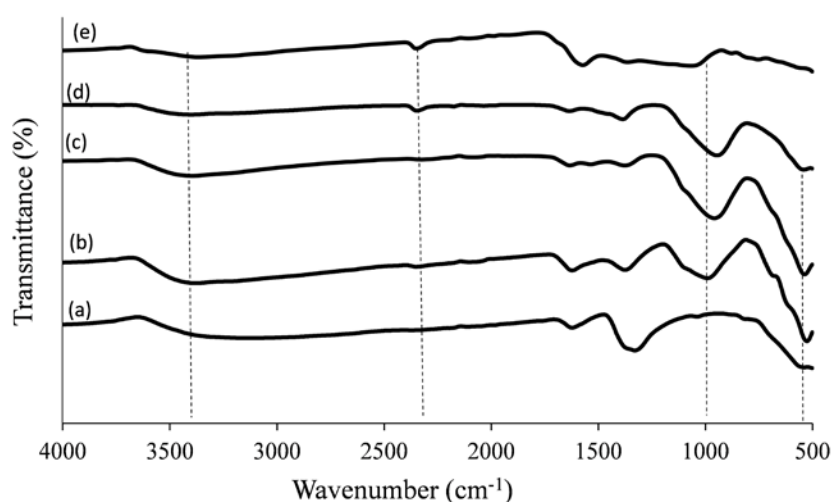


Figure 4.2: FTIR Results for (a) Fe<sub>3</sub>O<sub>4</sub>, (b) FeAC31, (c) FeAC11, (d) FeAC13, (e) AC

Besides, a peak observed at about  $1087\text{ cm}^{-1}$  for AC, FeAC11, FeAC13, and FeAC31 composite samples was attributed by C-O-C stretching due to the presence of C and O elements in activated carbon (Pan, et al., 2013). Tao, et al. (2015) also reported that the peak at around  $1040\text{ cm}^{-1}$  was ascribed by C-OH stretching which involving the elements of C and O. On the other hand,  $\text{Fe}_3\text{O}_4$ , FeAC11, FeAC13 and FeAC31 which consists of iron precursor showed a peak at approximately  $560\text{ cm}^{-1}$ . The peak could be ascribed by the stretching of Fe-O (Yang, et al., 2018). Rattanachueskul, et al. (2017) reported similar spectrum with the appearance of the peak at  $600\text{-}670\text{ cm}^{-1}$  indicated the presence of  $\text{Fe}_3\text{O}_4$  particle. Meanwhile, Li, et al. (2018) reported that the peak at about  $570\text{ cm}^{-1}$  represented the Fe-O vibration in the bulk  $\text{Fe}_3\text{O}_4$ .

#### 4.1.3 SEM-EDX Results

The surface morphology of the synthesised  $\text{Fe}_3\text{O}_4$ , AC and  $\text{Fe}_3\text{O}_4/\text{AC}$  at discrepant weight ratios were studied by utilising SEM as depicted in Figure 4.3. It was observable that  $\text{Fe}_3\text{O}_4$  displayed fine particle structures with irregular shape (Figure 4.3 (a)). As reported by Liu, et al. (2018b), the synthesised  $\text{Fe}_3\text{O}_4$  particles were present in irregular shape and consisted a combination of circular and square particles. Similar findings were obtained in this study.

Figure 4.3 (e) shows that the surface morphology of activated carbon was appeared as pieces-like in structure. Generally, the structure of sugarcane bagasse activated carbon is akin to plant tissue structures after subjecting to pyrolysis and activation process (Gonçalves, et al., 2015). The sample for FeAC31, FeAC11 and FeAC13 demonstrated a combined surface morphology for both  $\text{Fe}_3\text{O}_4$  and AC samples due to the samples were prepared by varying the weight ratio between Fe and activated carbon. FeAC11 with 1 to 1 weight ratio between Fe and activated carbon was identified to have similar amount of particle and pieces like structure as demonstrated in Figure 4.3 (c). On the other hand, Figure 4.3 (d) illustrates a large portion of pieces-like structure whereas Figure 4.3 (b) depicts the sample was occupied mostly by irregular shape particle. For the FeAC31 composite sample, the  $\text{Fe}_3\text{O}_4$  particles tend to be aggregated on the surface of AC, hence, majority of particles could be observed. On the other hand, FeAC13 illustrated the pieces-like

structure as the majority portion due to high proportion of activated carbon to Fe (Oh, Kim and Kim, 2015).

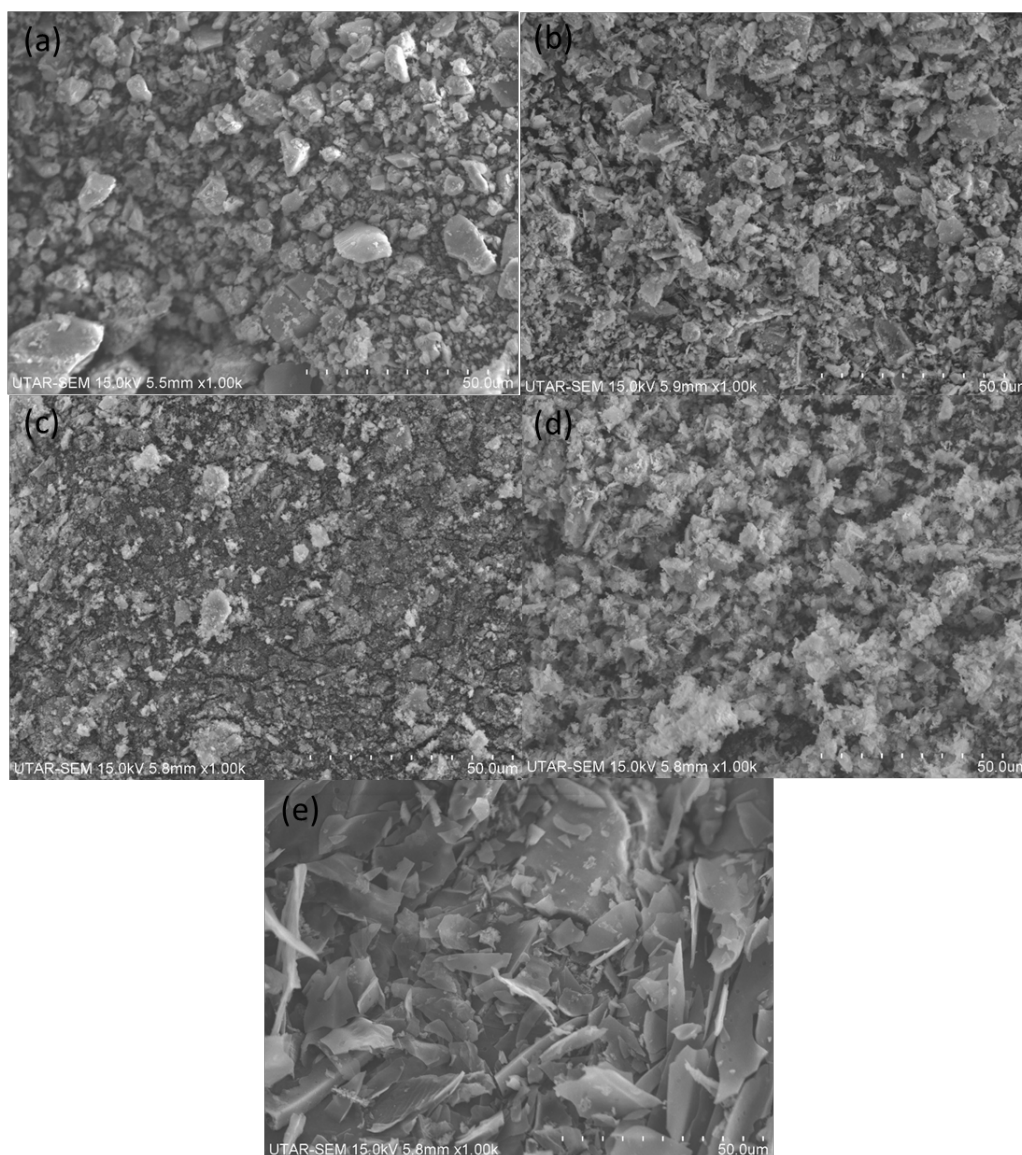


Figure 4.3: SEM Images of (a)  $\text{Fe}_3\text{O}_4$ , (b) FeAC31, (c) FeAC11, (d) FeAC13, (e) AC

With the coupled of EDX instrument, the elemental composition of synthesised  $\text{Fe}_3\text{O}_4$ , AC,  $\text{Fe}_3\text{O}_4/\text{AC}$  at different weight ratios were identified and illustrated in Table 4.1. The results show that the  $\text{Fe}_3\text{O}_4$  consisted the atomic percent ratio of approximately 3 to 4 for Fe to O elements. Therefore, the formation of  $\text{Fe}_3\text{O}_4$  was supported. It could be noticed that the amount of Fe was decreasing when increasing the amount of AC in the composite sample. Similarly, the C atomic

percent was detected to be higher upon increasing the amount of activated carbon in the composite sample.

Table 4.1: Atomic Percent for Synthesised Fe<sub>3</sub>O<sub>4</sub>, AC and Fe<sub>3</sub>O<sub>4</sub>/AC at Various Weight Ratios

Catalysts	Atomic Percent (At%)			
	C	O	K	Fe
Fe <sub>3</sub> O <sub>4</sub>	-	57.40	4.55	38.05
FeAC31	10.10	53.73	6.52	29.66
FeAC11	19.46	54.06	7.34	19.14
FeAC13	25.14	54.50	11.70	8.65
AC	78.53	19.55	1.92	-

#### 4.2 Catalytic Activities for Fe<sub>3</sub>O<sub>4</sub>, AC and Fe<sub>3</sub>O<sub>4</sub>/AC at Various Weight Ratios

The effect of various catalysts such as Fe<sub>3</sub>O<sub>4</sub>, AC and Fe<sub>3</sub>O<sub>4</sub>/AC at different weight ratios (3:1, 1:1, 1:3) on the heterogeneous photo Fenton and Fenton-like degradation of malachite green were studied and shown in Figure 4.4. It was observable that with the use of AC as catalyst, the degradation efficiency was only at 18.43 %, which is lower than Fe deposited composites. AC which utilised adsorption reaction to degrade the dye had lower degradation efficiency than Fe based catalyst which used heterogeneous photo Fenton and Fenton-like degradation (Fontecha-Cámara, et al., 2011). Similar findings was reported by (Liu, et al., 2017c), where the Fe based catalyst had higher degradation efficiency of phenol than pure AC catalyst.

As depicted in Figure 4.4, Fe<sub>3</sub>O<sub>4</sub> sample illustrated lower degradation efficiency of malachite green than FeAC13, FeAC31 and FeAC11. The degradation efficiency of malachite green for Fe<sub>3</sub>O<sub>4</sub>, FeAC13, FeAC31 and FeAC11 was 30.26, 73.00, 76.33 and 86.84 % respectively. It was anticipated that a combination of adsorption and heterogeneous photo Fenton and Fenton-like degradation was happened for the composite samples constitute both Fe<sub>3</sub>O<sub>4</sub> and activated carbon, leading to a higher degradation efficiency for malachite green. Among three different mixing ratios of Fe<sub>3</sub>O<sub>4</sub> to AC, FeAC13 showed a lower degradation efficiency than FeAC11 and FeAC31. It was deduced that AC was not evenly occupied by Fe<sub>3</sub>O<sub>4</sub>

due to the excessive amount of AC present in FeAC13. Messele, et al., (2012) reported that lower Fe/AC weight percent led to a decrease of phenol removal rate.

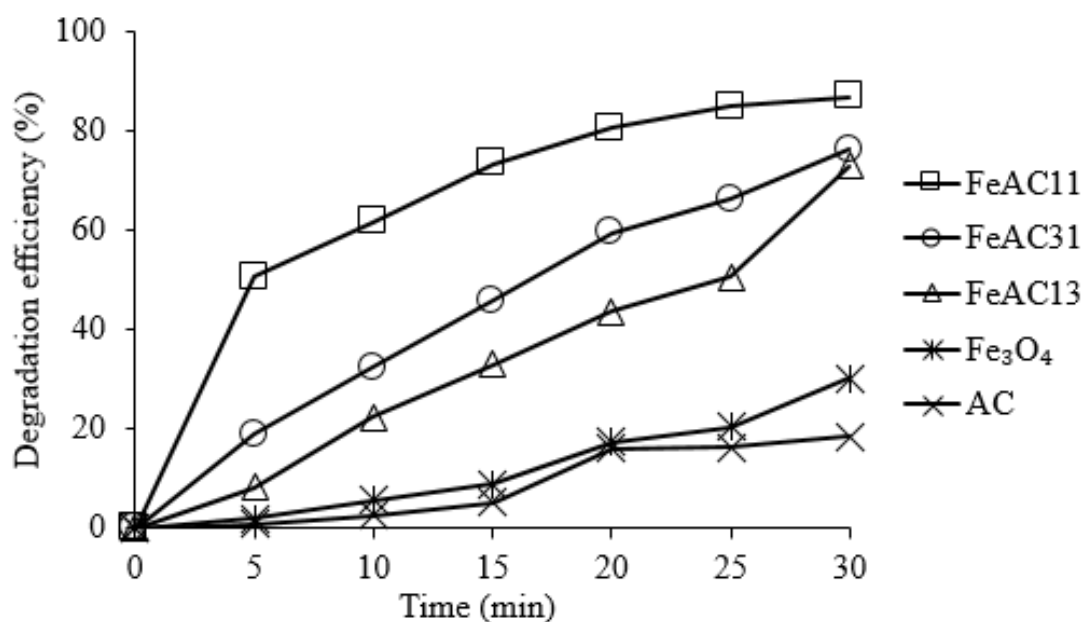


Figure 4.4: Heterogeneous Photo Fenton and Fenton-like Degradation Efficiency of Malachite Green in the Presence of Various Types of Catalysts (Catalyst Dosage = 1 g/L, Initial Dye Concentration = 30 ppm, Solution Temperature = 25 °C, pH =7, Reaction Time = 30 min)

On the other hand, FeAC31 demonstrated a lower degradation efficiency as compared to FeAC11. This could be attributed by the excessive amount of Fe<sub>3</sub>O<sub>4</sub> in the composite sample, causing the blockage of microporous sites of the activated carbon (Oh, Kim and Kim, 2015). The same situation was reported by Li, et al. (2008) when using TiO<sub>2</sub> deposited on activated carbon catalyst, where the degradation efficiency raised as the result of increasing the TiO<sub>2</sub> content up to a certain extend before falling to a lower degradation efficiency upon using excessive amount of TiO<sub>2</sub>. In short, FeAC11 composite sample with the optimal weight ratio possess the highest degradation activity.

### 4.3 Parameter Studies

#### 4.3.1 Effect of Organic Dye Concentration

The relationship between the malachite green concentration (30, 50, 70, 90 and 110 ppm) and the heterogeneous photo Fenton and Fenton-like degradation efficiency

was investigated. The results obtained were illustrated in Figure 4.5. It is notable that the degradation efficiency is in a dropping trend upon raising the concentration of organic dyes. The degradation efficiency was reduced from 86.84 to 61.23 % when the concentration of dyes used increased from 30 to 110 ppm. This could be attributed to the amount of reactive radicals such as  $\bullet\text{OH}$  radicals remain constant while the concentration of dyes had been risen. As the consequence, the number of available  $\bullet\text{OH}$  radicals not sufficient to degrade the higher amount of organic dyes, leading to a decrement in degradation efficiency (Akerdi, et al., 2017). Furthermore, the active sites available on the catalyst might be saturated by the excessive amount of organic dyes, retrenching the formation of  $\bullet\text{OH}$  radicals (Babuponnusami and Muthukumar, 2012). In a nutshell, malachite green with 30 ppm showed the highest degradation efficiency among other concentrations.

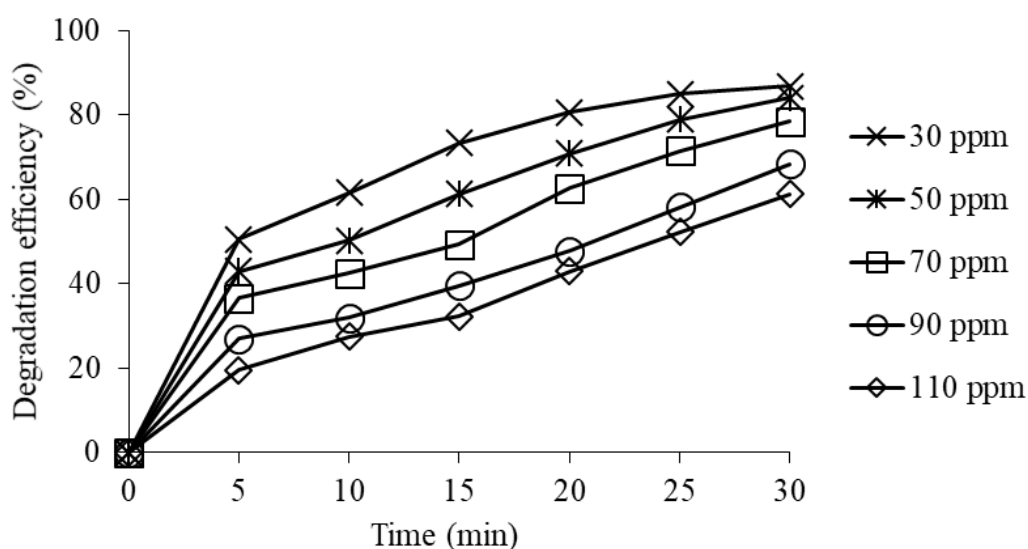


Figure 4.5: Effect of Malachite Green Concentration on the Heterogeneous Photo Fenton and Fenton-like Degradation Efficiency of Malachite Green (FeAC11 Dosage = 1 g/L, Solution Temperature = 25 °C, pH = 7, Reaction Time = 30 min)

Hassani, et al. (2018) reported that degradation of acid orange 7 also experienced the similar decreasing trend where the degradation efficiency reduced from 92.11 to 79.45 % upon increasing the concentration from 5 to 30 ppm. In addition, Peternel, et al. (2007) reported that degradation of reactive red 45 was also encountered a plunge in degradation efficiency from 98.3 to 65.5 % by escalating the concentration of dyes from 20 to 120 ppm. They claimed that the amount of dyes

adsorbed on the catalyst surface was deduced to raise in fold and led to a lower light absorption by the catalyst.

### 4.3.2 Effect of Catalyst Dosage

The effect of catalyst dosage (0, 0.2, 0.4, 0.6, 0.8, 1.0 and 1.2 g/L) on the heterogeneous photo Fenton and Fenton-like degradation of malachite green was studied. The results were depicted in Figure 4.6. The degradation efficiency of malachite green was only 1.9 % in the absence of FeAC11 composite sample. There was only photolysis taking place without any catalyst, hence, a very low degradation efficiency was obtained. Cardoso, Bessegato and Boldrin Zanoni (2016) reported the same outcome where the photolysis degradation efficiency of dyes was much lower as compare to photocatalysis and photoelectrocatalysis.

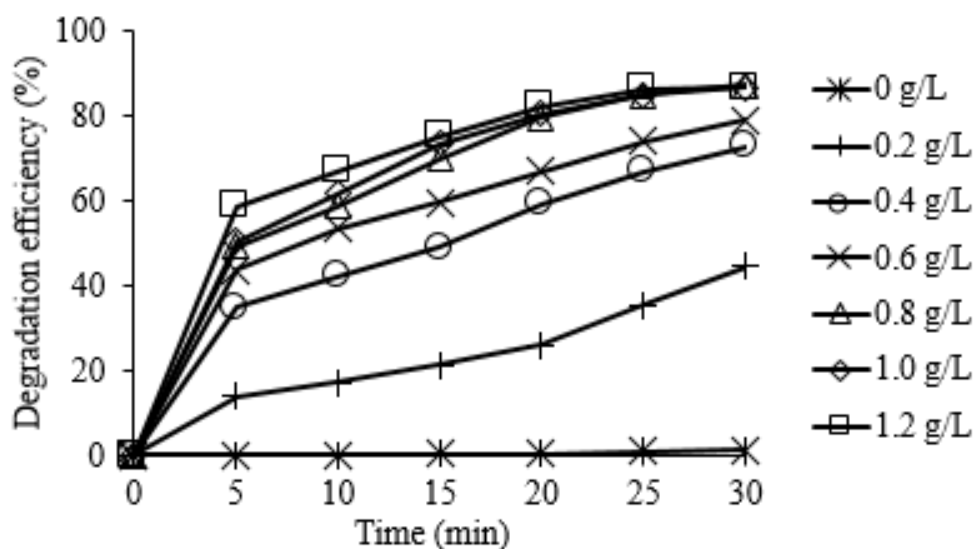


Figure 4.6: Effect of Catalyst Dosage on the Heterogeneous Photo Fenton and Fenton-like Degradation Efficiency of Malachite Green (Dyes Concentration = 30 ppm, Solution Temperature = 25 °C, pH = 7, Reaction Time = 30 min)

The degradation efficiency was raised from around 44.47 % up to a stagnant level at approximately 87 % with the increase of catalyst dosage from 0.2 to 0.8 g/L. A greater amount of active sites were available on the catalyst surface upon increasing the catalyst dosage. Besides, the generation of hydroxyl radical was enhanced with increasing the active sites. These factors accelerated the degradation process and improved the overall degradation efficiency (Wan and Wang, 2017).

Similar trend was reported by Liu, et al. (2017b), where the degradation efficiency of methyl orange was rocketed to 98 % upon raising the catalyst dosage from 0.1 to 0.4 g/L.

Nonetheless, the degradation efficiency experienced a small drop from 87.39 to 86.84 and 86.83 % if further increasing the catalyst dosage from 0.8 to 1.0 and 1.2 g/L respectively. Excessive amount of catalyst might inhibit the light penetration in the dye solution. This decreased the number of photons and subsequently generated lesser amount of  $\bullet\text{OH}$  radicals (Yu, et al., 2016). Liao, Sun and Gao (2009) also reported that abundant dosage of catalyst led to the decrement of the degradation process. Hence, the optimal catalyst dosage was at 0.8 g/L as it generated the highest degradation efficiency.

#### 4.3.3 Effect of Solution pH

The effect of solution pH on the heterogeneous photo Fenton and Fenton-like degradation of malachite green was identified. The solution pH value was varied in the range of pH 1, 3, 5, 7 and 9 with the aid of 0.1 M NaOH and 0.1 M HCl. The outcome of the experiment was illustrated in Figure 4.7. The degradation efficiency was enhanced dramatically from 34.03 to 88.43 % when adjusting the pH from 1 to 5 before a plateau point reached at 88 % upon further increasing the pH to 7 and 9.

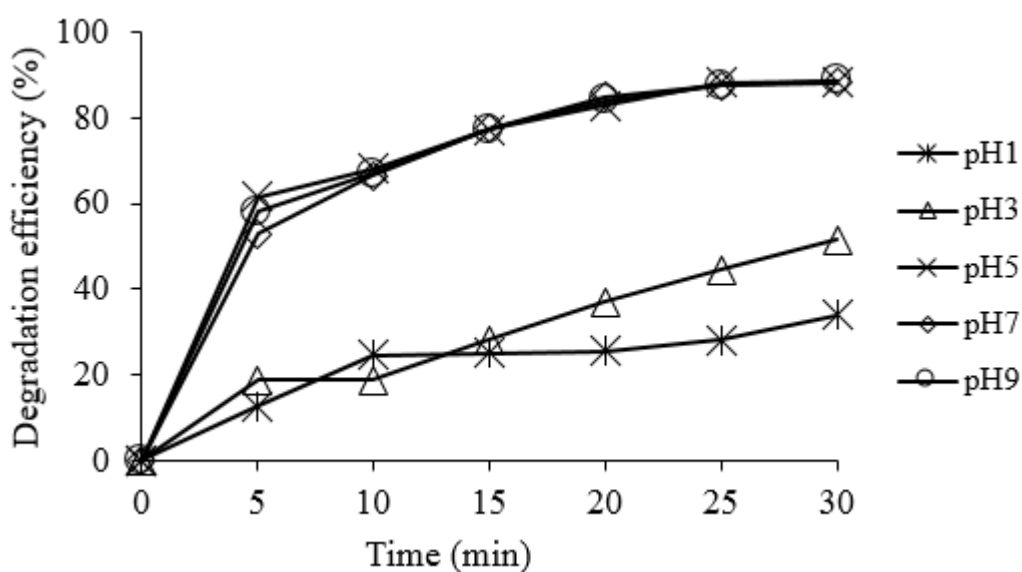


Figure 4.7: Effect of pH Solution on the Heterogeneous Photo Fenton and Fenton-like Degradation Efficiency of Malachite Green (Dyes Concentration = 30 ppm, FeAC11 Dosage = 0.8 g/L, Solution Temperature = 25 °C, Reaction Time = 30 min)



The lowest degradation efficiency at pH 1 was ascribed by the weak interaction between malachite green and catalyst surface in acidic environment. Malachite green is a cationic dye which might experience a repulsive force with the positively charged catalyst surface as the result of protonation effect. In addition, there could be a competition between positively charged ions such as  $H^+$  and dye molecules for the same binding site on the catalyst surface in acidic solution (Chowdhury and Saha, 2011). As discussed by Samiey and Toosi (2010), low amount of malachite green adsorbed on the positively charged catalyst surface due to the occurrence of  $H^+$  ions that would compete for the active site on the catalyst. The improvement in performance at higher solution pH value was mostly because of the different charges between organic dyes and catalyst surface. When the solution was approaching neutral or alkaline condition, the surface of the catalyst tends to be more negatively charged due to the accumulation of  $OH^-$  ions produced at high pH condition. Subsequently, a strong electrostatic force formed between the  $OH^-$  ions on the catalyst surface and the cationic dyes which led to a better degradation efficiency. In addition, slightly alkali condition was favourable for the generation of  $\bullet OH$  radicals (Nirmaladevi, Makeswari and Santhi, 2018). Similar trend was reported by Chowdhury and Saha (2011), where the degradation efficiency increased from pH 2 to around pH 6 before levelling out at higher pH value.

#### **4.3.4 Effect of $H_2O_2$ Dosage**

The effect of  $H_2O_2$  dosage (0, 1, 2, 3, 4, 5 and 6 mM) on heterogeneous photo Fenton and Fenton-like degradation efficiency of malachite green was analysed and shown in Figure 4.8. It was notable that the degradation efficiency was increased from 14.53 to 89.22 % when increasing the  $H_2O_2$  dosage from 0 to 4 mM, respectively. The degradation efficiency was enhanced with larger amount of  $H_2O_2$  supplied due to the growing amount of  $\bullet OH$  radicals produced (Lin, et al., 2014). Wu, et al. (2015) acquired the similar upward trend where the degradation efficiency raised when the  $H_2O_2$  dosage was increased from 5 to 7.4 mM as the result of escalating the number of  $\bullet OH$  radicals produced.

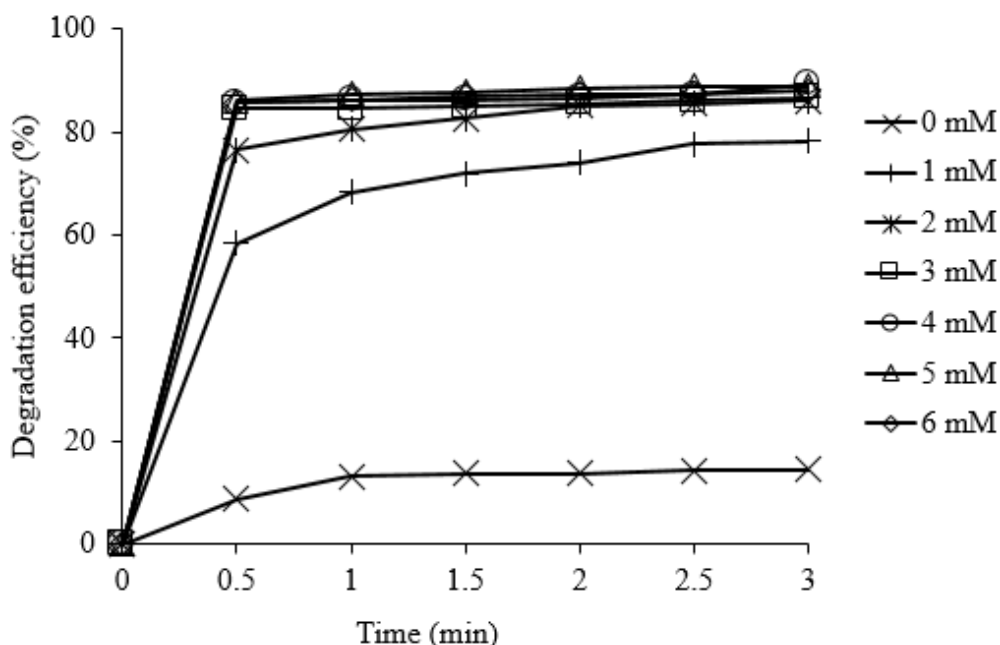


Figure 4.8: Effect of  $\text{H}_2\text{O}_2$  Dosage on the Heterogeneous Photo Fenton and Fenton-like Degradation Efficiency of Malachite Green (Dyes Concentration = 30 ppm, FeAC11 Dosage = 0.8 g/L, pH = 5, Solution Temperature = 25 °C, Reaction Time = 3 min)

Degradation efficiency was dropped slightly to 88.85 and 87.96 % upon increment of  $\text{H}_2\text{O}_2$  dosage to 5 and 6 mM, respectively. This indicated that the increment of degradation efficiency was halted when exceeding 4 mM of  $\text{H}_2\text{O}_2$ . This situation could be explained by the scavenging effect of excessive  $\text{H}_2\text{O}_2$  that could led to the production of  $\text{HO}_2\cdot$  radicals, which had lower reactivity than  $\cdot\text{OH}$  radicals. Pouran, et al. (2018) reported that the availability of  $\cdot\text{OH}$  radicals declined with excessive amount of  $\text{H}_2\text{O}_2$ , reducing the overall degradation efficiency. According to the study conducted by Zheng, et al. (2017), resembling scenario was encountered where the degradation efficiency raised upon increasing the dosage of  $\text{H}_2\text{O}_2$  from 1500 to 2000 mg/L before a deceleration at the dosage above 3000 mg/L.

#### 4.4 Kinetic Study

Kinetic studies were conducted on the basis of the degradation of malachite green in order to identify the order of reaction for heterogeneous photo Fenton and Fenton-like degradation of malachite green. The graph for pseudo zero, first and second orders were plotted for the experimental data obtained using malachite green at an

initial concentration of 30 ppm with various pH value. Since  $\bullet\text{OH}$  radicals are the main oxidants serve to degrade the organic matter in heterogeneous photo Fenton and Fenton-like processes, the reaction kinetics on the degradation of malachite green is depicted as Equation (4.1).

$$-\frac{dC_{MG}}{dt} = kC_{MG}^m C_{\bullet OH}^n \quad (4.1)$$

where

$C_{MG}$  = concentration of malachite green at time t, ppm

$C_{\bullet OH}$  = concentration of hydroxyl radicals at time t, ppm

$m$  = reaction order with respect to malachite green

$n$  = reaction order with respect to hydroxyl radicals

$t$  = reaction time, min

$k$  = reaction rate constant

It is arduous to measure and consider the hydroxyl radicals as a constant value at certain time as its life time is relative short (around 2.7  $\mu\text{s}$ ) (Wu, et al., 2018). Hence, Equation (4.1) can be modified in the form as Equation (4.2).

$$-\frac{dC_{MG}}{dt} = k_{app}C_{MG}^m \quad (4.2)$$

where

$k_{app}$  = apparent reaction rate constant

In this study, pseudo second-order was fitted well for all the data. Similar result was reported by Wu, et al. (2015), where heterogeneous Fenton-like degradation of malachite green by using iron-based nanoparticles fitted well to pseudo second-order model. Since the reaction was well fitted to pseudo second-order,  $m$  is equal to 2. By integrating Equation (4.2), the equation relating the concentration of malachite green to the reaction time can be modified to Equation (4.3).

$$\frac{1}{C_t} - \frac{1}{C_o} = k_{app}t \quad (4.3)$$

where

$C_o$  = concentration of malachite green (ppm) at time,  $t = 0$

$C_t$  = concentration of malachite green (ppm) at certain time,  $t$

In Figure 4.9, the plot of  $(1/C_t - 1/C_o)$  vs  $t$  for five different solution pH values. Linear relationship for the rate constant and time was identified from the plot. This indicated that heterogeneous photo Fenton and Fenton-like degradation of malachite green at different solution pH value was obeyed pseudo second-order reaction. The rate constants and the corresponding correlation coefficients at different solution pH values were calculated and summarised in Table 4.2.

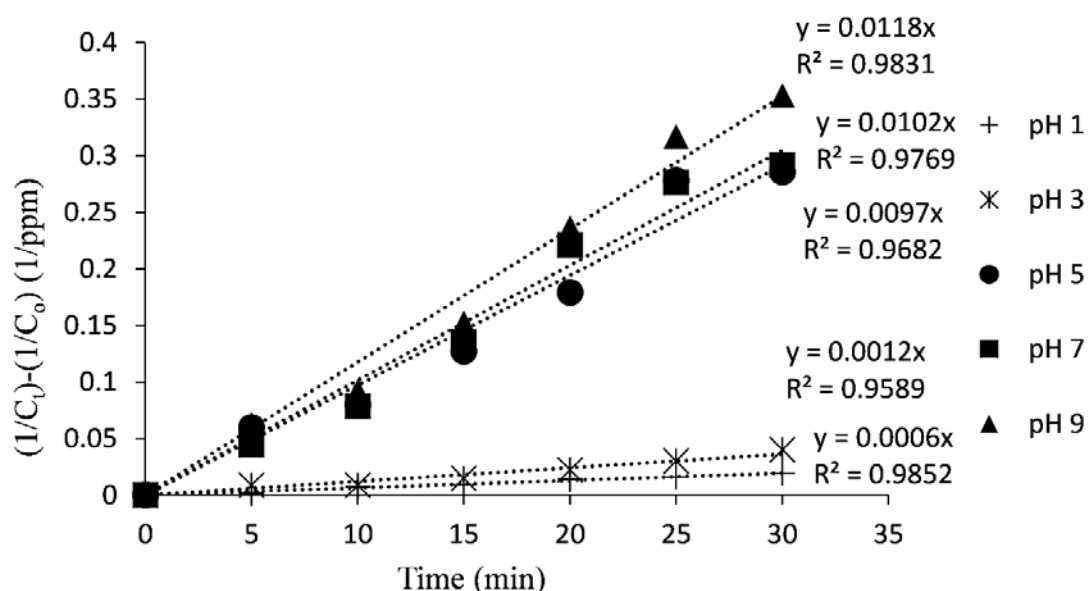


Figure 4.9: Pseudo Second-order Reaction Kinetics Plot for Heterogeneous Photo Fenton and Fenton-like Degradation of Malachite Green at Different Solution pH Values

Table 4.2: Rate Coefficients for Heterogeneous Photo Fenton and Fenton-like Degradation of Malachite Green by FeAC11 at Different Solution pH Values

pH Value	Pseudo Zero-order		Pseudo First-order		Pseudo Second-order	
	$R^2$	$k_{app}$ (ppm/min)	$R^2$	$k_{app}$ (min <sup>-1</sup> )	$R^2$	$k_{app}$ (ppm·min) <sup>-1</sup>
1	0.9678	0.3280	0.9812	0.0145	0.9852	0.0006
3	0.9446	0.4793	0.9744	0.0236	0.9589	0.0012
5	0.3974	0.8406	0.8844	0.0839	0.9682	0.0097
7	0.4647	0.9629	0.8722	0.0841	0.9769	0.0102
9	0.3298	1.0180	0.8364	0.0842	0.9831	0.0118

Table 4.2 indicates that pseudo second-order was well fitted due to the highest determination of coefficient ( $R^2 > 0.95$ ) could be obtained when pseudo second-order was applied. This signifies that the reaction kinetic of malachite green onto FeAC11 was well followed pseudo second-order kinetic model. Hence, the slope of the straight line was equivalent to the apparent reaction rate constant ( $k_{app}$ ). It was noticed that the  $k_{app}$  value raised from 0.0006 to 0.0118 ppm<sup>-1</sup>·min<sup>-1</sup> with the increase of pH value from pH 1 to 9. This could be attributed by the presence of excess amount of H<sup>+</sup> ions under acidic environment, creating a repulsive force between cationic dye molecules (malachite green) and the positively charged on the catalyst. On the contrary, a strong electrostatic interaction occurred in alkali environment as there would be more OH<sup>-</sup> ions appeared, enhancing the adsorption capacity between cationic malachite green and negatively charged FeAC11 (Hosseinzadeh and Ramin, 2018). The resemblance result was reported by Magdalane, et al. (2017), where increased of solution pH would enhance the degradation efficiency of malachite green.

#### 4.5 ICP-OES Results

To ensure the catalyst function consistently for a long period, stability of a catalyst is desirable. The degradation efficiency of the catalyst might be reduced as the result of leaching. It was reported that the degradation efficiency of phenol dropped from 99.96 % to 88.3 % after 3 repetitive runs and the situation could be

attributed by leaching of metal from the catalyst (Liu, et al., 2018a). Thus, it is important to study the stability of catalysts with the aid of ICP-OES where the concentration of dissolved iron in the final solution after 3 min reaction under optimum condition (Carrasco-Díaz, et al., 2016). Department of Environment had stipulated the acceptable condition for discharge of industrial effluent of Standard B in which the maximum allowable concentration of Fe is below 5 mg/L (Department of Environment, 2010).

The concentration of leached iron detected in the final solution on heterogeneous photo Fenton and Fenton-like degradation of malachite green was plotted in Figure 4.10. Based on ICP results, the concentration of leached iron in the final solution was 4 mg/L. The concentration of leached iron could be considered relatively low as the values were in the acceptable range for discharge of iron (less than 5 mg/L).

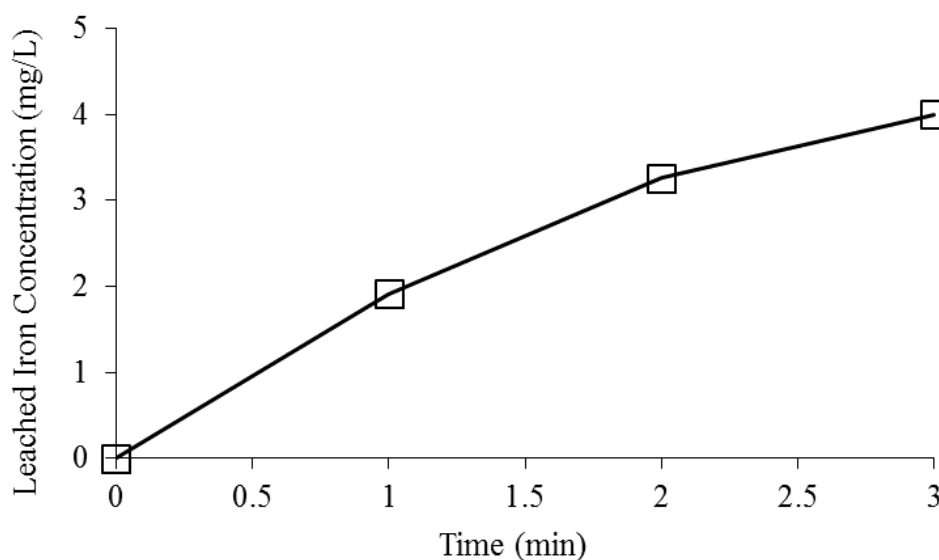


Figure 4.10: Leached Iron Concentration on the Heterogeneous Photo Fenton and Fenton-like Degradation of Malachite Green under Optimal Condition (Dyes Concentration = 30 ppm, FeAC11 Dosage = 0.8 g/L, pH = 5, Solution Temperature = 25 °C, Reaction Time = 3 min)

It was reported that the leaching of metal ions from the catalyst would reduce with an increase in solution pH value. The metal ions in the solution was inactivate because of hydrolysis and precipitation at higher solution pH value (Wang, et al.,

2016). Singh, Rekha and Chand (2016) had reported that the amount of leached copper dropped from 13.85 to 2.73 mg/L upon increasing the pH from 5 to 9. Besides the pH of solution, the concentration of leached metal is subjected to the chemical structure of the catalyst. It was found that the leaching of Fe could reached as high as 7.1 mg/L upon depositing on ligands and as low as 0.1 mg/L when impregnated on cobalt oxide nanocages.

## CHAPTER 5

### CONCLUSIONS AND RECOMMENDATIONS

#### 5.1 Conclusions

In this study, the  $\text{Fe}_3\text{O}_4$ , AC and  $\text{Fe}_3\text{O}_4/\text{AC}$  composite samples at various weight ratios were prepared by chemical impregnation of  $\text{Fe}_3\text{O}_4$  onto AC, followed by calcination under inert environment at  $550\text{ }^\circ\text{C}$  for 2 hours. The synthesised samples were then characterised by using SEM-EDX, XRD and FTIR. SEM depicted that  $\text{Fe}_3\text{O}_4$  was irregular particles whilst the AC was pieces-like in structure.  $\text{Fe}_3\text{O}_4/\text{AC}$  composite samples at various weight ratios showed a combination of irregular shapes and pieces-like structure. EDX demonstrated that the amount of Fe and C elements increased upon raising the weight ratio of  $\text{Fe}_3\text{O}_4$  and AC in the composite sample. In addition, the atomic ratio of Fe and O for  $\text{Fe}_3\text{O}_4$  was approximately 3 to 4. On the other hand, FTIR analysis indicated that several functional groups such as O-H,  $\text{C}\equiv\text{C}$  and C-O-C bonding present in AC sample. Furthermore, Fe-O stretching at  $570\text{ cm}^{-1}$  indicated the presence of  $\text{Fe}_3\text{O}_4$ . Among the composite samples synthesised, FeAC11 showed the highest degradation activity due to its appropriate amount of  $\text{Fe}_3\text{O}_4$  present in the AC and caused less blockage of active site.

The effect of different parameters such as malachite green concentration (30, 50, 70, 90 and 110 ppm), catalyst dosage (0, 0.2, 0.4, 0.6, 0.8, 1.0 and 1.2 g/L), solution pH (pH 1, 3, 5, 7 and 9) and  $\text{H}_2\text{O}_2$  dosage (0, 1, 2, 3, 4, 5 and 6 mM) for heterogeneous photo Fenton and Fenton-like degradation were investigated to identify the optimum condition. The optimum conditions for degrading malachite green were acquired at initial dye concentration of 30 ppm, FeAC11 dosage of 0.8 g/L, pH 5,  $\text{H}_2\text{O}_2$  dosage of 4 mM with the degradation efficiency of 89.22 % after 3 min of reaction time.

Besides, ICP-OES results demonstrated that the synthesised composite sample had high stability as only small amount of leached iron (about 4 mg/L) detected in the treated solution. The reaction kinetics of heterogeneous photo Fenton and Fenton-like degradation of malachite green at various solution pH (pH 1, 3, 5, 7 and 9) were followed pseudo second-order kinetics.



## **5.2 Recommendations for Future Study**

Other than SEM-EDX, FTIR and XRD analysis, the synthesised composite samples should also be characterised by thermogravimetric analysis (TGA) and Brunauer-Emmett-Teller (BET) surface analysis. TGA could be used to further identify the weight loss at different temperatures. Besides, the thermal stability of the composite samples is able to be identified with the aid of TGA analysis (Sohni, et al., 2018).

On the other hand, BET surface analysis enables the specific surface area and porosity of synthesised composite samples to be determined. Specific surface area is a crucial property for synthesised composite samples since it will affect the catalytic activity of heterogeneous photo Fenton and Fenton-like degradation on organic dye.

## REFERENCES

- Adegoke, K. A. and Bello, O. S., 2015. Dye sequestration using agricultural wastes as adsorbents. *Water Resources and Industry*, 12, pp. 8–24.
- Afroz, R. and Rahman, A., 2017. Health impact of river water pollution in Malaysia. *International journal of advanced and applied sciences*, 4(5), pp. 78–85.
- Ahmad, A., Buang, A. and Bhat, A. H., 2016. Renewable and sustainable bioenergy production from microalgal co-cultivation with palm oil mill effluent (POME): A review. *Renewable and Sustainable Energy Reviews*, 65, pp. 214–234.
- Ahmad, M., Rajapaksha, A. U., Lim, J. E., M., Bolan, N., Mohan, D., Vithanage, M., Lee, S. S. and Ok, Y. S., 2014. Biochar as a sorbent for contaminant management in soil and water: A review. *Chemosphere*, 99, pp. 19–23.
- Akerdi, A. G., Es'Haghzade, Z., Bahrami, S. H. and Arami, M., 2017. Comparative study of GO and reduced GO coated graphite electrodes for decolorization of acidic and basic dyes from aqueous solutions through heterogeneous electro-Fenton process. *Journal of Environmental Chemical Engineering*, 5(3), pp. 2313–2324.
- Almazán-Sánchez, P. T., Linares-Hernández, I., Martínez-Miranda, V., Lugo-Lugo, V. and Guadalupe Fonseca-Montes De Oca, R. M., 2014. Wastewater treatment of methyl methacrylate (MMA) by Fenton's reagent and adsorption. *Catalysis Today*, 220–222, pp. 39–48.
- Araujo, F. V. F., Yokoyama, L., Teixeira, L. A. C. and Campos, J. C., 2011. Heterogeneous Fenton process using the mineral hematite for the discoloration of a reactive dye solution. *Brazilian Journal of Chemical Engineering*, 28(4), pp. 605–616.
- Arimi, M. M., 2017. Modified natural zeolite as heterogeneous Fenton catalyst in treatment of recalcitrants in industrial effluent. *Progress in Natural Science: Materials International*, 27(2), pp. 275–282.
- Ariyanti, D., Maillot, M. and Gao, W., 2018. Photo-assisted degradation of dyes in a binary system using TiO<sub>2</sub> under simulated solar radiation. *Journal of Environmental Chemical Engineering*, 6(1), pp. 539–548.
- Azmi, N. B., Bashir, M. J. K., Sethupathi, S., Wei, L. J. and Aun, N. C., 2015. Stabilized landfill leachate treatment by sugarcane bagasse derived activated carbon for removal of color, COD and NH<sub>3</sub> - N - Optimization of preparation conditions by RSM. *Journal of Environmental Chemical Engineering*, 3(2), pp. 1287–1294.
- Babuponnusami, A. and Muthukumar, K., 2014. A review on Fenton and improvements to the Fenton process for wastewater treatment. *Journal of Environmental Chemical Engineering*, 2(1), pp. 557–572.

- Babuponnusami, A. and Muthukumar, K., 2012. Removal of phenol by heterogenous photo electro Fenton-like process using nano-zero valent iron. *Separation and Purification Technology*, 98, pp. 130–135.
- Balbuena, J., Cruz-Yusta, M., Pastor, A. and Sánchez, L., 2018.  $\alpha$ -Fe<sub>2</sub>O<sub>3</sub>/SiO<sub>2</sub> composites for the enhanced photocatalytic NO oxidation. *Journal of Alloys and Compounds*, 735(2), pp. 1553–1561.
- Bamdad, H., Hawboldt, K. and Macquarrie, S., 2018. A review on common adsorbents for acid gases removal: Focus on biochar. *Renewable and Sustainable Energy Reviews*, 81, pp. 1705–1720.
- Barbieri, L., Andreola, F., Lancellotti, I. and Taurino, R., 2013. Management of agricultural biomass wastes: Preliminary study on characterization and valorisation in clay matrix bricks. *Waste Management*, 33(11), pp. 2307–2315.
- Bethi, B., Sonawane, S. H., Bhanvase, B. A. and Gumfekar, S. P., 2016. Nanomaterials-based advanced oxidation processes for wastewater treatment: A review. *Chemical Engineering and Processing: Process Intensification*, 109, pp. 178–189.
- Bokare, A. D. and Choi, W., 2014. Review of iron-free Fenton-like systems for activating H<sub>2</sub>O<sub>2</sub> in advanced oxidation processes. *Journal of Hazardous Materials*, 275, pp. 121–135.
- Bunaciu, A. A., Udriștioiu, E. G. and Aboul-Enein, H. Y., 2015. X-Ray diffraction: Instrumentation and applications. *Critical Reviews in Analytical Chemistry*, 45(4), pp. 289–299.
- Cao, X., Sun, S. and Sun, R., 2017. Application of biochar-based catalysts in biomass upgrading: A review. *Royal Society of Chemistry*, 7(77), pp. 48793–48805.
- Cao, Z., Qin, M., Gu, Y., Jia, B., Chen, P. and Qu, X., 2016. Synthesis and characterization of Sn-doped hematite as visible light photocatalyst. *Materials Research Bulletin*, 77, pp. 41–47.
- Cardoso, J. C., Bessegato, G. G. and Boldrin Zanoni, M. V., 2016. Efficiency comparison of ozonation, photolysis, photocatalysis and photoelectrocatalysis methods in real textile wastewater decolorization. *Water Research*, 98, pp. 39–46.
- Carrasco-Díaz, M. R., Castillejos-López, E., Cerpa-Naranjo, A. and Rojas-Cervantes, M. L., 2016. Efficient removal of paracetamol using LaCu<sub>1-x</sub>M<sub>x</sub>O<sub>3</sub> (M = Mn, Ti) perovskites as heterogeneous Fenton-like catalysts. *Chemical Engineering Journal*, 304, pp. 408–418.
- Cha, J. S., Park, S. H., Jung, S. C., Ryu, C., Jeon, J. K., Shin, M. C. and Park, Y. K., 2016. Production and utilization of biochar: A review. *Journal of Industrial and Engineering Chemistry*, 40, pp. 1–15.

Chai, S., Bai, X., Li, J., Liu, C., Ding, T., Tian, Y., Liu, C., Xian, H., Mi, W. and Li, X., 2017. Effect of phase interaction on catalytic CO oxidation over the SnO<sub>2</sub>/Al<sub>2</sub>O<sub>3</sub> model catalyst. *Applied Surface Science*, 402, pp. 12–20.

Chan, N. W., 2012. Managing urban rivers and water quality in Malaysia for sustainable water resources. *International Journal of Water Resources Development*, 28(2), pp. 343–354.

Chen, J., Liu, S., Yan, J., Wen, J., Hu, Y. and Zhang, W., 2017. Intensive removal efficiency and mechanisms of carbon and ammonium in municipal wastewater treatment plant tail water by ozone oyster shells fix-bed bioreactor - membrane bioreactor combined system. *Ecological Engineering*, 101, pp. 75–83.

Chen, X., Wu, Z., Gao, Z. and Ye, B. C., 2017. Effect of different activated carbon as carrier on the photocatalytic activity of Ag-N-ZnO photocatalyst for methyl orange degradation under visible light irradiation. *Nanomaterials*, 7(9), p. 258.

Chen, Y., Li, N., Zhang, Y. and Zhang, L., 2014. Novel low-cost Fenton-like layered Fe-titanate catalyst: Preparation, characterization and application for degradation of organic colorants. *Journal of Colloid and Interface Science*, 422, pp. 9–15.

Chen, Y., Zhang, X., Chen, W., Yang, H. and Chen, H., 2017. The structure evolution of biochar from biomass pyrolysis and its correlation with gas pollutant adsorption performance. *Bioresource Technology*, 246, pp. 101–109.

Cheng, B. H., Zeng, R. J. and Jiang, H., 2017. Recent developments of post-modification of biochar for electrochemical energy storage. *Bioresource Technology*, 246, pp. 224–233.

Cheng, M., Lai, C., Liu, Y., Zeng, G., Huang, D., Zhang, C., Qin, L., Hu, L., Zhou, C. and Xiong, W., 2018. Metal-organic frameworks for highly efficient heterogeneous Fenton-like catalysis, *Coordination Chemistry Reviews*, 368, pp. 80–92.

Chowdhury, S. and Saha, P., 2011. Adsorption thermodynamics and kinetics of malachite green onto Ca(OH)<sub>2</sub> - Treated Fly Ash. *Journal of Environmental Engineering*, pp. 388–398.

Clarizia, L., Russo, D., Somma, I. Di, Marotta, R. and Andreozzi, R., 2017. Environmental homogeneous photo-Fenton processes at near neutral pH: A review. *Applied Catalysis B: Environmental*, 209, pp. 358–371.

Cruz, A., Couto, L., Esplugas, S. and Sans, C., 2017. Study of the contribution of homogeneous catalysis on heterogeneous Fe(III)/alginate mediated photo-Fenton process. *Chemical Engineering Journal*, 318, pp. 272–280.

Deng, J., Li, M. and Wang, Y., 2016. Biomass-derived carbon: synthesis and applications in energy storage and conversion. *Green Chem*, 18(18), pp. 4824–4854.

Department of Environment, 2010. Environmental requirements: A guide for investors. [online] Available at: <<http://www.doe.gov.my/eia/wp-content/uploads/2012/03/A-Guide-For-Investors1.pdf>> [Accessed 19 August 2018].

Dewil, R., Mantzavinos, D., Poulios, I. and Rodrigo, M. A., 2017. New perspectives for advanced oxidation processes. *Journal of Environmental Management*, 195, pp. 93–99.

Diao, Z. H., Xu, X. R., Jiang, D., Li, G., Liu, J. J., Kong, L. J. and Zuo, L. Z., 2017. Enhanced catalytic degradation of ciprofloxacin with FeS<sub>2</sub>/SiO<sub>2</sub> microspheres as heterogeneous Fenton catalyst: Kinetics, reaction pathways and mechanism. *Journal of Hazardous Materials*, 327, pp. 108–115.

Dias, F. F., Oliveira, A. A. S., Arcanjo, A. P., Moura, F. C. C. and Pacheco, J. G. A., 2016. Residue-based iron catalyst for the degradation of textile dye via heterogeneous photo-Fenton. *Applied Catalysis B: Environmental*, 186, pp. 136–142.

Duarte, F. M., Maldonado-hódar, F. J. and Madeira, L. M., 2013. Influence of the iron precursor in the preparation of heterogeneous Fe/activated carbon Fenton-like catalysts. *Applied Catalysis A: General*, 458, pp. 39–47.

Fang, Z. D., Zhang, K., Liu, J., Fan, J. Y. and Zhao, Z. W., 2017. Fenton-like oxidation of azo dye in aqueous solution using magnetic Fe<sub>3</sub>O<sub>4</sub>-MnO<sub>2</sub> nanocomposites as catalysts. *Water Science and Engineering*, 10(4), pp. 326–333.

Feng, D., Zhang, Y., Zhao, Y., Sun, S. and Gao, J., 2018. Improvement and maintenance of biochar catalytic activity for in-situ biomass tar reforming during pyrolysis and H<sub>2</sub>O/CO<sub>2</sub> gasification. *Fuel Processing Technology*, 172, pp. 106–114.

Fida, H., Zhang, G., Guo, S. and Naeem, A., 2017. Heterogeneous Fenton degradation of organic dyes in batch and fixed bed using La-Fe montmorillonite as catalyst. *Journal of Colloid and Interface Science*, 490, pp. 859–868.

Fischbacher, A., Sonntag, C. Von and Schmidt, T. C., 2017. Hydroxyl radical yields in the Fenton process under various pH, ligand concentrations and hydrogen peroxide/Fe (II) ratios. *Chemosphere*, 182, pp. 738–744.

Fontecha-Cámara, M. A., Álvarez-Merino, M. A., Carrasco-Marín, F., López-Ramón, M. V. and Moreno-Castilla, C., 2011. Heterogeneous and homogeneous Fenton processes using activated carbon for the removal of the herbicide amitrole from water. *Applied Catalysis B: Environmental*, 101, pp. 425–430.

Gao, M., Zhang, D., Li, W., Chang, J., Lin, Q., Xu, D. and Ma, H., 2016. Degradation of methylene blue in a heterogeneous Fenton reaction catalysed by chitosan crosslinked ferrous complex. *Journal of the Taiwan Institute of Chemical Engineers*, 67, pp. 355–361.

Garcia-Segura, S. and Brillas, E., 2017. Applied photoelectrocatalysis on the degradation of organic pollutants in wastewaters. *Journal of Photochemistry and Photobiology C: Photochemistry Reviews*, 31, pp. 1–35.

Godlewska, P., Schmidt, H. P., Ok, Y. S. and Oleszczuk, P., 2017. Biochar for composting improvement and contaminants reduction. A review. *Bioresource Technology*, 246, pp. 193–202.

Gonçalves, G. D. C., Pereira, N. C. and Veit, M. T., 2016. Production of bio-oil and activated carbon from sugarcane bagasse and molasses. *Biomass and Bioenergy*, 85, pp. 178–186.

Gonçalves, S. P. C., Strauss, M., Delite, F. S., Clemente, Z., Castro, V. L. and Martinez, D. S. T., 2015. Activated carbon from pyrolysed sugarcane bagasse: Silver nanoparticle modification and ecotoxicity assessment. *Science of the Total Environment*, 565, pp. 833–840.

Guin, J. P., Bhardwaj, Y. K. and Varshney, L., 2017. Mineralization and biodegradability enhancement of methyl orange dye by an effective advanced oxidation process. *Applied Radiation and Isotopes*, 122, pp. 153–157.

Gupta, R. K., Dubey, M., Kharel, P., Gu, Z. and Fan, Q. H., 2015. Biochar activated by oxygen plasma for supercapacitors. *Journal of Power Sources*, 274, pp. 1300–1305.

Hamid, S. A., Shahadat, M. and Ismail, S., 2017. Development of cost effective bentonite adsorbent coating for the removal of organic pollutant. *Applied Clay Science*, 149, pp. 79–86.

Hassani, A., Çelikdağ, G., Eghbali, P., Sevim, M., Karaca, S. and Metin, Ö., 2018. Heterogeneous sono-Fenton-like process using magnetic cobalt ferrite-reduced graphene oxide (CoFe<sub>2</sub>O<sub>4</sub>-rGO) nanocomposite for the removal of organic dyes from aqueous solution. *Ultrasonics Sonochemistry*, 40, pp. 841–852.

He, D., Chen, Y., Situ, Y., Zhong, L. and Huang, H., 2017. Synthesis of ternary g-C<sub>3</sub>N<sub>4</sub>/Ag/γ-FeOOH photocatalyst: An integrated heterogeneous Fenton-like system for effectively degradation of azo dye methyl orange under visible light. *Applied Surface Science*, 425, pp. 862–872.

Hermosilla, D., Cortijo, M. and Pao, C., 2009. Optimizing the treatment of landfill leachate by conventional fenton and photo-fenton processes. *Science of the Total Environment*, 407(11), pp. 3473–3481.

Hosseinzadeh, H. and Ramin, S., 2018. Fabrication of starch-graft-poly(acrylamide)/graphene oxide/hydroxyapatite nanocomposite hydrogel adsorbent for removal of malachite green dye from aqueous solution. *International Journal of Biological Macromolecules*, 106, pp. 101–115.

Hu, Y., Li, Y., He, J., Liu, T., Zhang, K., Huang, X., Kong, L. and Liu, J., 2018. EDTA-Fe(III) Fenton-like oxidation for the degradation of malachite green. *Journal of Environmental Management*, 226, pp. 256–263.

Huang, Y., Ma, E. and Zhao, G., 2015. Thermal and structure analysis on reaction mechanisms during the preparation of activated carbon fibers by KOH activation from liquefied wood-based fibers. *Industrial Crops and Products*, 69, pp. 447–455.

Huang, Z., Li, Y., Chen, W., Shi, J., Zhang, N., Wang, X., Li, Z., Gao, L. and Zhang, Y., 2017. Modified bentonite adsorption of organic pollutants of dye wastewater. *Materials Chemistry and Physics*, 202, pp. 266–276.

- Ibhadon, A. and Fitzpatrick, P., 2013. Heterogeneous photocatalysis: Recent advances and applications. *Catalysts*, 3(1), pp. 189–218.
- Inyang, M. and Dickenson, E., 2015. The potential role of biochar in the removal of organic and microbial contaminants from potable and reuse water: A review. *Chemosphere*, 134, pp. 232–240.
- Islam, M. A., Ahmed, M. J., Khanday, W. A., Asif, M. and Hameed, B. H., 2017. Mesoporous activated carbon prepared from NaOH activation of rattan (*Lacosperma secundiflorum*) hydrochar for methylene blue removal. *Ecotoxicology and Environmental Safety*, 138, pp. 279–285.
- Jiang, C., Gao, Z., Qu, H., Li, J., Wang, X., Li, P. and Liu, H., 2013. A new insight into Fenton and Fenton-like processes for water treatment: Part II. Influence of organic compounds on Fe (III)/ Fe (II) interconversion and the course of reactions. *Journal of Hazardous Materials*, 250–251, pp. 76–81.
- Joshi, M., Bhattacharyya, A. and Ali, S. W., 2008. Characterization techniques for nanotechnology applications in textiles. *Indian Journal of Fibre and Textile Research*, 33(3), pp. 304–317.
- Kadir, A. A. and Maasom, N., 2013. Recycling sugarcane bagasse waste into fired clay brick. *International Journal of Zero Waste Generation*, 1(1), pp. 21–26.
- Karunanayake, A. G., Adele, O., Crowley, M., Ricchetti, L., Pittman, C. U., Anderson, R., Mohan, D. and Mlsna, T., 2018. Lead and cadmium remediation using magnetized and nonmagnetized biochar from Douglas fir. *Chemical Engineering Journal*, 331, pp. 480–491.
- Kausar, A., Iqbal, M., Javed, A., Aftab, K., Nazli, Z.-H., Bhatti, H. N. and Nouren, S., 2018. Dyes adsorption using clay and modified clay: A review. *Journal of Molecular Liquids*, 256, pp. 395–407.
- Kaushik, C. P., Tuteja, R., Kaushik, N. and Sharma, J. K., 2009. Minimization of organic chemical load in direct dyes effluent using low cost adsorbents. *Chemical Engineering Journal*, 155, pp. 234–240.
- Khan, S. B., Hou, M., Shuang, S. and Zhang, Z., 2017. Morphological influence of TiO<sub>2</sub> nanostructures (nanozigzag, nanohelics and nanorod) on photocatalytic degradation of organic dyes. *Applied Surface Science*, 400, pp. 184–193.
- Khandpur, R. S., 2015. *Handbook of analytical instruments*. New Delhi, India: McGraw-Hill.
- Khataee, A. R. and Kasiri, M. B., 2010. Photocatalytic degradation of organic dyes in the presence of nanostructured titanium dioxide: Influence of the chemical structure of dyes. *Journal of Molecular Catalysis A: Chemical*, 328, pp. 8–26.

Khataee, A. R., Zarei, M. and Ordikhani-Seyedlar, R., 2011. Heterogeneous photocatalysis of a dye solution using supported TiO<sub>2</sub> nanoparticles combined with homogeneous photoelectrochemical process: Molecular degradation products. *Journal of Molecular Catalysis A: Chemical*, 338, pp. 84–91.

Khataee, A., Gholami, P. and Sheydaei, M., 2016. Heterogeneous Fenton process by natural pyrite for removal of a textile dye from water: Effect of parameters and intermediate identification. *Journal of the Taiwan Institute of Chemical Engineers*, 58, pp. 366–373.

Khataee, A., Kayan, B., Gholami, P., Kalderis, D. Akay, S., Dinpazhoh, L., 2017. Sonocatalytic degradation of reactive yellow 39 using synthesized ZrO<sub>2</sub> nanoparticles on biochar. *Ultrasonics Sonochemistry*, 39, pp. 540–549.

Khataee, A., Salahpour, F., Fathinia, M., Seyyedi, B. and Vahid, B., 2015. Iron rich laterite soil with mesoporous structure for heterogeneous Fenton-like degradation of an azo dye under visible light. *Journal of Industrial and Engineering Chemistry*, 26, pp. 129–135.

Klančar, A., Trontelj, J., Kristl, A., Meglič, A., Rozina, T., Justin, M. Z. and Roškar, R., 2016. An advanced oxidation process for wastewater treatment to reduce the ecological burden from pharmacotherapy and the agricultural use of pesticides. *Ecological Engineering*, 97, pp. 186–195.

Kshirsagar, A. S., Gautam, A. and Khanna, P. K., 2017. Efficient photo-catalytic oxidative degradation of organic dyes using CuInSe<sub>2</sub>/TiO<sub>2</sub> hybrid hetero-nanostructures. *Journal of Photochemistry and Photobiology A: Chemistry*, 349, pp. 73–90.

Kumar, A., Kumar, A., Sharma, G., Naushad, M., Stadler, F. J., Ghfar, A. A., Dhiman, P. and Saini, R. V., 2017. Sustainable nano-hybrids of magnetic biochar supported g-C<sub>3</sub>N<sub>4</sub>/FeVO<sub>4</sub> for solar powered degradation of noxious pollutants - Synergism of adsorption, photocatalysis & photo-ozonation. *Journal of Cleaner Production*, 165, pp. 431–451.

Labiadh, L., Oturan, M. A., Panizza, M., Hamadi, N. Ben and Ammar, S., 2015. Complete removal of AHPS synthetic dye from water using new electro-fenton oxidation catalyzed by natural pyrite as heterogeneous catalyst. *Journal of Hazardous Materials*, 297, pp. 34–41.

Lam, S. S., Liew, R. K., Cheng, C. K. and Chase, H. A., 2015. Catalytic microwave pyrolysis of waste engine oil using metallic pyrolysis char. *Applied Catalysis B: Environmental*, 176–177(1), pp. 601–617.

Lam, S. S., Liew, R. K., Wong, Y. M., Yek, P. N. Y., Ma, N. L., Lee, C. L. and Chase, H. A., 2017. Microwave-assisted pyrolysis with chemical activation, an innovative method to convert orange peel into activated carbon with improved properties as dye adsorbent. *Journal of Cleaner Production*, 162, pp. 1376–1387.

Lee, J., Kim, K. H. and Kwon, E. E., 2017. Biochar as a catalyst. *Renewable and Sustainable Energy Reviews*, 77, pp. 70–79.



- Li, H., Dong, X., Silva, D. E. B., Oliveira, D. L. M., Chen, Y. and Ma, L. Q., 2017. Mechanisms of metal sorption by biochars: Biochar characteristics and modifications. *Chemosphere*, 178, pp. 466–478.
- Li, S., Han, K., Li, J., Li, M. and Lu, C., 2017. Preparation and characterization of super activated carbon produced from gulfweed by KOH activation. *Microporous and Mesoporous Materials*, 243, pp. 291–300.
- Li, H., Li, Y., Xiang, L., Huang, Q., Qiu, J., Zhang, H., Sivaiah, M. V., Baron, F., Barrault, J., Petit, S. and Valange, S., 2015. Heterogeneous photo-Fenton decolorization of Orange II over Al-pillared Fe-smectite: Response surface approach, degradation pathway, and toxicity evaluation, *Journal of Hazardous Materials*, 287, pp. 32–41.
- Li, W., Wu, X., Li, S., Tang, W. and Chen, Y., 2018. Magnetic porous Fe<sub>3</sub>O<sub>4</sub>/carbon octahedra derived from iron-based metal-organic framework as heterogeneous Fenton-like catalyst. *Applied Surface Science*, 436, pp. 252–262.
- Li, Y., Sun, S., Ma, M., Ouyang, Y. and Yan, W., 2008. Kinetic study and model of the photocatalytic degradation of rhodamine B (RhB) by a TiO<sub>2</sub>-coated activated carbon catalyst: Effects of initial RhB content, light intensity and TiO<sub>2</sub> content in the catalyst. *Chemical Engineering Journal*, 142(2), pp. 147–155.
- Liang, X., He, Z., Zhong, Y., Tan, W., He, H., Yuan, P., Zhu, J. and Zhang, J., 2013. The effect of transition metal substitution on the catalytic activity of magnetite in heterogeneous Fenton reaction: In interfacial view. *Colloids and Surfaces A: Physicochemical and Engineering Aspects*, 435, pp. 28–35.
- Liao, Q., Sun, J. and Gao, L., 2009. Degradation of phenol by heterogeneous Fenton reaction using multi-walled carbon nanotube supported Fe<sub>2</sub>O<sub>3</sub> catalysts. *Colloids and Surfaces A: Physicochemical and Engineering Aspects*, 345(1–3), pp. 95–100.
- Lin, Z. R., Ma, X. H., Zhao, L. and Dong, Y. H., 2014. Kinetics and products of PCB28 degradation through a goethite-catalyzed Fenton-like reaction. *Chemosphere*, 101, pp. 15–20.
- Liu, Y., Jin, W., Zhao, Y., Zhang, G. and Zhang, W., 2017a. Enhanced catalytic degradation of methylene blue by A-Fe<sub>2</sub>O<sub>3</sub>/graphene oxide via heterogeneous photo-Fenton reactions. *Applied Catalysis B: Environmental*, 206, pp. 642–652.
- Liu, Y., Zhang, G., Chong, S., Zhang, N., Chang, H., Huang, T. and Fang, S., 2017b. NiFe(C<sub>2</sub>O<sub>4</sub>)<sub>x</sub> as a heterogeneous Fenton catalyst for removal of methyl orange. *Journal of Environmental Management*, 192, pp. 150–155.
- Liu, Z. L., Meng, H. L., Zhang, H., Cao, J. S., Zhou, K. and Lian, J. J., 2018a. Highly efficient degradation of phenol wastewater by microwave induced H<sub>2</sub>O<sub>2</sub>-CuO<sub>x</sub>/GAC catalytic oxidation process. *Separation and Purification Technology*, 193, pp. 49–57.

Liu, Z., Li, X., Rao, Z. and Hu, F., 2018b. Treatment of landfill leachate biochemical effluent using the nano-Fe<sub>3</sub>O<sub>4</sub>/Na<sub>2</sub>S<sub>2</sub>O<sub>8</sub> system: Oxidation performance, wastewater spectral analysis, and activator characterization. *Journal of Environmental Management*, 208, pp. 159–168.

Liu, X. L., Yin, H. L., Lin, A. G. and Guo, Z. Q., 2017c. Effective removal of phenol by using activated carbon supported iron prepared under microwave irradiation as a reusable heterogeneous Fenton-like catalyst. *Journal of Environmental Chemical Engineering*, 5(1), pp. 870–876.

Ma, J., Zhou, L., Dan, W., Zhang, H., Shao, Y., Bao, C. and Jing, L., 2015. Novel magnetic porous carbon spheres derived from chelating resin as a heterogeneous Fenton catalyst for the removal of methylene blue from aqueous solution. *Journal of Colloid and Interface Science*, 446, pp. 298–306.

Ma, Xi. J., Zhou, W. R. and Chen, Y., 2017. Structure and photocatalytic properties of Mn-Doped TiO<sub>2</sub> loaded on wood-based activated carbon fiber composites. *Materials*, 10, pp. 631-640

Magdalane, C. M., Kaviyarasu, K., Vijaya, J. J., Jayakumar, C., Maaza, M. and Jeyaraj, B., 2017. Photocatalytic degradation effect of malachite green and catalytic hydrogenation by UV-illuminated CeO<sub>2</sub>/CdO multilayered nanoplatelet arrays: Investigation of antifungal and antimicrobial activities. *Journal of Photochemistry and Photobiology B: Biology*, 169, pp. 110–123.

Majeed, A. A., Malik, R. N., Iqbal, M., Nadeem, M. A., Hussain, I., Yousaf, S., Zeshan, Mustafa, G., Zafar, M. I. and Nadeem, M. A., 2016. Photocatalytic degradation of textile dyes on Cu<sub>2</sub>O - CuO /TiO<sub>2</sub> anatase powder. *Journal of Environmental Chemical Engineering*, 4, pp. 2138–2146.

Mao, H., Zhou, D., Hashisho, Z., Wang, S., Chen, H. and Wang, H., 2015. Preparation of pinewood- and wheat straw-based activated carbon via a microwave-assisted potassium hydroxide treatment and an analysis of the effects of the microwave activation conditions. *BioResources*, 10(1), pp. 809–821.

Mark, C., Masooda, Q., Hajira, T., Sitara, R., Sehar, M., Sundus, A. and Mohsin, A., 2017. The oxidative response and viable reaction mechanism of the textile dyes by Fenton reagent. *Environ. Chem.*, 18(2), pp. 143–154.

Mendonça, F. G. D., Cunha, I. T. D., Soares, R. R., Tristão, J. C. and Lago, R. M., 2017. Tuning the surface properties of biochar by thermal treatment. *Bioresource Technology*, 246, pp. 28-33.

Meng, S., Ning, X., Chang, S., Fu, X., Ye, X. and Chen, S., 2018. Simultaneous dehydrogenation and hydrogenolysis of aromatic alcohols in one reaction system via visible-light-driven heterogeneous photocatalysis. *Journal of Catalysis*, 357, pp. 247–256.

Meng, X., Zhang, Z. and Li, X., 2015. Synergetic photoelectrocatalytic reactors for environmental remediation: A review. *Journal of Photochemistry and Photobiology C: Photochemistry Reviews*, 24, pp. 83–101.

Messele, S. A., Stüber, F., Bengoa, C., Fortuny, A., Fabregat, A. and Font, J., 2012. Phenol degradation by heterogeneous Fenton-like reaction using Fe supported over activated carbon. *Procedia Engineering*, 42, pp. 1373–1377.

Mirzaei, A., Chen, Z., Haghghat, F. and Yerushalmi, L., 2017. Removal of pharmaceuticals from water by homo/heterogonous fenton-type processes – A review. *Chemosphere*, 174, pp. 665–688.

Mohamed, A. R., Mohammadi, M. and Darzi, G. N., 2010. Preparation of carbon molecular sieve from lignocellulosic biomass: A review. *Renewable and Sustainable Energy Reviews*, 14(6), pp. 1591–1599.

Mohan, D., Sarswat, A., Ok, Y. S. and Pittman, C. U., 2014. Organic and inorganic contaminants removal from water with biochar, a renewable, low cost and sustainable adsorbent - A critical review. *Bioresourc Technology*, 160, pp. 191–202.

Moreira, F. C., Soler, J., Alpendurada, M. F., Boaventura, R. A. R., Brillas, E. and Vilar, V. J. P., 2016. Tertiary treatment of a municipal wastewater toward pharmaceuticals removal by chemical and electrochemical advanced oxidation processes. *Water Research*, 105, pp. 251–263.

Mubarak, N. M., Alicia, R. F., Abdullah, E. C., Sahu, J. N., Haslija, A. B. A. and Tan, J., 2013. Statistical optimization and kinetic studies on removal of  $Zn^{2+}$  using functionalized carbon nanotubes and magnetic biochar. *Biochemical Pharmacology*, 1(3), pp. 486–495.

Munoz, M., Pedro, Z. M. D., Casas, J. A. and Rodriguez, J. J., 2015. Preparation of magnetite-based catalysts and their application in heterogeneous Fenton oxidation - A review. *Applied Catalysis B: Environmental*, 176–177, pp. 249–265.

Nahar, S., Zain, M., Kadhum, A., Hasan, H. and Hasan, M., 2017. Advances in photocatalytic  $CO_2$  reduction with water: A review. *Materials*, 10(6), pp. 629–640.

Nair, V. and Vinu, R., 2016. Peroxide-assisted microwave activation of pyrolysis char for adsorption of dyes from wastewater. *Bioresourc Technology*, 216, pp. 511–519.

Nakason, K., Panyapinyopol, B. and Kanokkantapong, V., 2017a. Characteristics of hydrochar and liquid fraction from hydrothermal carbonization of cassava rhizome. *Journal of the Energy Institute*, 91, pp. 184–193.

Neamtu, M., Catrinescu, C. and Kettrup, A., 2004. Effect of dealumination of iron (III) - Exchanged Y zeolites on oxidation of reactive yellow 84 azo dye in the presence of hydrogen peroxide. *Applied Catalysis B: Environmental*, 51(3), pp. 149–157.

Nirmaladevi, V., Makeswari, M. and Santhi, T., 2018. Malachite green dye degradation using  $ZnCl_2$  activated ricinus communis stem by sunlight irradiation, *Rasayan J. Chem*, 11(1), pp. 219–227.

- Nizamuddin, S., Ahmed, H., Gri, G. J., Mubarak, N. M., Bhutto, W., Abro, R., Ali, S. and Si, B., 2017. An overview of effect of process parameters on hydrothermal carbonization of biomass. *Renewable and Sustainable Energy Reviews*, 73, pp. 1289–1299.
- Noor, N. M., Othman, R., Mubarak, N. M. and Abdullah, E. C., 2017. Agricultural biomass-derived magnetic adsorbents: Preparation and application for heavy metals removal. *Journal of the Taiwan Institute of Chemical Engineers*, 78, pp. 168–177.
- Noraini, M. N., Abdullah, E. C., Othman, R. and Mubarak, N. M., 2016. Single-route synthesis of magnetic biochar from sugarcane bagasse by microwave-assisted pyrolysis. *Materials Letters*, 184, pp. 315–319.
- Oh, I., Kim, M. and Kim, J., 2015. Deposition of Fe<sub>3</sub>O<sub>4</sub> on oxidized activated carbon by hydrazine reducing method for high performance supercapacitor. *Microelectronics Reliability*, 55(1), pp. 114–122.
- Oliveira, F. R., Patel, A. K., Jaisi, D. P., Adhikari, S., Lu, H. and Khanal, S. K., 2017. Environmental application of biochar: Current status and perspectives. *Bioresource Technology*, 246, pp. 110–122.
- Ozturk, M., Saba, N., Altay, V., Iqbal, R., Hakeem, K. R., Jawaid, M. and Ibrahim, F. H., 2017. Biomass and bioenergy: An overview of the development potential in Turkey and Malaysia. *Renewable and Sustainable Energy Reviews*, 79, pp. 1285–1302.
- Pan, J., Cheng, X., Yan, X. and Zhang, C., 2013. Preparation and hierarchical porous structure of biomorphic woodceramics from sugarcane bagasse. *Journal of the European Ceramic Society*, 33(3), pp. 575–581.
- Pang, Y. L. and Abdullah, A. Z., 2013. Current status of textile industry wastewater management and research progress in Malaysia: A review. *Clean - Soil, Air, Water*, 41(8), pp. 751–764.
- Pang, Y. L., Lim, S., Ong, H. C. and Chong, W. T., 2016. Research progress on iron oxide-based magnetic materials: Synthesis techniques and photocatalytic applications. *Ceramics International*, 42(1), pp. 9–34.
- Park, J., Wang, J. J., Xiao, R., Tafti, N., Delaune, R. D. and Seo, D., 2018. Degradation of orange G by Fenton-like reaction with Fe-impregnated biochar catalyst. *Bioresource Technology*, 249, pp. 368–376.
- Paul Guin, J., Bhardwaj, Y. K. and Varshney, L., 2017. Mineralization and biodegradability enhancement of methyl orange dye by an effective advanced oxidation process. *Applied Radiation and Isotopes*, 122, pp. 153–157.
- Peternel, I. T., Koprivanac, N., Božić, A. M. L. and Kušić, H. M., 2007. Comparative study of UV/TiO<sub>2</sub>, UV/ZnO and photo-Fenton processes for the organic reactive dye degradation in aqueous solution. *Journal of Hazardous Materials*, 148(1–2), pp. 477–484.

Pouran, S. R., Bayrami, A., Shafeeyan, M. S., Raman, A. A. A. and Daud, W. M. A. W., 2018. A comparative study on a cationic dye removal through homogeneous and heterogeneous Fenton oxidation systems. *Acta Chimica Slovenica*, 65(1), pp. 166–171.

Pouran, S. R., Raman, A. A. A. and Daud, W. M. A.W., 2014. Review on the application of modified iron oxides as heterogeneous catalysts in Fenton reactions. *Journal of Cleaner Production*, 64, pp. 24–35.

Qian, K., Kumar, A., Zhang, H., Bellmer, D. and Huhnke, R., 2015. Recent advances in utilization of biochar. *Renewable and Sustainable Energy Reviews*, 42, pp. 1055–1064.

Qiao, Y. H., Teng, J., Wang, S. and Ma, H., 2017. Amine - functionalized sugarcane bagasse: A renewable catalyst for efficient continuous flow Knoevenagel condensation reaction at room temperature. *Molecules*, 23(1), pp. 1–13.

Rajapaksha, A. U., Chen, S. S., Tsang, D. C. W., Zhang, M., Vithanage, M., Mandal, S., Gao, B., Bolan, N. S. and Ok, Y. S., 2016. Engineered/designer biochar for contaminant removal/immobilization from soil and water: Potential and implication of biochar modification. *Chemosphere*, 148, pp. 276–291.

Rajoriya, S., Bargole, S., George, S. and Saharan, V. K., 2018. Treatment of textile dyeing industry effluent using hydrodynamic cavitation in combination with advanced oxidation reagents. *Journal of Hazardous Materials*, 344, pp. 1109–1115.

Ramírez-Montoya, L. A., Hernández-Montoya, V. and Montes-Morán, M. A., 2014. Optimizing the preparation of carbonaceous adsorbents for the selective removal of textile dyes by using Taguchi methodology. *Journal of Analytical and Applied Pyrolysis*, 109, pp. 9–20.

Rangabhashiyam, S., Anu, N. and Selvaraju, N., 2013. Sequestration of dye from textile industry wastewater using agricultural waste products as adsorbents. *Journal of Environmental Chemical Engineering*, 1(4), pp. 629–641.

Rangabhashiyam, S. and Balasubramanian, P., 2018. Performance of novel biosorbents prepared using native and NaOH treated *Peltophorum pterocarpum* fruit shells for the removal of malachite green. *Bioresource Technology Reports*, 3, pp. 75–81.

Rattanachueskul, N., Saning, A., Kaowphong, S., Chumha, N. and Chuenchom, L., 2017. Magnetic carbon composites with a hierarchical structure for adsorption of tetracycline, prepared from sugarcane bagasse via hydrothermal carbonization coupled with simple heat treatment process. *Bioresource Technology*, 226, pp. 164–172.

Rauf, M. A. and Ashraf, S. S., 2009. Fundamental principles and application of heterogeneous photocatalytic degradation of dyes in solution. *Chemical Engineering Journal*, 151(1–3), pp. 10–18.

- Rezania, S., Din, M. F. M., Taib, S. M., Dahalan, F. A., Songip, A. R., Singh, L. and Kamyab, H., 2016. The efficient role of aquatic plant (water hyacinth) in treating domestic wastewater in continuous system. *International Journal of Phytoremediation*, 18(7), pp. 679–685.
- Río, J. C., Lino, A. G., Colodette, J. L., Lima, C. F., Gutiérrez, A., Martínez, Á. T., Lu, F., Ralph, J. and Rencoret, J., 2015. Differences in the chemical structure of the lignins from sugarcane bagasse and straw. *Biomass and Bioenergy*, 81, pp. 322–338.
- Roonasi, P. and Nezhad, A. Y., 2015. A comparative study of a series of ferrite nanoparticles as heterogeneous catalysts for phenol removal at neutral pH. *Materials Chemistry and Physics*, 172, pp. 143–149.
- Sajjadi, S. H. and Goharshadi, E. K., 2017. Highly monodispersed hematite cubes for removal of ionic dyes. *Journal of Environmental Chemical Engineering*, 5(1), pp. 1096–1106.
- Salama, A., Etri, S., Mohamed, S. A. A. and El-sakhawy, M., 2018. Carboxymethyl cellulose prepared from mesquite tree: New source for promising nanocomposite materials. *Carbohydrate Polymers*, 189, pp. 138–144.
- Samiey, B. and Toosi, A. R., 2010. Adsorption of malachite green on silica gel: Effects of NaCl, pH and 2-propanol. *Journal of Hazardous Materials*, 184, pp. 739–745.
- Shafie, S. M., Mahlia, T. M. I., Masjuki, H. H. and Ahmad-Yazid, A., 2012. A review on electricity generation based on biomass residue in Malaysia. *Renewable and Sustainable Energy Reviews*, 16(8), pp. 5879–5889.
- Sham, A. Y. W. and Notley, S. M., 2018. Adsorption of organic dyes from aqueous solutions using surfactant exfoliated graphene. *Journal of Environmental Chemical Engineering*, 6(1), pp. 495–504.
- Sharma, S., Buddhdev, J., Patel, M. and Ruparelia, J. P., 2013. Studies on degradation of reactive red 135 dye in wastewater using ozone. *Procedia Engineering*, 51, pp. 451–455.
- Shen, J., Horng, J., Wang, Y. and Zeng, Y., 2017. The use of reactive index of hydroxyl radicals to investigate the degradation of acid orange 7 by Fenton process. *Chemosphere*, 182, pp. 364–372.
- Singh, L., Rekha, P. and Chand, S., 2016. Cu-impregnated zeolite Y as highly active and stable heterogeneous Fenton-like catalyst for degradation of Congo red dye. *Separation and Purification Technology*, 170, pp. 321–336.
- Singh, R. K., Philip, L. and Ramanujam, S., 2017. Removal of 2,4-dichlorophenoxyacetic acid in aqueous solution by pulsed corona discharge treatment: Effect of different water constituents, degradation pathway and toxicity assay. *Chemosphere*, 184, pp. 207–214.

- Sizmur, T., Fresno, T., Akgül, G., Frost, H. and Moreno-Jiménez, E., 2017. Biochar modification to enhance sorption of inorganics from water. *Bioresource Technology*, 246, pp. 34-47.
- Skoog, D. A., Holler, F. J. and Crouch, S. R., 2007. *Principles of instrumental analysis*. California, USA: Thomson Higher Education.
- Sohni, S., Norulaini, N. A. N., Hashim, R., Bahadar, S., Fadhullah, W. and Omar, A. K. M., 2018. Industrial crops & products physicochemical characterization of Malaysian crop and agro-industrial biomass residues as renewable energy resources. *Industrial Crops & Products*, 111, pp. 642–650.
- Spasiano, D., Marotta, R., Malato, S., Fernandez-Ibañez, P. and Di Somma, I., 2015. Solar photocatalysis: Materials, reactors, some commercial, and pre-industrialized applications. A comprehensive approach. *Applied Catalysis B: Environmental*, 170–171, pp. 90–123.
- Sugrañez, R., Balbuena, J., Cruz-Yusta, M., Martín, F., Morales, J. and Sánchez, L., 2015. Efficient behaviour of hematite towards the photocatalytic degradation of NO<sub>x</sub> gases. *Applied Catalysis B: Environmental*, 165, pp. 529–536.
- Sun, Y., Chen, Z., Wu, G., Wu, Q., Zhang, F., Niu, Z. and Hu, H. Y., 2016. Characteristics of water quality of municipal wastewater treatment plants in China: Implications for resources utilization and management. *Journal of Cleaner Production*, 131, pp. 1–9.
- Tan, X. F., Liu, S. B., Liu, Y. G., Gu, Y. L., Zeng, G. M., Hu, X. J., Wang, X., Liu, S. H. and Jiang, L. H., 2017. Biochar as potential sustainable precursors for activated carbon production: Multiple applications in environmental protection and energy storage. *Bioresource Technology*, 227, pp. 359–372.
- Tan, X. F., Liu, Y. G., Gu, Y. L., Xu, Y., Zeng, G. M., Hu, X. J., Liu, S. B., Wang, X., Liu, S. M. and Li, J., 2016. Biochar-based nano-composites for the decontamination of wastewater: A review. *Bioresource Technology*, 212, pp. 318–333.
- Tan, Z., Lin, C. S. K., Ji, X. and Rainey, T. J., 2017. Returning biochar to fields: A review. *Applied Soil Ecology*, 116, pp. 1–11.
- Tao, H. C., Zhang, H. R., Li, J. B. and Ding, W. Y., 2015. Biomass based activated carbon obtained from sludge and sugarcane bagasse for removing lead ion from wastewater. *Bioresource Technology*, 192, pp. 611–617.
- Thines, K. R., Abdullah, E. C., Mubarak, N. M. and Ruthiraan, M., 2017. Synthesis of magnetic biochar from agricultural waste biomass to enhancing route for waste water and polymer application: A review. *Renewable and Sustainable Energy Reviews*, 67, pp. 257–276.
- Tizaoui, C. and Grima, N., 2011. Kinetics of the ozone oxidation of reactive orange 16 azo-dye in aqueous solution. *Chemical Engineering Journal*, 173(2), pp. 463–473.

Tripathi, M., Sahu, J. N. and Ganesan, P., 2016. Effect of process parameters on production of biochar from biomass waste through pyrolysis: A review. *Renewable and Sustainable Energy Reviews*, 55, pp. 467–481.

Trojanowicz, M., Bojanowska-Czajka, A., Bartosiewicz, I. and Kulisa, K., 2018. Advanced oxidation/reduction processes treatment for aqueous perfluorooctanoate (PFOA) and perfluorooctanesulfonate (PFOS) – A review of recent advances. *Chemical Engineering Journal*, 336, pp. 170–199.

Truskewycz, A., Shukla, R. and Ball, A. S., 2016. Iron nanoparticles synthesized using green tea extracts for the Fenton-like degradation of concentrated dye mixtures at elevated temperatures. *Journal of Environmental Chemical Engineering*, 4(4), pp. 4409–4417.

Tzvetkov, G., Mihaylova, S., Stoitchkova, K., Tzvetkov, P. and Spassov, T., 2016. Mechanochemical and chemical activation of lignocellulosic material to prepare powdered activated carbons for adsorption applications. *Powder Technology*, 299, pp. 41–50.

Udaiyappan, A. F. M., Hasan, H. A., Takriff, M. S. and Abdullah, S. R. S., 2017. A review of the potentials, challenges and current status of microalgae biomass applications in industrial wastewater treatment. *Journal of Water Process Engineering*, 20, pp. 8–21.

Urbaniec, K. and Bakker, R. R., 2015. Biomass residues as raw material for dark hydrogen fermentation - A review. *International Journal of Hydrogen Energy*, 40(9), pp. 3648–3658.

Varma, A. K. and Mondal, P., 2017. Pyrolysis of sugarcane bagasse in semi batch reactor: Effects of process parameters on product yields and characterization of products. *Industrial Crops and Products*, 95, pp. 704–717.

Vyavahare, G. D., Gurav, R. G., Jadhav, P. P., Patil, R. R., Aware, C. B. and Jadhav, J. P., 2018. Response surface methodology optimization for sorption of malachite green dye on sugarcane bagasse biochar and evaluating the residual dye for phyto and cytogenotoxicity. *Chemosphere*, 194, pp. 306–315.

Wan, Z. and Wang, J., 2017. Degradation of sulfamethazine using Fe<sub>3</sub>O<sub>4</sub>-Mn<sub>3</sub>O<sub>4</sub>/reduced graphene oxide hybrid as Fenton-like catalyst. *Journal of Hazardous Materials*, 324, pp. 653–664.

Wang, L., Yao, Y., Sun, L., Mao, Y., Lu, W., Huang, S. and Chen, W., 2014. Rapid removal of dyes under visible irradiation over activated carbon fibers supported Fe (III) - citrate at neutral pH. *Separation and Purification Technology*, 122, pp. 449–455.

Wang, N., Zheng, T., Zhang, G. and Wang, P., 2016. A review on Fenton-like processes for organic wastewater treatment. *Journal of Environmental Chemical Engineering*, 4(1), pp. 762–787.



- Wang, S. H. and Zhou, X., 2017. Recent advances in hybrid measurement methods based on atomic force microscopy and surface sensitive measurement techniques. *RSC Advances*, 7, pp. 47464-47499.
- Wang, S., Kong, L., Long, J., Su, M., Diao, Z., Chang, X., Chen, D., Song, G. and Shih, K., 2018. Adsorption of phosphorus by calcium-flour biochar: Isotherm, kinetic and transformation studies. *Chemosphere*, 195, pp. 666–672.
- Wang, S., Zhao, C., Shan, R., Wang, Y. and Yuan, H., 2017. A novel peat biochar supported catalyst for the transesterification reaction. *Energy Conversion and Management*, 139, pp. 89–96.
- Wu, J. M., Sun, Y. G., Chang, W. E. and Lee, J. T., 2018. Piezoelectricity induced water splitting and formation of hydroxyl radical from active edge sites of MoS<sub>2</sub> nanoflowers. *Nano Energy*, 46, pp. 372–382.
- Wu, Y., Zeng, S., Wang, F., Megharaj, M., Naidu, R. and Chen, Z., 2015. Heterogeneous Fenton-like oxidation of malachite green by iron-based nanoparticles synthesized by tea extract as a catalyst. *Separation and Purification Technology*, 154, pp. 161–167.
- Xiao, J., Xie, Y. and Cao, H., 2015. Organic pollutants removal in wastewater by heterogeneous photocatalytic ozonation. *Chemosphere*, 121, pp. 1–17.
- Xiong, X., Yu, I. K. M., Cao, L., Tsang, D. C. W., Zhang, S. and Ok, Y. S., 2017. A review of biochar-based catalysts for chemical synthesis, biofuel production, and pollution control. *Bioresource Technology*, 246, pp. 254-270.
- Xu, X., Schierz, A., Xu, N. and Cao, X., 2016. Comparison of the characteristics and mechanisms of Hg(II) sorption by biochars and activated carbon. *Journal of Colloid and Interface Science*, 463, pp. 55–60.
- Yan, R., Yang, F., Wu, Y., Hu, Z., Nath, B., Yang, L. and Fang, Y., 2011. Cadmium and mercury removal from non-point source wastewater by a hybrid bioreactor. *Bioresource Technology*, 102(21), pp. 9927–9932.
- Yang, L., Tian, J., Meng, J., Zhao, R., Li, C., Ma, J. and Jin, T., 2018. Modification and characterization of Fe<sub>3</sub>O<sub>4</sub> nanoparticles for use in adsorption of alkaloids. *Molecules*, 23, pp. 1–10.
- You, S., Ok, Y. S., Chen, S. S., Tsang, D. C. W., Kwon, E. E., Lee, J. and Wang, C. H., 2017. A critical review on sustainable biochar system through gasification: Energy and environmental applications. *Bioresource Technology*, 246, pp. 242-253.
- Yu, J. X., Chi, R. A., Zhang, Y. F., Xu, Z. G., Xiao, C. Q. and Guo, J., 2012. A situ co-precipitation method to prepare magnetic PMDA modified sugarcane bagasse and its application for competitive adsorption of methylene blue and basic magenta. *Bioresource Technology*, 110, pp. 160–166.

Yu, K. L., Lau, B. F., Show, P. L., Ong, H. C., Ling, T. C., Chen, W. H., Ng, E. P. and Chang, J. S., 2017. Recent developments on algal biochar production and characterization. *Bioresource Technology*, 246, pp. 2-11.

Yu, L., Chen, J., Liang, Z., Xu, W., Chen, L. and Ye, D., 2016. Degradation of phenol using Fe<sub>3</sub>O<sub>4</sub>-GO nanocomposite as a heterogeneous photo-Fenton catalyst. *Separation and Purification Technology*, 171, pp. 80-87.

Yu, S., Zhang, T., Xie, Y., Wang, Q., Gao, X., Zhang, R., Zhang, Y. and Su, H., 2014. Synthesis and characterization of iron-based catalyst on mesoporous titania for photo-thermal F-T synthesis. *International Journal of Hydrogen Energy*, 40(1), pp. 870-877.

Yuan, Y., Bolan, N., PrévotEAU, A., Vithanage, M., Biswas, J. K., Ok, Y. S. and Wang, H., 2017. Applications of biochar in redox-mediated reactions. *Bioresource Technology*, 246, pp. 271-281.

Zhang, H., Liu, D., Ren, S. and Zhang, H., 2017. Kinetic studies of direct blue photodegradation over flower-like TiO<sub>2</sub>. *Research on Chemical Intermediates*, 43(3), pp. 1529-1542.

Zhang, H., Xue, G., Chen, H. and Li, X., 2018. Magnetic biochar catalyst derived from biological sludge and ferric sludge using hydrothermal carbonization: Preparation, characterization and its circulation in Fenton process for dyeing wastewater treatment. *Chemosphere*, 191, pp. 64-71.

Zhang, J., Li, F. and Sun, Q., 2018. Rapid and selective adsorption of cationic dyes by a unique metal-organic framework with decorated pore surface. *Applied Surface Science*, 440, pp. 1219-1226.

Zhang, Q., Zhang, X., Zhu, Z., Zhang, A., Zhang, C., Wang, X. and Liu, C., 2018. Mechanocatalytic solvent-free esterification of sugarcane bagasse. *Polymers*, 10(3), pp. 1-13.

Zheng, C. M., Yang, C. W., Cheng, X. Z., Xu, S. C., Fan, Z. P., Wang, G. H., Wang, S. B., Guan, X. F. and Sun, X. H., 2017. Specifically enhancement of heterogeneous Fenton-like degradation activities for ofloxacin with synergetic effects of bimetallic Fe-Cu on ordered mesoporous silicon. *Separation and Purification Technology*, 189, pp. 357-365.

Zhou, L., Ma, J., Zhang, H., Shao, Y. and Li, Y., 2015. Fabrication of magnetic carbon composites from peanut shells and its application as a heterogeneous Fenton catalyst in removal of methylene blue. *Applied Surface Science*, 324, pp. 490-498.

Zhou, Y., Zhang, L. and Cheng, Z., 2015. Removal of organic pollutants from aqueous solution using agricultural wastes: A review. *Journal of Molecular Liquids*, 212, pp. 739-762.

Zuo, R., Du, G., Zhang, W., Liu, L., Liu, Y., Mei, L. and Li, Z., 2014. Photocatalytic degradation of methylene blue using TiO<sub>2</sub> impregnated diatomite. *Advances in Materials Science and Engineering*, 10, pp. 1-7.

## APPENDICES

### APPENDIX A: Preparation of Various Concentrations of Organic Dyes

Dilution process is the method used to obtain the concentration of organic dyes required from the stock solution. With the knowledge on the concentration of a stock solution, desired concentration and volume of organic dyes, the volume from stock solution needed to achieve the desired concentration can be calculated as follow:

$$C_1V_1 = C_2V_2$$

where

$C_1$  = Concentration of stock solution, ppm

$V_1$  = Volume of stock solution, L

$C_2$  = Concentration of diluted solution, ppm

$V_2$  = Volume of diluted solution, L

Once the value of  $V_1$  required is calculated, the amount will be pipetted to a volumetric cylinder, followed by adding the distilled water to the desired volume. In order to obtain the solution of 50 % malachite green with the concentration of 500 ppm in 0.5 L, the mass of malachite green powder required can be computed as follow:

$$\begin{aligned} \text{Mass of malachite green} &= 1/0.50 \times 500 \text{ ppm} \times 0.5 \text{ L} \\ &= 500 \text{ mg} \\ &= 0.5 \text{ g} \end{aligned}$$

Hence, 0.5 g of malachite green is necessary to be dissolved in 0.5 L of distilled water to acquire desired stock solution with 500 ppm in 0.5 L. Volume of 50 % malachite green with 500 ppm required to prepare various concentration in 0.1 L solution is shown Table A.1. The volume of 50 % malachite green stock solution with 500 ppm required to prepare 0.1 L of diluted malachite green solution with concentration of 20 ppm is computed as follow:

$$(500 \text{ ppm})(V_1) = (30 \text{ ppm})(0.1 \text{ L})$$

$$V_1 = 0.006 \text{ L or } 6 \text{ mL}$$

Therefore, 6 mL of malachite green stock solution is pipetted from the 500 ppm stock solution before mixing with distilled water until the volume achieve 100 mL.

Table A.1: Volume of 50 % Malachite Green Stock Solutions with 500 ppm Required to Prepare Different Concentration of Organic Dyes in 100 mL Solution

<b>Concentration of Malachite Green (ppm)</b>	<b>Volume of 50 % Malachite Green Stock Solution with 500 ppm Required (mL)</b>
30	6
50	10
70	14
90	18
110	22

## APPENDIX B: Preparation of 0.1 M HCl from a 37 % HCl Solution

Molarity of 37 % HCl is first identified as follow:

$$\text{HCl} - 37 \% \text{ v/v} = 37 \text{ mL} / 100 \text{ mL}$$

$$\text{Specific gravity of 37 \% HCl} = 1.19 \text{ g/mL}$$

$$\text{Molecular weight of HCl} = 36.46 \text{ g/mol}$$

$$\begin{aligned} \text{Concentration of HCl in g/L} &= 37 \text{ mL} / 100\text{mL} \times 1.19 \text{ g/mL} \\ &= 0.4403 \text{ g/mL} \times 1000 \text{ mL} / \text{L} \\ &= 440.3 \text{ g/L} \end{aligned}$$

$$\begin{aligned} \text{Molarity of HCl} &= 440.3 \text{ g/L} \times 1 \text{ mol} / 36.46 \text{ g} \\ &= 12.07 \text{ mol/L} \end{aligned}$$

Volume of 0.37 % HCl needed can be calculated in order to get 0.1 M by using the equation as follow:

$$M_1V_1 = M_2V_2$$

where

$M_1$  = Concentration of 37 % HCl solution, mol/L

$V_1$  = Volume from 37 % HCl solution, L

$M_2$  = Concentration of diluted HCl solution, mol/L

$V_2$  = Volume from diluted HCl solution, L

$$M_1 = 12.07 \text{ M}, M_2 = 0.1 \text{ M}, V_2 = 0.5 \text{ L}$$

Therefore,

$$\begin{aligned} V_1 &= M_2V_2 / M_1 \\ &= 0.1 \text{ M} \times 0.5 \text{ L} / 12.07 \text{ M} \\ &= 0.00414 \text{ L or } 4.14 \text{ mL} \end{aligned}$$

Hence, 4.14 mL of 37 % HCl is pipetted and mixed with distilled water until the volume reach 500 mL.

## APPENDIX C: Preparation of 0.1 M NaOH from a 97 % NaOH

In order to obtain 0.1 M of NaOH in 500 mL solution, the mass of NaOH powder needed is calculated as below:

$$\begin{aligned}\text{Number of moles of NaOH} &= \text{Molarity (mol/L)} \times \text{Volume (L)} \times \text{Purity} \\ &= 0.1 \text{ mol/L} \times 500 \text{ mL} \times 1 \text{ L}/1000 \text{ mL} \times 100/97 \\ &= 0.052 \text{ mol}\end{aligned}$$

$$\text{Molecular weight of NaOH} = 40 \text{ g/mol}$$

Mass of NaOH

$$\begin{aligned}&= \text{Number of moles of NaOH (mol)} \times \text{Molecular Weight of NaOH (g/mol)} \\ &= 0.052 \text{ mol} \times 40 \text{ g/mol} \\ &= 2.08 \text{ g}\end{aligned}$$

Hence, 2.08 g of NaOH powder is needed to be dissolved in 500 mL of distilled water to get 0.1 M of NaOH solution.

APPENDIX D: Preparation of 0.1 M H<sub>2</sub>O<sub>2</sub> from 30 % H<sub>2</sub>O<sub>2</sub>

Concentration of H<sub>2</sub>O<sub>2</sub> utilised in this experiment was 30 % H<sub>2</sub>O<sub>2</sub> (w/w) in H<sub>2</sub>O. This indicates that 30 g of H<sub>2</sub>O<sub>2</sub> is present in 100 g of solution. Density of 30 % H<sub>2</sub>O<sub>2</sub> is 1.11 g/mL. Volume for 100 g of 30 % H<sub>2</sub>O<sub>2</sub> solution is computed as follow:

$$\rho = m/V$$

where

$\rho$  = Density, g/mL

$m$  = Mass, g

$V$  = Volume, mL

$$\begin{aligned} V &= m/\rho \\ &= 100 \text{ g} / 1.11 \text{ g/mL} \\ &= 90.09 \text{ mL} \end{aligned}$$

Then, the percentage concentration (w/v) of H<sub>2</sub>O<sub>2</sub> solution is calculated as below:

$$\begin{aligned} \text{Percent concentration (w/v)} &= 100 \times \text{Amount of solute (g)} / \text{Amount of solution (mL)} \\ &= 100 \times 30 \text{ g} / 90.09 \text{ mL} \\ &= 33.30 \text{ g/mL} \end{aligned}$$

Moles of H<sub>2</sub>O<sub>2</sub> occurred in 33.30 g of H<sub>2</sub>O is computed.

$$\begin{aligned} \text{Moles} &= \text{Mass of substance (g)} / \text{Atomic weight (g/mol)} \\ &= 33.30 \text{ g} / 34.01 \text{ g/mol} \\ &= 0.98 \text{ mol of H}_2\text{O}_2 \end{aligned}$$

Hence, 0.98 mol of H<sub>2</sub>O<sub>2</sub> is present in 100 mL solution. Now, the molarity of H<sub>2</sub>O<sub>2</sub> solution is computed as follow:

$$\text{Molarity} = \text{Number of moles of solutes (mol)} / \text{Volume of solution (L)}$$



$$= 0.98 \text{ mol/ 1 L}$$

$$= 0.98 \text{ M}$$

Volume of 0.30 % H<sub>2</sub>O<sub>2</sub> needed can be calculated to obtain the desired concentration of H<sub>2</sub>O<sub>2</sub> by using the equation as below:

$$M_1V_1 = M_2V_2$$

where

$M_1$  = Concentration of 30 % H<sub>2</sub>O<sub>2</sub> solution, mol/L

$V_1$  = Volume from 30 % H<sub>2</sub>O<sub>2</sub> solution, L

$M_2$  = Concentration of diluted H<sub>2</sub>O<sub>2</sub> solution, mol/L

$V_2$  = Volume from diluted H<sub>2</sub>O<sub>2</sub> solution, L

Once the value of  $V_1$  is known, the amount of stock solution is pipetted and is mixed with distilled water until the volume achieve  $V_2$  value. Volume of 30 % H<sub>2</sub>O<sub>2</sub> needed to prepare different dosage in 100 mL solution is shown in Table D.1. The volume of H<sub>2</sub>O<sub>2</sub> required is computed as follow:

$$(9.8 \text{ M})(V_1) = (1 \text{ mM})(100 \text{ mL})$$

$$V_1 = 0.01 \text{ mL}$$

Table D.1: Volume of H<sub>2</sub>O<sub>2</sub> Required to Prepare Different Dosage in 100 mL Solution

<b>H<sub>2</sub>O<sub>2</sub> Dosage (mM)</b>	<b>Volume of 30% H<sub>2</sub>O<sub>2</sub> Solution Required (mL)</b>
1	0.01
2	0.02
3	0.03
4	0.04
5	0.05
6	0.06

## APPENDIX E: Preparation of Standard Solution for ICP-OES Analysis

To acquire the concentration of  $\text{Fe}(\text{NO}_3)_3$  needed from the stock solution, dilution process is necessary. The desired volume and concentration of  $\text{Fe}(\text{NO}_3)_3$  from stock solution can be computed by using formula below:

$$C_1V_1 = C_2V_2$$

where

$C_1$  = Concentration of stock solution, g/L

$V_1$  = Volume of stock solution, L

$C_2$  = Concentration of diluted solution, g/L

$V_2$  = Volume of diluted solution, L

Upon knowing the value of  $V_1$ , the amount is pipetted and diluted by adding distilled water till the volume reach  $V_2$  value.

In order to prepare the stock solution of  $\text{Fe}(\text{NO}_3)_3$  with concentration of 1000 mg/L in 100 mL, the mass of  $\text{Fe}(\text{NO}_3)_3$  powder required can be computed as below:

$$\text{Mass of } \text{Fe}(\text{NO}_3)_3 = (1000 \text{ mg/L})(1 \text{ L} / 1000 \text{ mL})(100 \text{ mL})$$

$$V_1 = 100 \text{ mg or } 0.1 \text{ g}$$

Hence, 0.1 g of  $\text{Fe}(\text{NO}_3)_3$  was dissolved in 100 mL distilled water to acquire 1000 mg/L of stock solution.

The volume of stock solution with 1000 mg/L needed to prepare the various concentration of  $\text{Fe}(\text{NO}_3)_3$  in 40 mL solution was depicted in Table E.1. The formula used to calculate the volume of 1000 mg/L stock solution needed to achieve the diluted concentration of 2 mg/L as the final solution is shown as follow:

$$(1000 \text{ mg/L})(V_1) = (1 \text{ mg/L}) (40 \text{ mL})$$

$$V_1 = 0.04 \text{ mL}$$

As calculated, 2 mL of  $\text{Fe}(\text{NO}_3)_3$  stock solution was pipetted and then diluted by adding distilled water until the volume reached 40 mL.

Table E.1: Volume of 1000 mg/L Stock Solution Needed to Prepare Various Concentration of  $\text{Fe}(\text{NO}_3)_3$  in 40 mL Solution

<b>Concentration of <math>\text{Fe}(\text{NO}_3)_3</math> (mg/L)</b>	<b>Volume of 1000 mg/L <math>\text{Fe}(\text{NO}_3)_3</math> solution required (mL)</b>
1	0.04
2	0.08
3	0.12
4	0.16
5	0.20

## APPENDIX F: Calibration Curve of Organic Dye

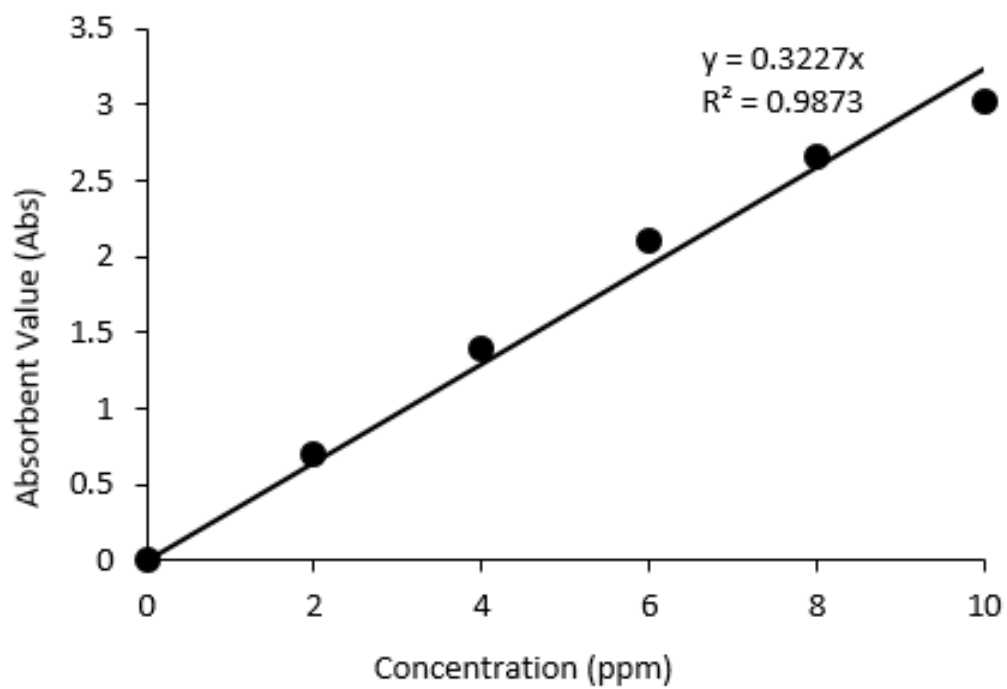


Figure F.1: Calibration Curve of Malachite Green

APPENDIX G: Calibration Curve of Standard Solution for ICP-OES Analysis and  
Curve for Extended Reaction Time for Leached Iron Concentration Detection

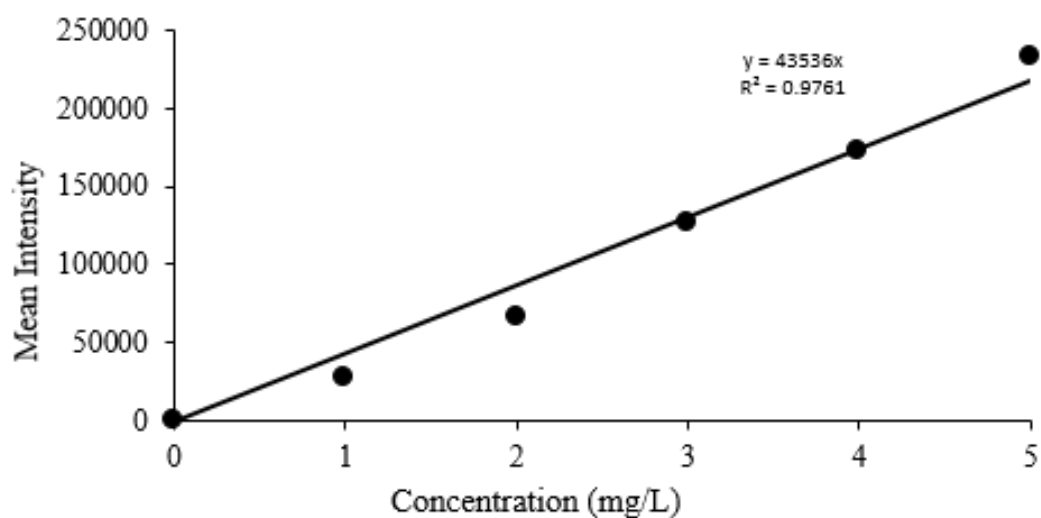


Figure G.1: Calibration Curve of Standard Solution for ICP-OES Analysis of Fe

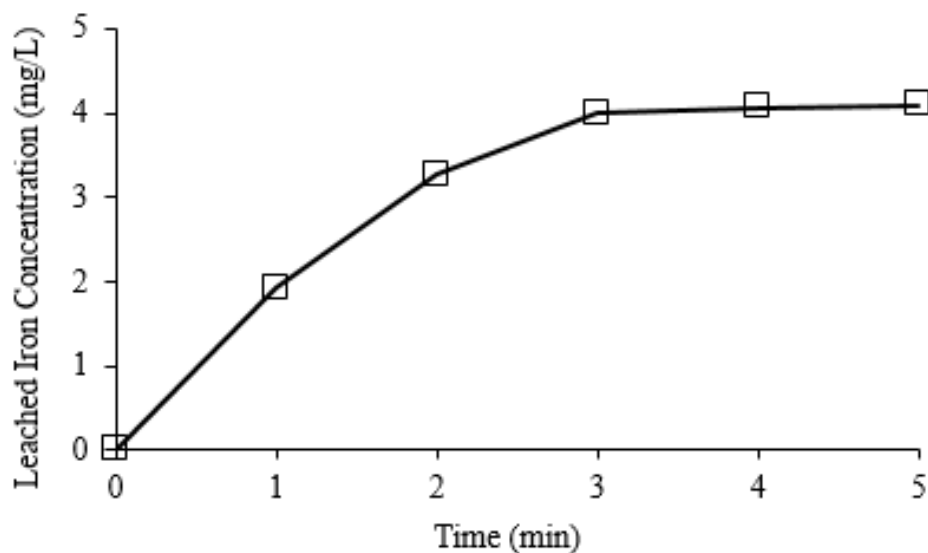


Figure G.2: Leached Iron Concentration on the Heterogeneous Photo Fenton and Fenton-like Degradation of Malachite Green under Optimal Condition (Dyes Concentration = 30 ppm, FeAC11 Dosage = 0.8 g/L, pH = 5, Solution Temperature = 25 °C, Reaction Time = 5 min)

## APPENDIX H: Reaction Kinetics Plot

The kinetics of heterogeneous photo Fenton and Fenton-like degradation of malachite green can be shown as below:

$$-dC_{MG}/dt = k_{app} C_{MG}^m$$

where

$C_{MG}$  = concentration of malachite green at time  $t$ , mg/L

$m$  = reaction order with respect to malachite green

$t$  = reaction time, min

$k_{app}$  = reaction rate constant

For pseudo zero-order reaction, the  $m$  is equal to 0. Hence, the equation above can be integrated and simplified as below:

$$C_t = C_o - k_o t$$

$C_t$  against  $t$  was plotted and depicted in Figure I.1.

For pseudo first-order reaction, the  $m$  is equivalent to 1. Therefore, the integrated equation becomes:

$$\ln C_o/C_t = k_{app} t$$

$\ln C_o/C_t$  against  $t$  was plotted and illustrated in Figure I.2.

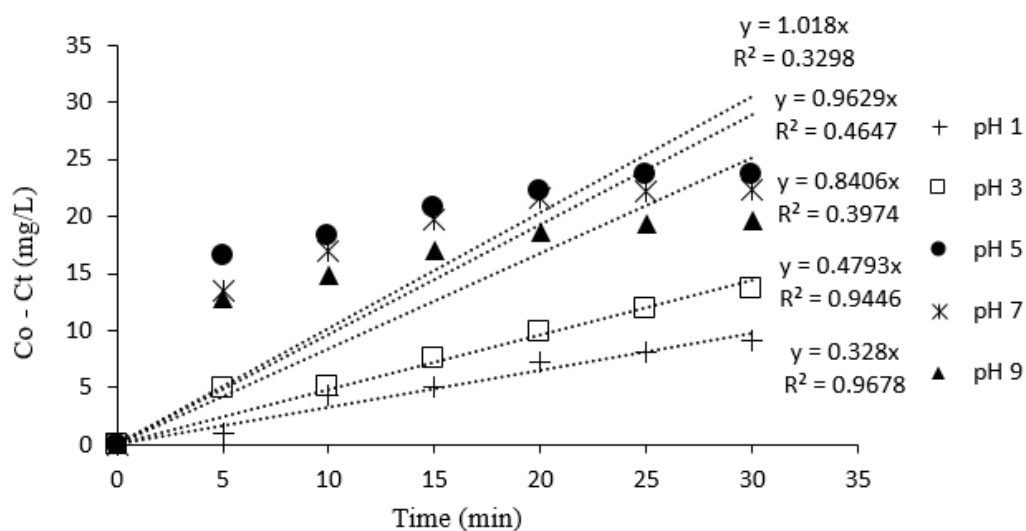


Figure I.1: Pseudo Zero-order Reaction Kinetics Plot for Heterogeneous Photo Fenton and Fenton-like Degradation of Malachite Green at Different pH Values

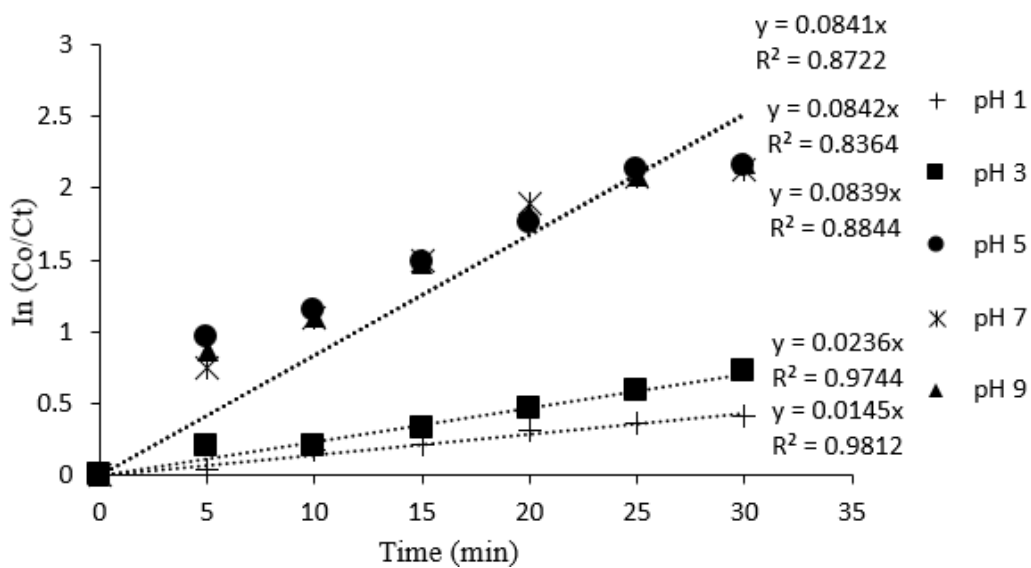


Figure I.2: Pseudo First-order Reaction Kinetics Plot for Heterogeneous Photo Fenton and Fenton-like Degradation of Malachite Green at Different pH Values

## APPENDIX I: Safety Data Sheet (SDS)



## SAFETY DATA SHEET

Creation Date 07-Aug-2014

Revision Date 18-Jan-2018

Revision Number 3

### 1. Identification

**Product Name** Malachite Green (Technical)  
**Cat No. :** A779-500  
**Synonyms** Acryl Brilliant Green; Aniline Green; China Green  
**Recommended Use** Laboratory chemicals.  
**Uses advised against** Not for food, drug, pesticide or biocidal product use

#### Details of the supplier of the safety data sheet

##### Company

Fisher Scientific  
One Reagent Lane  
Fair Lawn, NJ 07410  
Tel: (201) 796-7100

##### **Emergency Telephone Number**

CHEMTREC®, Inside the USA: 800-424-9300  
CHEMTREC®, Outside the USA: 001-703-527-3887

### 2. Hazard(s) identification

#### Classification

This chemical is considered hazardous by the 2012 OSHA Hazard Communication Standard (29 CFR 1910.1200)

Acute oral toxicity	Category 4
Serious Eye Damage/Eye Irritation	Category 1
Reproductive Toxicity	Category 2

#### Label Elements

##### **Signal Word**

Danger

##### **Hazard Statements**

Harmful if swallowed  
Causes serious eye damage  
Suspected of damaging the unborn child



#### **Precautionary Statements**

**Prevention**

Obtain special instructions before use  
 Do not handle until all safety precautions have been read and understood  
 Use personal protective equipment as required  
 Wash face, hands and any exposed skin thoroughly after handling  
 Do not eat, drink or smoke when using this product

**Response**

IF exposed or concerned: Get medical attention/advice

**Eyes**

IF IN EYES: Rinse cautiously with water for several minutes. Remove contact lenses, if present and easy to do. Continue rinsing  
 Immediately call a POISON CENTER or doctor/physician

**Ingestion**

IF SWALLOWED: Call a POISON CENTER or doctor/physician if you feel unwell

Rinse mouth

**Storage**

Store locked up

**Disposal**

Dispose of contents/container to an approved waste disposal plant

**Hazards not otherwise classified (HNOC)**

Very toxic to aquatic life with long lasting effects

### 3. Composition/Information on Ingredients

Component	CAS-No	Weight %
Malachite green	569-64-2	100

### 4. First-aid measures

<b>Eye Contact</b>	Rinse immediately with plenty of water, also under the eyelids, for at least 15 minutes. Immediate medical attention is required.
<b>Skin Contact</b>	Wash off immediately with plenty of water for at least 15 minutes. Get medical attention if symptoms occur.
<b>Inhalation</b>	Move to fresh air. If breathing is difficult, give oxygen. Do not use mouth-to-mouth method if victim ingested or inhaled the substance; give artificial respiration with the aid of a pocket mask equipped with a one-way valve or other proper respiratory medical device. Obtain medical attention.
<b>Ingestion</b>	Do not induce vomiting. Call a physician or Poison Control Center immediately.
<b>Most important symptoms and effects</b>	Causes eye burns.
<b>Notes to Physician</b>	Treat symptomatically

### 5. Fire-fighting measures

<b>Suitable Extinguishing Media</b>	Use water spray, alcohol-resistant foam, dry chemical or carbon dioxide.
<b>Unsuitable Extinguishing Media</b>	No information available
<b>Flash Point</b>	No information available
<b>Method -</b>	No information available
<b>Autoignition Temperature</b>	No information available
<b>Explosion Limits</b>	
<b>Upper</b>	No data available
<b>Lower</b>	No data available

**Sensitivity to Mechanical Impact** No information available  
**Sensitivity to Static Discharge** No information available

**Specific Hazards Arising from the Chemical**

Fine dust dispersed in air may ignite. Thermal decomposition can lead to release of irritating gases and vapors. Keep product and empty container away from heat and sources of ignition.

**Hazardous Combustion Products**

Carbon monoxide (CO) Carbon dioxide (CO<sub>2</sub>) Nitrogen oxides (NO<sub>x</sub>)

**Protective Equipment and Precautions for Firefighters**

As in any fire, wear self-contained breathing apparatus pressure-demand, MSHA/NIOSH (approved or equivalent) and full protective gear.

**NFPA**

Health	Flammability	Instability	Physical hazards
2	1	0	N/A

**6. Accidental release measures**

**Personal Precautions** Use personal protective equipment. Ensure adequate ventilation. Avoid dust formation. Avoid contact with skin, eyes and clothing.

**Environmental Precautions** Should not be released into the environment.

**Methods for Containment and Clean Up** Sweep up or vacuum up spillage and collect in suitable container for disposal. Avoid dust formation.

**7. Handling and storage**

**Handling** Wear personal protective equipment. Ensure adequate ventilation. Avoid dust formation. Avoid contact with skin, eyes and clothing. Avoid ingestion and inhalation.

**Storage** Keep containers tightly closed in a dry, cool and well-ventilated place.

**8. Exposure controls / personal protection**

**Exposure Guidelines** This product does not contain any hazardous materials with occupational exposure limits established by the region specific regulatory bodies.

**Engineering Measures** Ensure adequate ventilation, especially in confined areas. Ensure that eyewash stations and safety showers are close to the workstation location.

**Personal Protective Equipment**

**Eye/face Protection** Wear appropriate protective eyeglasses or chemical safety goggles as described by OSHA's eye and face protection regulations in 29 CFR 1910.133 or European Standard EN166.

**Skin and body protection** Wear appropriate protective gloves and clothing to prevent skin exposure.

**Respiratory Protection** Follow the OSHA respirator regulations found in 29 CFR 1910.134 or European Standard EN 149. Use a NIOSH/MSHA or European Standard EN 149 approved respirator if exposure limits are exceeded or if irritation or other symptoms are experienced.

**Hygiene Measures** Handle in accordance with good industrial hygiene and safety practice.

**9. Physical and chemical properties**

<b>Physical State</b>	Solid
<b>Appearance</b>	Brown

Odor	Odorless
Odor Threshold	No information available
pH	No information available
Melting Point/Range	No data available
Boiling Point/Range	Not applicable
Flash Point	No information available
Evaporation Rate	No information available
Flammability (solid,gas)	No information available
Flammability or explosive limits	
Upper	No data available
Lower	No data available
Vapor Pressure	No information available
Vapor Density	No information available
Specific Gravity	No information available
Solubility	Soluble in water
Partition coefficient; n-octanol/water	No data available
Autoignition Temperature	No information available
Decomposition Temperature	No information available
Viscosity	No information available
Molecular Formula	C <sub>23</sub> H <sub>25</sub> N <sub>2</sub> Cl
Molecular Weight	364.92

## 10. Stability and reactivity

<b>Reactive Hazard</b>	None known, based on information available
<b>Stability</b>	Stable under normal conditions.
<b>Conditions to Avoid</b>	Avoid dust formation. Incompatible products. Excess heat.
<b>Incompatible Materials</b>	Strong oxidizing agents
<b>Hazardous Decomposition Products</b>	Carbon monoxide (CO), Carbon dioxide (CO <sub>2</sub> ), Nitrogen oxides (NO <sub>x</sub> )
<b>Hazardous Polymerization</b>	Hazardous polymerization does not occur.
<b>Hazardous Reactions</b>	None under normal processing.

## 11. Toxicological information

### Acute Toxicity

**Product Information** No acute toxicity information is available for this product

**Component Information**  
**Toxicologically Synergistic Products** No information available

### Delayed and immediate effects as well as chronic effects from short and long-term exposure

**Irritation** Severe eye irritant

**Sensitization** No information available

**Carcinogenicity** The table below indicates whether each agency has listed any ingredient as a carcinogen.

Component	CAS-No	IARC	NTP	ACGIH	OSHA	Mexico
Malachite green	569-64-2	Not listed	Not listed	Not listed	Not listed	Not listed

**Mutagenic Effects** No information available

**Reproductive Effects** No information available.

**Developmental Effects** No information available.

<b>Teratogenicity</b>	No information available.
<b>STOT - single exposure</b>	None known
<b>STOT - repeated exposure</b>	None known
<b>Aspiration hazard</b>	No information available
<b>Symptoms / effects, both acute and delayed</b>	No information available
<b>Endocrine Disruptor Information</b>	No information available
<b>Other Adverse Effects</b>	The toxicological properties have not been fully investigated.

## 12. Ecological information

### Ecotoxicity

Very toxic to aquatic organisms, may cause long-term adverse effects in the aquatic environment.

<b>Persistence and Degradability</b>	No information available
<b>Bioaccumulation/ Accumulation</b>	No information available.
<b>Mobility</b>	No information available.

## 13. Disposal considerations

**Waste Disposal Methods** Chemical waste generators must determine whether a discarded chemical is classified as a hazardous waste. Chemical waste generators must also consult local, regional, and national hazardous waste regulations to ensure complete and accurate classification.

## 14. Transport information

<b>DOT</b>	Not regulated
<b>TDG</b>	Not regulated
<b>IATA</b>	Not regulated
<b>IMDG/IMO</b>	Not regulated

## 15. Regulatory information

**All of the components in the product are on the following Inventory lists:** Australia X = listed China Canada Europe TSCA Korea Philippines Japan

### International Inventories

Component	TSCA	DSL	NDSL	EINECS	ELINCS	NLP	PICCS	ENCS	AICS	IECSC	KECL
Malachite green	X	X	-	209-322-8	-		X	X	X	X	X

#### Legend:

X - Listed

E - Indicates a substance that is the subject of a Section 5(e) Consent order under TSCA.

F - Indicates a substance that is the subject of a Section 5(f) Rule under TSCA.

N - Indicates a polymeric substance containing no free-radical initiator in its inventory name but is considered to cover the designated polymer made with any free-radical initiator regardless of the amount used.

P - Indicates a commenced PMN substance

R - Indicates a substance that is the subject of a Section 6 risk management rule under TSCA.

S - Indicates a substance that is identified in a proposed or final Significant New Use Rule

T - Indicates a substance that is the subject of a Section 4 test rule under TSCA.

XU - Indicates a substance exempt from reporting under the Inventory Update Rule, i.e. Partial Updating of the TSCA Inventory Data Base Production and Site Reports (40 CFR 710(B)).

Y1 - Indicates an exempt polymer that has a number-average molecular weight of 1,000 or greater.

Y2 - Indicates an exempt polymer that is a polyester and is made only from reactants included in a specified list of low concern reactants that comprises one of the eligibility criteria for the exemption rule.

**U.S. Federal Regulations**

TSCA 12(b) Not applicable

**SARA 313**

Component	CAS-No	Weight %	SARA 313 - Threshold Values %
Malachite green	569-64-2	100	1.0

SARA 311/312 Hazard Categories See section 2 for more information

CWA (Clean Water Act) Not applicable

Clean Air Act Not applicable

OSHA Occupational Safety and Health Administration  
Not applicable

CERCLA Not applicable

California Proposition 65 This product does not contain any Proposition 65 chemicals

**U.S. State Right-to-Know Regulations**

Component	Massachusetts	New Jersey	Pennsylvania	Illinois	Rhode Island
Malachite green	X	X	X	-	-

**U.S. Department of Transportation**Reportable Quantity (RQ): N  
DOT Marine Pollutant N  
DOT Severe Marine Pollutant N**U.S. Department of Homeland Security**

This product does not contain any DHS chemicals.

**Other International Regulations**

Mexico - Grade No information available

**16. Other information**Prepared By Regulatory Affairs  
Thermo Fisher Scientific  
Email: EMSDS.RA@thermofisher.com

Creation Date 07-Aug-2014

Revision Date 18-Jan-2018

Print Date 18-Jan-2018

Revision Summary This document has been updated to comply with the US OSHA HazCom 2012 Standard replacing the current legislation under 29 CFR 1910.1200 to align with the Globally Harmonized System of Classification and Labeling of Chemicals (GHS).

**Disclaimer**

The information provided in this Safety Data Sheet is correct to the best of our knowledge, information and belief at the date of its publication. The information given is designed only as a guidance for safe handling, use, processing, storage, transportation, disposal and release and is not to be considered a warranty or quality specification. The information relates only to the specific material designated and may not be valid for such material used in combination with any other materials or in any process, unless specified in the text

**End of SDS**

## SAFETY DATA SHEET

according to Occupational Safety And Health (Classification,  
Labelling And Safety Data Sheet Of Hazardous Chemicals)  
Regulations 2013 (CLASS 2013)

Revision Date 15.12.2017

Version 1.2

---

### SECTION 1. Identification of the substance/mixture and of the company/undertaking

#### 1.1 Product identifier

Catalogue No. 103883  
Product name Iron(III) nitrate nonahydrate for analysis EMSURE® ACS, Reag. Ph Eur

REACH Registration Number A registration number is not available for this substance as the substance or its use are exempted from registration according to Article 2 REACH Regulation (EC) No 1907/2006, the annual tonnage does not require a registration or the registration is envisaged for a later registration deadline.

CAS-No. 7782-61-8

#### 1.2 Relevant identified uses of the substance or mixture and uses advised against

Identified uses Reagent for analysis  
For additional information on uses please refer to the Merck Chemicals portal ([www.merckgroup.com](http://www.merckgroup.com)).

#### 1.3 Details of the supplier of the safety data sheet

Company Merck KGaA \* 64271 Darmstadt \*Germany\* Telefon:+49 6151 72-0  
Responsible Department LS-QHC \* e-mail: [prodsafe@merckgroup.com](mailto:prodsafe@merckgroup.com)  
Regional representation Merck Sdn. Bhd. (Co. No: 178145), No. 4, Jalan U1/26, Section U1,  
Hicom Glenmarie Industrial Park, 40150 Shah Alam, Selangor. Tel:  
03-74943688 Fax: 03-74910850

**1.4 Emergency telephone Customer Call Centre: + 62 0800 140 1253 (Toll Free)**



# SAFETY DATA SHEET

according to Occupational Safety And Health (Classification,  
Labelling And Safety Data Sheet Of Hazardous Chemicals)  
Regulations 2013 (CLASS 2013)

Catalogue No.	103883
Product name	Iron(III) nitrate nonahydrate for analysis EMSURE® ACS,Reag. Ph Eur

---

number

---

## SECTION 2. Hazards identification

### 2.1 Classification of the substance or mixture

#### Classification according to CLASS regulations 2013

Skin irritation, Category 2, H315

Eye irritation, Category 2, H319

For the full text of the H-Statements mentioned in this Section, see Section 16.

### 2.2 Label elements

#### Labelling according to CLASS regulations 2013

##### *Hazard pictograms*



##### *Signal word*

Warning

##### *Hazard statements*

H315 Causes skin irritation.

H319 Causes serious eye irritation.

##### *Precautionary statements*

Response

P302 + P352 IF ON SKIN: Wash with plenty of soap and water.

P305 + P351 + P338 IF IN EYES: Rinse cautiously with water for several minutes. Remove contact lenses, if present and easy to do. Continue rinsing.

# SAFETY DATA SHEET

according to Occupational Safety And Health (Classification,  
Labelling And Safety Data Sheet Of Hazardous Chemicals)  
Regulations 2013 (CLASS 2013)

Catalogue No. 103883  
Product name Iron(III) nitrate nonahydrate for analysis EMSURE® ACS, Reag. Ph Eur

---

## Reduced labelling (≤125 ml)

*Hazard pictograms*



*Signal word*

Warning

CAS-No. 7782-61-8

## 2.3 Other hazards

None known.

---

## SECTION 3. Composition/information on ingredients

### 3.1 Substance

Formula	Fe(NO <sub>3</sub> ) <sub>3</sub> * 9 H <sub>2</sub> O	FeN <sub>3</sub> O <sub>9</sub> * 9 H <sub>2</sub> O FeN <sub>3</sub> O <sub>9</sub> * 9 H <sub>2</sub> O (Hill)
EC-No.	233-899-5	
Molar mass	403.95 g/mol	

### Hazardous components according to CLASS regulations 2013

*Chemical name (Concentration)*

CAS-No.	Registration number	Classification
---------	---------------------	----------------

Eisentrinitrat-Nonahydrat (>= 80 % - <= 100 % )

7782-61-8	*)	
-----------	----	--

Skin irritation, Category 2, H315

Eye irritation, Category 2, H319

\*) A registration number is not available for this substance as the substance or its use are exempted from registration according to Article 2 REACH Regulation (EC) No 1907/2006, the annual tonnage does not require a registration or the registration is envisaged for a later registration deadline.

# SAFETY DATA SHEET

according to Occupational Safety And Health (Classification,  
Labelling And Safety Data Sheet Of Hazardous Chemicals)  
Regulations 2013 (CLASS 2013)

Catalogue No.	103883
Product name	Iron(III) nitrate nonahydrate for analysis EMSURE® ACS, Reag. Ph Eur

---

For the full text of the H-Statements mentioned in this Section, see Section 16.

## 3.2 Mixture

Not applicable

---

## SECTION 4. First aid measures

### 4.1 Description of first aid measures

After inhalation: fresh air.

In case of skin contact: Take off immediately all contaminated clothing. Rinse skin with water/  
shower.

After eye contact: rinse out with plenty of water. Call in ophthalmologist. Remove contact lenses.

After swallowing: immediately make victim drink water (two glasses at most). Consult a  
physician.

### 4.2 Most important symptoms and effects, both acute and delayed

The following applies to nitrites/nitrates in general: methaemoglobinaemia after the uptake of  
large quantities.

The following applies to soluble iron compounds: nausea and vomiting after swallowing. The  
absorption of large quantities is followed by cardiovascular disorders. Toxic effect on liver and  
kidneys.

irritant effects, gastric pain, bloody diarrhoea, Nausea, Vomiting, collapse

### 4.3 Indication of any immediate medical attention and special treatment needed

No information available.

---

## SECTION 5. Firefighting measures

### 5.1 Extinguishing media

*Suitable extinguishing media*

---

# SAFETY DATA SHEET

according to Occupational Safety And Health (Classification,  
Labelling And Safety Data Sheet Of Hazardous Chemicals)  
Regulations 2013 (CLASS 2013)

Catalogue No.	103883
Product name	Iron(III) nitrate nonahydrate for analysis EMSURE® ACS, Reag. Ph Eur

---

Use extinguishing measures that are appropriate to local circumstances and the surrounding environment.

### *Unsuitable extinguishing media*

For this substance/mixture no limitations of extinguishing agents are given.

## 5.2 Special hazards arising from the substance or mixture

Not combustible.

Has a fire-promoting effect due to release of oxygen.

Ambient fire may liberate hazardous vapours.

Fire may cause evolution of:

nitrous gases, nitrogen oxides

## 5.3 Advice for firefighters

### *Special protective equipment for firefighters*

Stay in danger area only with self-contained breathing apparatus. Prevent skin contact by keeping a safe distance or by wearing suitable protective clothing.

### *Further information*

Suppress (knock down) gases/vapours/mists with a water spray jet. Prevent fire extinguishing water from contaminating surface water or the ground water system.

---

## SECTION 6. Accidental release measures

### 6.1 Personal precautions, protective equipment and emergency procedures

Advice for non-emergency personnel: Avoid inhalation of dusts. Avoid substance contact. Ensure adequate ventilation. Evacuate the danger area, observe emergency procedures, consult an expert.

Advice for emergency responders:

Protective equipment see section 8.

### 6.2 Environmental precautions

# SAFETY DATA SHEET

according to Occupational Safety And Health (Classification,  
Labelling And Safety Data Sheet Of Hazardous Chemicals)  
Regulations 2013 (CLASS 2013)

Catalogue No.	103883
Product name	Iron(III) nitrate nonahydrate for analysis EMSURE® ACS, Reag. Ph Eur

---

Do not let product enter drains.

## 6.3 Methods and materials for containment and cleaning up

Cover drains. Collect, bind, and pump off spills. Observe possible material restrictions (see sections 7 and 10). Take up dry. Dispose of properly. Clean up affected area. Avoid generation of dusts.

## 6.4 Reference to other sections

Indications about waste treatment see section 13.

---

## SECTION 7. Handling and storage

### 7.1 Precautions for safe handling

#### *Advice on safe handling*

Observe label precautions.

#### *Hygiene measures*

Immediately change contaminated clothing. Apply preventive skin protection. Wash hands and face after working with substance.

### 7.2 Conditions for safe storage, including any incompatibilities

#### *Storage conditions*

Protected from light.

Tightly closed. Do not store near combustible materials.

Recommended storage temperature see product label.

### 7.3 Specific end use(s)

Apart from the uses mentioned in section 1.2 no other specific uses are stipulated.

---

## SECTION 8. Exposure controls/personal protection

### 8.1 Control parameters

---

The Safety Data Sheets for catalogue items are available at [www.merckgroup.com](http://www.merckgroup.com)

# SAFETY DATA SHEET

according to Occupational Safety And Health (Classification,  
Labelling And Safety Data Sheet Of Hazardous Chemicals)  
Regulations 2013 (CLASS 2013)

Catalogue No. 103883

Product name Iron(III) nitrate nonahydrate for analysis EMSURE® ACS, Reag. Ph Eur

---

## *Eisentrinitrat-Nonahydrat (7782-61-8)*

MY OEL Time Weighted Average 1 mg/m<sup>3</sup> Expressed as: as Fe  
(TWA):

## 8.2 Exposure controls

### Engineering measures

Technical measures and appropriate working operations should be given priority over the use of personal protective equipment.

See section 7.1.

### Individual protection measures

Protective clothing needs to be selected specifically for the workplace, depending on concentrations and quantities of the hazardous substances handled. The chemical resistance of the protective equipment should be enquired at the respective supplier.

#### *Eye/face protection*

Safety glasses

#### *Hand protection*

full contact:

Glove material:	Nitrile rubber
Glove thickness:	0.11 mm
Break through time:	> 480 min

splash contact:

Glove material:	Nitrile rubber
Glove thickness:	0.11 mm
Break through time:	> 480 min

The protective gloves to be used must comply with the specifications of EC Directive 89/686/EEC and the related standard EN374, for example KCL 741 Dermatril® L (full contact), KCL 741 Dermatril® L (splash contact).

# SAFETY DATA SHEET

according to Occupational Safety And Health (Classification,  
Labelling And Safety Data Sheet Of Hazardous Chemicals)  
Regulations 2013 (CLASS 2013)

Catalogue No. 103883  
Product name Iron(III) nitrate nonahydrate for analysis EMSURE® ACS, Reag. Ph Eur

---

The breakthrough times stated above were determined by KCL in laboratory tests acc. to EN374 with samples of the recommended glove types.

This recommendation applies only to the product stated in the safety data sheet(>,<)> supplied by us and for the designated use. When dissolving in or mixing with other substances and under conditions deviating from those stated in EN374 please contact the supplier of CE-approved gloves (e.g. KCL GmbH, D-36124 Eichenzell, Internet: [www.kcl.de](http://www.kcl.de)).

#### *Other protective equipment*

protective clothing

#### *Respiratory protection*

required when dusts are generated.

Recommended Filter type: Filter P 2 (acc. to DIN 3181) for solid and liquid particles of harmful substances

The entrepreneur has to ensure that maintenance, cleaning and testing of respiratory protective devices are carried out according to the instructions of the producer. These measures have to be properly documented.

#### **Environmental exposure controls**

Do not let product enter drains.

---

## **SECTION 9. Physical and chemical properties**

### **9.1 Information on basic physical and chemical properties**

Form	solid
Colour	light blue
Odour	of nitric acid
Odour Threshold	No information available.

# SAFETY DATA SHEET

according to Occupational Safety And Health (Classification,  
Labelling And Safety Data Sheet Of Hazardous Chemicals)  
Regulations 2013 (CLASS 2013)

Catalogue No. 103883  
Product name Iron(III) nitrate nonahydrate for analysis EMSURE® ACS, Reag. Ph Eur

---

pH	ca. 1.3 at 100 g/l 20 °C
Melting point	47 °C
Boiling point	No information available.
Flash point	Not applicable
Evaporation rate	No information available.
Flammability (solid, gas)	The product is not flammable.
Lower explosion limit	Not applicable
Upper explosion limit	Not applicable
Vapour pressure	No information available.
Relative vapour density	No information available.
Density	1.68 g/cm <sup>3</sup> at 20 °C
Relative density	No information available.
Water solubility	at 20 °C soluble
Partition coefficient: n- octanol/water	No information available.



# SAFETY DATA SHEET

according to Occupational Safety And Health (Classification,  
Labelling And Safety Data Sheet Of Hazardous Chemicals)  
Regulations 2013 (CLASS 2013)

Catalogue No.	103883
Product name	Iron(III) nitrate nonahydrate for analysis EMSURE® ACS, Reag. Ph Eur

---

Auto-ignition temperature	No information available.
Decomposition temperature	ca.100 °C Elimination of water of crystallisation  ca.125 °C decomposes
Viscosity, dynamic	No information available.
Explosive properties	Not classified as explosive.
Oxidizing properties	No information available.

## 9.2 Other data

Ignition temperature	Not applicable
Bulk density	ca.900 kg/m <sup>3</sup>

---

## SECTION 10. Stability and reactivity

### 10.1 Reactivity

See section 10.3

### 10.2 Chemical stability

sensitive to moisture

Sensitivity to light

### 10.3 Possibility of hazardous reactions

Risk of explosion with:

dimethyl sulfoxide, Reducing agents

# SAFETY DATA SHEET

according to Occupational Safety And Health (Classification,  
Labelling And Safety Data Sheet Of Hazardous Chemicals)  
Regulations 2013 (CLASS 2013)

Catalogue No.	103883
Product name	Iron(III) nitrate nonahydrate for analysis EMSURE® ACS, Reag. Ph Eur

---

increased reactivity with:  
organic combustible substances, Powdered metals

## 10.4 Conditions to avoid

Strong heating (decomposition).

## 10.5 Incompatible materials

no information available

## 10.6 Hazardous decomposition products

in the event of fire: See section 5.

---

## SECTION 11. Toxicological information

### 11.1 Information on toxicological effects

#### *Acute oral toxicity*

LD50 Rat: 3,250 mg/kg

(RTECS)

Symptoms: Irritations of mucous membranes in the mouth, pharynx, oesophagus and gastrointestinal tract., Nausea, Vomiting

#### *Acute inhalation toxicity*

Symptoms: Possible damages:, mucosal irritations

#### *Acute dermal toxicity*

This information is not available.

#### *Skin irritation*

Causes skin irritation.

#### *Eye irritation*

Causes serious eye irritation.

# SAFETY DATA SHEET

according to Occupational Safety And Health (Classification,  
Labelling And Safety Data Sheet Of Hazardous Chemicals)  
Regulations 2013 (CLASS 2013)

Catalogue No.	103883
Product name	Iron(III) nitrate nonahydrate for analysis EMSURE® ACS, Reag. Ph Eur

---

## *Sensitisation*

This information is not available.

## *Germ cell mutagenicity*

This information is not available.

## *Carcinogenicity*

This information is not available.

## *Reproductive toxicity*

This information is not available.

## *Teratogenicity*

This information is not available.

## *Specific target organ toxicity - single exposure*

This information is not available.

## *Specific target organ toxicity - repeated exposure*

This information is not available.

## *Aspiration hazard*

This information is not available.

## 11.2 Further information

After absorption:

gastric pain, bloody diarrhoea, Circulatory collapse

The following applies to nitrites/nitrates in general: methaemoglobinaemia after the uptake of large quantities.

The following applies to soluble iron compounds: nausea and vomiting after swallowing. The absorption of large quantities is followed by cardiovascular disorders. Toxic effect on liver and kidneys.

Other dangerous properties can not be excluded.

Handle in accordance with good industrial hygiene and safety practice.

---

## SECTION 12. Ecological information

# SAFETY DATA SHEET

according to Occupational Safety And Health (Classification,  
Labelling And Safety Data Sheet Of Hazardous Chemicals)  
Regulations 2013 (CLASS 2013)

Catalogue No. 103883

Product name Iron(III) nitrate nonahydrate for analysis EMSURE® ACS, Reag. Ph Eur

---

## 12.1 Toxicity

No information available.

## 12.2 Persistence and degradability

No information available.

## 12.3 Bioaccumulative potential

No information available.

## 12.4 Mobility in soil

No information available.

## 12.5 Results of PBT and vPvB assessment

PBT/vPvB assessment not available as chemical safety assessment not required/not conducted.

## 12.6 Other adverse effects

*Additional ecological information*

Discharge into the environment must be avoided.

# SAFETY DATA SHEET

according to Occupational Safety And Health (Classification,  
Labelling And Safety Data Sheet Of Hazardous Chemicals)  
Regulations 2013 (CLASS 2013)

Catalogue No. 103883  
Product name Iron(III) nitrate nonahydrate for analysis EMSURE® ACS, Reag. Ph Eur

---

---

## SECTION 13. Disposal considerations

### *Waste treatment methods*

Waste material must be disposed of in accordance with the national and local regulations. Leave chemicals in original containers. No mixing with other waste. Handle uncleaned containers like the product itself.

See [www.retrologistik.com](http://www.retrologistik.com) for processes regarding the return of chemicals and containers, or contact us there if you have further questions.

According to Quality Environment Regulation (Scheduled Waste) 2005, waste need to be sent to designated premise for recycle, treatment or disposal. Please contact Kualiti Alam for waste classification and correct disposal method.

---

## SECTION 14. Transport information

### Land transport (ADR/RID)

14.1 UN number	UN 1466
14.2 Proper shipping name	FERRIC NITRATE
14.3 Class	5.1
14.4 Packing group	III
14.5 Environmentally hazardous	--
14.6 Special precautions for user	yes
Tunnel restriction code	E

### Inland waterway transport (ADN)

Not relevant

### Air transport (IATA)

# SAFETY DATA SHEET

according to Occupational Safety And Health (Classification,  
Labelling And Safety Data Sheet Of Hazardous Chemicals)  
Regulations 2013 (CLASS 2013)

Catalogue No.	103883
Product name	Iron(III) nitrate nonahydrate for analysis EMSURE® ACS, Reag. Ph Eur

---

14.1 UN number	UN 1466
14.2 Proper shipping name	FERRIC NITRATE
14.3 Class	5.1
14.4 Packing group	III
14.5 Environmentally hazardous	--
14.6 Special precautions for user	no

## Sea transport (IMDG)

14.1 UN number	UN 1466
14.2 Proper shipping name	FERRIC NITRATE
14.3 Class	5.1
14.4 Packing group	III
14.5 Environmentally hazardous	--
14.6 Special precautions for user	yes

EmS F-A S-Q

14.7 Transport in bulk according to Annex II of MARPOL 73/78 and the IBC Code  
Not relevant

---

## SECTION 15. Regulatory information

### 15.1 Safety, health and environmental regulations/legislation specific for the substance or mixture

All national and local regulations, including Occupational Safety and Health (Classification, Labelling and Safety Data Sheet of Hazardous Chemicals) Regulations 2013, if applicable to the use, should be observed.

#### *National legislation*

Storage class 5.1B

### 15.2 Chemical safety assessment

# SAFETY DATA SHEET

according to Occupational Safety And Health (Classification,  
Labelling And Safety Data Sheet Of Hazardous Chemicals)  
Regulations 2013 (CLASS 2013)

Catalogue No. 103883  
Product name Iron(III) nitrate nonahydrate for analysis EMSURE® ACS, Reag. Ph Eur

---

For this product a chemical safety assessment was not carried out.

---

## SECTION 16. Other information

### Full text of H-Statements referred to under sections 2 and 3.

H315 Causes skin irritation.  
H319 Causes serious eye irritation.

### Training advice

Provide adequate information, instruction and training for operators.

### Labelling

#### *Hazard pictograms*



#### *Signal word*

Warning

#### *Hazard statements*

H315 Causes skin irritation.  
H319 Causes serious eye irritation.

#### *Precautionary statements*

##### Response

P302 + P352 IF ON SKIN: Wash with plenty of soap and water.

P305 + P351 + P338 IF IN EYES: Rinse cautiously with water for several minutes. Remove contact lenses, if present and easy to do. Continue rinsing.

P313 Get medical advice/ attention.

# SAFETY DATA SHEET

according to Occupational Safety And Health (Classification,  
Labelling And Safety Data Sheet Of Hazardous Chemicals)  
Regulations 2013 (CLASS 2013)

Catalogue No. 103883

Product name Iron(III) nitrate nonahydrate for analysis EMSURE® ACS, Reag. Ph Eur

---

## Key or legend to abbreviations and acronyms used in the safety data sheet

Used abbreviations and acronyms can be looked up at [www.wikipedia.org](http://www.wikipedia.org).

## Regional representation

Merck Sdn. Bhd. (Co. No: 178145), No. 4, Jalan U1/26, Section U1, Hicom Glenmarie Industrial Park, 40150 Shah Alam, Selangor. Tel: 03-74943688 Fax: 03-74910850

---

*The information contained herein is based on the present state of our knowledge. It characterises the product with regard to the appropriate safety precautions. It does not represent a guarantee of any properties of the product.*



## SAFETY DATA SHEET

Creation Date 28-Oct-2009

Revision Date 17-Jan-2018

Revision Number 7

### 1. Identification

**Product Name** Hydrogen peroxide, 30%

**Cat No. :** H325-4; H325-4LC; H325-30GAL; H325-100; H325-500; H325-500LC

**CAS-No** 7722-84-1

**Synonyms** Hydrogen Dioxide; Peroxide; Carbamide Peroxide

**Recommended Use** Laboratory chemicals.

**Uses advised against** Not for food, drug, pesticide or biocidal product use

#### Details of the supplier of the safety data sheet

##### Company

Fisher Scientific  
One Reagent Lane  
Fair Lawn, NJ 07410  
Tel: (201) 796-7100

##### **Emergency Telephone Number**

CHEMTREC®, Inside the USA: 800-424-9300  
CHEMTREC®, Outside the USA: 001-703-527-3887

### 2. Hazard(s) identification

#### Classification

This chemical is considered hazardous by the 2012 OSHA Hazard Communication Standard (29 CFR 1910.1200)

Oxidizing liquids	Category 2
Acute oral toxicity	Category 4
Serious Eye Damage/Eye Irritation	Category 1

#### Label Elements

##### **Signal Word**

Danger

##### **Hazard Statements**

May intensify fire; oxidizer  
Harmful if swallowed  
Causes serious eye damage



**Precautionary Statements****Prevention**

Wash face, hands and any exposed skin thoroughly after handling  
 Do not eat, drink or smoke when using this product  
 Wear protective gloves/protective clothing/eye protection/face protection  
 Keep away from heat/sparks/open flames/hot surfaces. - No smoking  
 Keep/Store away from clothing/ other combustible materials  
 Take any precaution to avoid mixing with combustibles

**Eyes**

IF IN EYES: Rinse cautiously with water for several minutes. Remove contact lenses, if present and easy to do. Continue rinsing  
 Immediately call a POISON CENTER or doctor/physician

**Ingestion**

IF SWALLOWED: Call a POISON CENTER or doctor/physician if you feel unwell  
 Rinse mouth

**Fire**

In case of fire: Use CO<sub>2</sub>, dry chemical, or foam for extinction

**Disposal**

Dispose of contents/container to an approved waste disposal plant

**Hazards not otherwise classified (HNOC)**

None identified

### 3. Composition/Information on Ingredients

Component	CAS-No	Weight %
Water	7732-18-5	65 - 80
Hydrogen peroxide	7722-84-1	20 - 35

### 4. First-aid measures

<b>General Advice</b>	If symptoms persist, call a physician.
<b>Eye Contact</b>	Rinse immediately with plenty of water, also under the eyelids, for at least 15 minutes. Get medical attention.
<b>Skin Contact</b>	Wash off immediately with plenty of water for at least 15 minutes. If skin irritation persists, call a physician.
<b>Inhalation</b>	Move to fresh air. If not breathing, give artificial respiration. Get medical attention if symptoms occur.
<b>Ingestion</b>	Clean mouth with water and drink afterwards plenty of water.
<b>Most important symptoms and effects</b>	Causes severe eye damage.
<b>Notes to Physician</b>	Treat symptomatically

### 5. Fire-fighting measures

<b>Suitable Extinguishing Media</b>	Use water spray or fog; do not use straight streams.
<b>Unsuitable Extinguishing Media</b>	No information available
<b>Flash Point</b>	No information available
<b>Method -</b>	No information available
<b>Autoignition Temperature</b>	No information available
<b>Explosion Limits</b>	

Upper	100%
Lower	40%
<b>Oxidizing Properties</b>	Oxidizer

**Sensitivity to Mechanical Impact** No information available  
**Sensitivity to Static Discharge** No information available

#### Specific Hazards Arising from the Chemical

Corrosive Material. Containers may explode when heated. Oxidizer: Contact with combustible/organic material may cause fire. In the event of fire and/or explosion do not breathe fumes. Thermal decomposition can lead to release of irritating gases and vapors. May ignite combustibles (wood paper, oil, clothing, etc.).

#### Hazardous Combustion Products

Hydrogen oxygen

#### Protective Equipment and Precautions for Firefighters

As in any fire, wear self-contained breathing apparatus pressure-demand, MSHA/NIOSH (approved or equivalent) and full protective gear.

#### NFPA

<b>Health</b>	<b>Flammability</b>	<b>Instability</b>	<b>Physical hazards</b>
3	0	1	OX

### 6. Accidental release measures

**Personal Precautions** Ensure adequate ventilation. Use personal protective equipment.

Do not use steel or aluminum tools or equipment

**Environmental Precautions** Should not be released into the environment. Do not flush into surface water or sanitary sewer system.

**Methods for Containment and Clean Up** Soak up with inert absorbent material. Keep in suitable, closed containers for disposal. Sweep up and shovel into suitable containers for disposal.

### 7. Handling and storage

**Handling** Wear personal protective equipment. Do not get in eyes, on skin, or on clothing. Avoid ingestion and inhalation. Ensure adequate ventilation. Keep away from clothing and other combustible materials.

**Storage** Keep containers tightly closed in a dry, cool and well-ventilated place. To maintain product quality. Keep refrigerated. Keep away from direct sunlight. Do not store in metal containers. Containers should be vented periodically in order to overcome pressure buildup. Do not store near combustible materials.

### 8. Exposure controls / personal protection

#### Exposure Guidelines

Component	ACGIH TLV	OSHA PEL	NIOSH IDLH	Mexico OEL (TWA)
Hydrogen peroxide	TWA: 1 ppm	(Vacated) TWA: 1 ppm (Vacated) TWA: 1.4 mg/m <sup>3</sup> TWA: 1 ppm TWA: 1.4 mg/m <sup>3</sup>	IDLH: 75 ppm TWA: 1 ppm TWA: 1.4 mg/m <sup>3</sup>	TWA: 1 ppm TWA: 1.5 mg/m <sup>3</sup> STEL: 2 ppm STEL: 3 mg/m <sup>3</sup>

#### Legend

ACGIH - American Conference of Governmental Industrial Hygienists

OSHA - Occupational Safety and Health Administration

NIOSH IDLH: The National Institute for Occupational Safety and Health Immediately Dangerous to Life or Health

#### Engineering Measures

Ensure that eyewash stations and safety showers are close to the workstation location.  
 Ensure adequate ventilation, especially in confined areas.

**Personal Protective Equipment**

<b>Eye/face Protection</b>	Wear appropriate protective eyeglasses or chemical safety goggles as described by OSHA's eye and face protection regulations in 29 CFR 1910.133 or European Standard EN166.
<b>Skin and body protection</b>	Long sleeved clothing.
<b>Respiratory Protection</b>	Follow the OSHA respirator regulations found in 29 CFR 1910.134 or European Standard EN 149. Use a NIOSH/MSHA or European Standard EN 149 approved respirator if exposure limits are exceeded or if irritation or other symptoms are experienced.
<b>Hygiene Measures</b>	Handle in accordance with good industrial hygiene and safety practice.

**9. Physical and chemical properties**

<b>Physical State</b>	Liquid
<b>Appearance</b>	Colorless
<b>Odor</b>	Slight
<b>Odor Threshold</b>	No information available
<b>pH</b>	3.3
<b>Melting Point/Range</b>	-33 °C / -27.4 °F
<b>Boiling Point/Range</b>	108 °C / 226.4 °F @ 760 mmHg
<b>Flash Point</b>	No information available
<b>Evaporation Rate</b>	1.0 (Butyl acetate = 1.0)
<b>Flammability (solid,gas)</b>	Not applicable
<b>Flammability or explosive limits</b>	
<b>Upper</b>	100%
<b>Lower</b>	40%
<b>Vapor Pressure</b>	No information available
<b>Vapor Density</b>	1.10
<b>Specific Gravity</b>	1.110
<b>Solubility</b>	Soluble in water
<b>Partition coefficient; n-octanol/water</b>	No data available
<b>Autoignition Temperature</b>	No information available
<b>Decomposition Temperature</b>	> 125°C
<b>Viscosity</b>	No information available

**10. Stability and reactivity**

<b>Reactive Hazard</b>	Yes
<b>Stability</b>	Sensitivity to light. Oxidizer: Contact with combustible/organic material may cause fire.
<b>Conditions to Avoid</b>	Incompatible products. Excess heat. Exposure to light. Combustible material.
<b>Incompatible Materials</b>	Strong oxidizing agents, Metals, Reducing agents, Alcohols, Ammonia, copper, Copper alloys, lead oxides, Cyanides, Sulfides, lead, Acetone, Aluminium, , Strong reducing agents, Combustible material
<b>Hazardous Decomposition Products</b>	Hydrogen, oxygen
<b>Hazardous Polymerization</b>	Hazardous polymerization does not occur.
<b>Hazardous Reactions</b>	None under normal processing.

**11. Toxicological information****Acute Toxicity**

**Product Information****Oral LD50**

Category 4. ATE = 300 - 2000 mg/kg.

**Dermal LD50**

Based on ATE data, the classification criteria are not met. ATE &gt; 2000 mg/kg.

**Vapor LC50**

Based on ATE data, the classification criteria are not met. ATE &gt; 20 mg/l.

**Component Information**

Component	LD50 Oral	LD50 Dermal	LC50 Inhalation
Water	-	Not listed	Not listed
Hydrogen peroxide	376 mg/kg ( Rat ) (90%) 910 mg/kg ( Rat ) (20-60%) 1518 mg/kg ( Rat ) (8-20% sol)	>2000 mg/kg ( Rabbit )	LC50 = 2 g/m <sup>3</sup> ( Rat ) 4 h

**Toxicologically Synergistic Products**

No information available

**Delayed and immediate effects as well as chronic effects from short and long-term exposure****Irritation**

Causes severe eye burns May cause irritation

**Sensitization**

No information available

**Carcinogenicity**

The table below indicates whether each agency has listed any ingredient as a carcinogen.

Component	CAS-No	IARC	NTP	ACGIH	OSHA	Mexico
Water	7732-18-5	Not listed	Not listed	Not listed	Not listed	Not listed
Hydrogen peroxide	7722-84-1	Not listed	Not listed	A3	Not listed	A3

*IARC: (International Agency for Research on Cancer)**IARC: (International Agency for Research on Cancer)**Group 1 - Carcinogenic to Humans**Group 2A - Probably Carcinogenic to Humans**Group 2B - Possibly Carcinogenic to Humans**A1 - Known Human Carcinogen**A2 - Suspected Human Carcinogen**A3 - Animal Carcinogen**ACGIH: (American Conference of Governmental Industrial Hygienists)**ACGIH: (American Conference of Governmental Industrial Hygienists)**Mexico - Occupational Exposure Limits - Carcinogens**A1 - Confirmed Human Carcinogen**A2 - Suspected Human Carcinogen**A3 - Confirmed Animal Carcinogen**A4 - Not Classifiable as a Human Carcinogen**A5 - Not Suspected as a Human Carcinogen**Mexico - Occupational Exposure Limits - Carcinogens***Mutagenic Effects**

No information available

**Reproductive Effects**

No information available.

**Developmental Effects**

No information available.

**Teratogenicity**

No information available.

**STOT - single exposure**

None known

**STOT - repeated exposure**

None known

**Aspiration hazard**

No information available

**Symptoms / effects, both acute and delayed**

No information available

**Endocrine Disruptor Information**

No information available

**Other Adverse Effects**

The toxicological properties have not been fully investigated.

**12. Ecological information****Ecotoxicity**

Contains a substance which is: Harmful to aquatic organisms, may cause long-term adverse effects in the aquatic environment.

Component	Freshwater Algae	Freshwater Fish	Microtox	Water Flea
-----------	------------------	-----------------	----------	------------

Hydrogen peroxide	EC50 2.5 mg/L/72h	LC50: 16.4 mg/L/96h (P.promelas)	Not listed	EC50 7.7 mg/L/24h
-------------------	-------------------	-------------------------------------	------------	-------------------

**Persistence and Degradability** Persistence is unlikely Decomposes Soluble in water based on information available.

**Bioaccumulation/ Accumulation** No information available.

**Mobility** Will likely be mobile in the environment due to its water solubility.

Component	log Pow
Hydrogen peroxide	-1.1

### 13. Disposal considerations

**Waste Disposal Methods** Chemical waste generators must determine whether a discarded chemical is classified as a hazardous waste. Chemical waste generators must also consult local, regional, and national hazardous waste regulations to ensure complete and accurate classification.

### 14. Transport information

#### DOT

UN-No UN2014  
 Proper Shipping Name HYDROGEN PEROXIDE, AQUEOUS SOLUTIONS  
 Hazard Class 5.1  
 Subsidiary Hazard Class 8  
 Packing Group II

#### TDG

UN-No UN2014  
 Proper Shipping Name HYDROGEN PEROXIDE, AQUEOUS SOLUTIONS  
 Hazard Class 5.1  
 Subsidiary Hazard Class 8  
 Packing Group II

#### IATA

UN-No UN2014  
 Proper Shipping Name HYDROGEN PEROXIDE, AQUEOUS SOLUTION  
 Hazard Class 5.1  
 Subsidiary Hazard Class 8  
 Packing Group II

#### IMDG/IMO

UN-No UN2014  
 Proper Shipping Name HYDROGEN PEROXIDE, AQUEOUS SOLUTION  
 Hazard Class 5.1  
 Subsidiary Hazard Class 8  
 Packing Group II

### 15. Regulatory information

All of the components in the product are on the following Inventory lists: X = listed

#### International Inventories

Component	TSCA	DSL	NDSL	EINECS	ELINCS	NLP	PICCS	ENCS	AICS	IECSC	KECL
Water	X	X	-	231-791-2	-		X	-	X	X	X
Hydrogen peroxide	X	X	-	231-765-0	-		X	X	X	X	X

#### Legend:

X - Listed

E - Indicates a substance that is the subject of a Section 5(e) Consent order under TSCA.

F - Indicates a substance that is the subject of a Section 5(f) Rule under TSCA.

N - Indicates a polymeric substance containing no free-radical initiator in its inventory name but is considered to cover the designated polymer made with any free-radical initiator regardless of the amount used.

P - Indicates a commenced PMN substance

R - Indicates a substance that is the subject of a Section 6 risk management rule under TSCA.

S - Indicates a substance that is identified in a proposed or final Significant New Use Rule

T - Indicates a substance that is the subject of a Section 4 test rule under TSCA.

XU - Indicates a substance exempt from reporting under the Inventory Update Rule, i.e. Partial Updating of the TSCA Inventory Data Base Production and Site Reports (40 CFR 710(B)).

Y1 - Indicates an exempt polymer that has a number-average molecular weight of 1,000 or greater.

Y2 - Indicates an exempt polymer that is a polyester and is made only from reactants included in a specified list of low concern reactants that comprises one of the eligibility criteria for the exemption rule.

### U.S. Federal Regulations

<b>TSCA 12(b)</b>	Not applicable
<b>SARA 313</b>	Not applicable
<b>SARA 311/312 Hazard Categories</b>	See section 2 for more information
<b>CWA (Clean Water Act)</b>	Not applicable
<b>Clean Air Act</b>	Not applicable
<b>OSHA Occupational Safety and Health Administration</b>	

Component	Specifically Regulated Chemicals	Highly Hazardous Chemicals
Hydrogen peroxide	-	TQ: 7500 lb

**CERCLA** This material, as supplied, contains one or more substances regulated as a hazardous substance under the Comprehensive Environmental Response Compensation and Liability Act (CERCLA) (40 CFR 302)

Component	Hazardous Substances RQs	CERCLA EHS RQs
Hydrogen peroxide	-	1000 lb

**California Proposition 65** This product does not contain any Proposition 65 chemicals

### U.S. State Right-to-Know Regulations

Component	Massachusetts	New Jersey	Pennsylvania	Illinois	Rhode Island
Water	-	-	X	-	-
Hydrogen peroxide	X	X	X	-	X

### U.S. Department of Transportation

Reportable Quantity (RQ):	N
DOT Marine Pollutant	N
DOT Severe Marine Pollutant	N

### U.S. Department of Homeland Security

This product contains the following DHS chemicals:

Component	DHS Chemical Facility Anti-Terrorism Standard
Hydrogen peroxide	2000 lb STQ (concentration of at least 30%)

### Other International Regulations

**Mexico - Grade** No information available

## 16. Other information

**Prepared By** Regulatory Affairs  
Thermo Fisher Scientific  
Email: EMSDS.RA@thermofisher.com

**Creation Date** 28-Oct-2009  
**Revision Date** 17-Jan-2018

**Print Date**

17-Jan-2018

**Revision Summary**

This document has been updated to comply with the US OSHA HazCom 2012 Standard replacing the current legislation under 29 CFR 1910.1200 to align with the Globally Harmonized System of Classification and Labeling of Chemicals (GHS).

**Disclaimer**

The information provided in this Safety Data Sheet is correct to the best of our knowledge, information and belief at the date of its publication. The information given is designed only as a guidance for safe handling, use, processing, storage, transportation, disposal and release and is not to be considered a warranty or quality specification. The information relates only to the specific material designated and may not be valid for such material used in combination with any other materials or in any process, unless specified in the text

**End of SDS**



---

### 1. SECTION 1: Identification of the hazardous chemical and of the supplier

#### 1.1 Product identifiers

Product name : Potassium iodide

Product Number : P4286

Brand : Sigma

#### 1.2 Other means of identification

No data available

#### 1.3 Recommended use of the chemical and restrictions on use

For R&D use only. Not for pharmaceutical, household or other uses.

#### 1.4 Details of the supplier of the safety data sheet

Company : Merck Sdn. Bhd. Malaysia  
Level 3, Menara Sunway Annexe Jalan  
Lagoon Timur (PJS9/1)  
Bandar Sunway  
Petaling Jaya  
46150 SELANGOR DARUL EHSAN  
MALAYSIA

Telephone : +60 3 7494 3688

Fax : +60 3 7491 0850

#### 1.5 Emergency telephone number

Emergency Phone # : +62 08001401253

---

### 2. HAZARDS IDENTIFICATION

#### 2.1 Classification of the hazardous chemical

##### Classification according to CLASS regulations 2013

Specific target organ toxicity - repeated exposure, Oral (Category 1), Thyroid

#### 2.2 Label elements

##### Labelling according to CLASS regulations 2013

Pictogram



Signal word

Danger

Hazard statement(s)  
H372

Causes damage to organs (Thyroid) through prolonged or repeated exposure if swallowed.

Precautionary statement(s)

Prevention

P260 Do not breathe dust/ fume/ gas/ mist/ vapours/ spray.  
P264 Wash skin thoroughly after handling.  
P270 Do not eat, drink or smoke when using this product.

Response

P314 Get medical advice/ attention if you feel unwell.

Disposal

P501 Dispose of contents/ container to an approved waste disposal plant.

**2.3 Other hazards - none**

---

**3. SECTION 3: Composition and information of the ingredients of the hazardous chemical**

**3.1 Substances**

**Chemical identity**

Formula : IK  
Molecular weight : 166,00 g/mol  
CAS-No. : 7681-11-0

Component	Concentration
<b>Potassium iodide</b>	
CAS-No. 7681-11-0	<= 100 %
EC-No. 231-659-4	

---

**4. FIRST AID MEASURES**

**4.1 Description of first aid measures**

**General advice**

Consult a physician. Show this safety data sheet to the doctor in attendance.

**If inhaled**

If breathed in, move person into fresh air. If not breathing, give artificial respiration. Consult a physician.

**In case of skin contact**

Wash off with soap and plenty of water. Take victim immediately to hospital. Consult a physician.

**In case of eye contact**

Flush eyes with water as a precaution.

**If swallowed**

Never give anything by mouth to an unconscious person. Rinse mouth with water. Consult a physician.

**4.2 Most important symptoms and effects, both acute and delayed**

Prolonged exposure to iodides may produce iodism in sensitive individuals. Symptoms of exposure include: skin rash, running nose, headache and irritation of the mucous membrane. For severe cases the skin may show pimples, boils, hives, blisters and black and blue spots. Iodides are readily diffused across the placenta. Neonatal deaths from respiratory distress secondary to goiter have been reported. Iodides have been known to cause drug-induced fevers, which are usually of short duration.

To the best of our knowledge, the chemical, physical, and toxicological properties have not been thoroughly investigated.

**4.3 Indication of any immediate medical attention and special treatment needed**

No data available

---

## 5. FIREFIGHTING MEASURES

### 5.1 Extinguishing media

#### Suitable extinguishing media

Use water spray, alcohol-resistant foam, dry chemical or carbon dioxide.

### 5.2 Special hazards arising from the substance or mixture

No data available

### 5.3 Advice for firefighters

Wear self-contained breathing apparatus for firefighting if necessary.

### 5.4 Further information

No data available

---

## 6. ACCIDENTAL RELEASE MEASURES

### 6.1 Personal precautions, protective equipment and emergency procedures

Use personal protective equipment. Avoid dust formation. Avoid breathing vapours, mist or gas. Ensure adequate ventilation. Evacuate personnel to safe areas. Avoid breathing dust.

### 6.2 Environmental precautions

Prevent further leakage or spillage if safe to do so. Do not let product enter drains.

### 6.3 Methods and materials for containment and cleaning up

Pick up and arrange disposal without creating dust. Sweep up and shovel. Keep in suitable, closed containers for disposal.

### 6.4 Reference to other sections

For disposal see section 13.

---

## 7. HANDLING AND STORAGE

### 7.1 Precautions for safe handling

Avoid contact with skin and eyes. Avoid formation of dust and aerosols. Provide appropriate exhaust ventilation at places where dust is formed.

### 7.2 Conditions for safe storage, including any incompatibilities

Keep container tightly closed in a dry and well-ventilated place.

Air, light, and moisture sensitive. Store under inert gas.

### 7.3 Specific end use(s)

No data available

---

## 8. Exposure controls and personal protection

### 8.1 Control parameters

#### Permissible exposure limit

### 8.2 Exposure controls

#### Appropriate engineering controls

Handle in accordance with good industrial hygiene and safety practice. Wash hands before breaks and at the end of workday.

#### Personal protective equipment

##### Eye/face protection

Face shield and safety glasses Use equipment for eye protection tested and approved under appropriate government standards such as NIOSH (US) or EN 166(EU).

### **Skin protection**

Handle with gloves. Gloves must be inspected prior to use. Use proper glove removal technique (without touching glove's outer surface) to avoid skin contact with this product. Dispose of contaminated gloves after use in accordance with applicable laws and good laboratory practices. Wash and dry hands.

The selected protective gloves have to satisfy the specifications of EU Directive 89/686/EEC and the standard EN 374 derived from it.

#### Full contact

Material: Nitrile rubber

Minimum layer thickness: 0,11 mm

Break through time: 480 min

Material tested: Dermatril® (KCL 740 / Aldrich Z677272, Size M)

#### Splash contact

Material: Nitrile rubber

Minimum layer thickness: 0,11 mm

Break through time: 480 min

Material tested: Dermatril® (KCL 740 / Aldrich Z677272, Size M)

data source: KCL GmbH, D-36124 Eichenzell, phone +49 (0)6659 87300, e-mail sales@kcl.de, test method: EN374

If used in solution, or mixed with other substances, and under conditions which differ from EN 374, contact the supplier of the CE approved gloves. This recommendation is advisory only and must be evaluated by an industrial hygienist and safety officer familiar with the specific situation of anticipated use by our customers. It should not be construed as offering an approval for any specific use scenario.

### **Body Protection**

Complete suit protecting against chemicals, The type of protective equipment must be selected according to the concentration and amount of the dangerous substance at the specific workplace.

### **Respiratory protection**

Where risk assessment shows air-purifying respirators are appropriate use a full-face particle respirator type N99 (US) or type P2 (EN 143) respirator cartridges as a backup to engineering controls. If the respirator is the sole means of protection, use a full-face supplied air respirator. Use respirators and components tested and approved under appropriate government standards such as NIOSH (US) or CEN (EU).

### **Thermal hazards**

No data available

---

## **9. PHYSICAL AND CHEMICAL PROPERTIES**

### **9.1 Information on basic physical and chemical properties**

- |  |                                     |
|--|-------------------------------------|
| a) Appearance                              | Form: solid<br>Colour: off-white    |
| b) Odour                                   | odourless                           |
| c) Odour Threshold                         | No data available                   |
| d) pH                                      | ca.6,9 at 50 g/l at 20 °C           |
| e) Melting point/freezing point            | Melting point: 685 °C at ca.975 hPa |
| f) Initial boiling point and boiling range | 1.325 °C at 1.013 hPa               |
| g) Flash point                             | does not flash                      |
| h) Evaporation rate                        | No data available                   |

i) Flammability (solid, gas)	The product is not flammable.
j) Upper/lower flammability or explosive limits	No data available
k) Vapour pressure	ca.1 hPa at 745 °C
l) Vapour density	No data available
m) Relative density	3,23 g/cm <sup>3</sup> at 25 °C
n) Water solubility	ca.1.430 g/l at 20 °C
o) Partition coefficient: n-octanol/water	Not applicable for inorganic substances
p) Auto-ignition temperature	No data available
q) Decomposition temperature	No data available
r) Viscosity	No data available

---

## 10. STABILITY AND REACTIVITY

### 10.1 Reactivity

No data available

### 10.2 Chemical stability

No data available

### 10.3 Possibility of hazardous reactions

No data available

### 10.4 Conditions to avoid

Tin/tin oxides

### 10.5 Incompatible materials

No data available

### 10.6 Hazardous decomposition products

Hazardous decomposition products formed under fire conditions. - Hydrogen iodide, Potassium oxides  
Other decomposition products - No data available

---

## 11. TOXICOLOGICAL INFORMATION

### 11.1 Information on toxicological effects

#### Acute toxicity

LD50 Dermal - Rat - male and female - > 2.000 mg/kg

#### Skin corrosion/irritation

Skin - Rabbit - No skin irritation - 4 h - OECD Test Guideline 404

#### Serious eye damage/eye irritation

Eyes - Rabbit - No eye irritation - OECD Test Guideline 405

#### Respiratory or skin sensitisation

Patch test: - Human - negative

Remarks: (ECHA)

#### Germ cell mutagenicity

Genotoxicity in vitro - Ames test - Salmonella typhimurium - negative (Lit.)

## Carcinogenicity

IARC: No component of this product present at levels greater than or equal to 0.1% is identified as probable, possible or confirmed human carcinogen by IARC.

## Reproductive toxicity

### Specific target organ toxicity - single exposure

### Specific target organ toxicity - repeated exposure

Ingestion - Causes damage to organs through prolonged or repeated exposure. - Thyroid

## Aspiration hazard

## Potential health effects

<b>Inhalation</b>	Toxic if inhaled. May cause respiratory tract irritation.
<b>Ingestion</b>	Toxic if swallowed.
<b>Skin</b>	Toxic if absorbed through skin. May cause skin irritation.
<b>Eyes</b>	May cause eye irritation.

## Signs and Symptoms of Exposure

Prolonged exposure to iodides may produce iodism in sensitive individuals. Symptoms of exposure include: skin rash, running nose, headache and irritation of the mucous membrane. For severe cases the skin may show pimples, boils, hives, blisters and black and blue spots. Iodides are readily diffused across the placenta. Neonatal deaths from respiratory distress secondary to goiter have been reported. Iodides have been known to cause drug-induced fevers, which are usually of short duration.

To the best of our knowledge, the chemical, physical, and toxicological properties have not been thoroughly investigated.

## Additional Information

RTECS: TT2975000

## Further information

After absorption of toxic quantities: drop in blood pressure, paralysis symptoms, agitation, Vomiting  
The following applies to iodides in general: Sensitisation possible in predisposed persons. Other dangerous properties can not be excluded. Handle in accordance with good industrial hygiene and safety practice.

---

## 12. ECOLOGICAL INFORMATION

### 12.1 Ecotoxicity

Toxicity to fish static test LC50 - Danio rerio (zebra fish) - > 100 mg/l - 96 h  
Method: OECD Test Guideline 203

### 12.2 Persistence and degradability

The methods for determining the biological degradability are not applicable to inorganic substances.

### 12.3 Bioaccumulative potential

### 12.4 Mobility in soil

### 12.5 Other adverse effects

---

## 13. SECTION 13: Disposal information

### 13.1 Waste treatment methods

#### Product

Offer surplus and non-recyclable solutions to a licensed disposal company. Dissolve or mix the material with a combustible solvent and burn in a chemical incinerator equipped with an afterburner and scrubber.

#### Contaminated packaging

Dispose of as unused product.

---

**14. TRANSPORT INFORMATION****14.1 UN number**

ADR/RID: -

IMDG: -

IATA-DGR: -

**14.2 UN proper shipping name**

ADR/RID:

Not dangerous goods

IMDG

Not dangerous goods

IATA-DGR:

Not dangerous goods

**14.3 Transport hazard class(es)**

ADR/RID: -

IMDG: -

IATA-DGR: -

**14.4 Packaging group**

ADR/RID: -

IMDG: -

IATA-DGR: -

**14.5 Environmental hazards**

ADR/RID: no

IMDG Marine pollutant: no

IATA-DGR: no

**14.6 Transport in bulk according to Annex II of MARPOL 73/78 and the IBC Code**

No data available

**14.7 Special precautions for user**

No data available

---

**15. REGULATORY INFORMATION****15.1 Safety, health and environmental regulations/legislation specific for the substance or mixture**

No data available

---

**16. OTHER INFORMATION****Further information**

Copyright 2016 Sigma-Aldrich Co. LLC. License granted to make unlimited paper copies for internal use only.

The above information is believed to be correct but does not purport to be all inclusive and shall be used only as a guide. The information in this document is based on the present state of our knowledge and is applicable to the product with regard to appropriate safety precautions. It does not represent any guarantee of the properties of the product. Sigma-Aldrich Corporation and its Affiliates shall not be held liable for any damage resulting from handling or from contact with the above product. See [www.sigma-aldrich.com](http://www.sigma-aldrich.com) and/or the reverse side of invoice or packing slip for additional terms and conditions of sale.

---

---

### 1. SECTION 1: Identification of the hazardous chemical and of the supplier

#### 1.1 Product identifiers

Product name : Hydrochloric acid

Product Number : 320331

Brand : Sigma-Aldrich

#### 1.2 Other means of identification

No data available

#### 1.3 Recommended use of the chemical and restrictions on use

For R&D use only. Not for pharmaceutical, household or other uses.

#### 1.4 Details of the supplier of the safety data sheet

Company : Merck Sdn. Bhd. Malaysia  
Level 3, Menara Sunway Annexe Jalan  
Lagoon Timur (PJS9/1)  
Bandar Sunway  
Petaling Jaya  
46150 SELANGOR DARUL EHSAN  
MALAYSIA

Telephone : +60 3 7494 3688

Fax : +60 3 7491 0850

#### 1.5 Emergency telephone number

Emergency Phone # : +62 08001401253

---

### 2. HAZARDS IDENTIFICATION

#### 2.1 Classification of the hazardous chemical

##### Classification according to CLASS regulations 2013

Corrosive to metals (Category 1)

Acute toxicity, Inhalation (Category 3)

Skin corrosion/irritation (Category 1B)

Serious eye damage/eye irritation (Category 1)

#### 2.2 Label elements

##### Labelling according to CLASS regulations 2013

Pictogram



Signal word

Danger



Hazard statement(s)	
H290	May be corrosive to metals.
H314	Causes severe skin burns and eye damage.
H331	Toxic if inhaled.
Precautionary statement(s)	
Prevention	
P264	Wash skin thoroughly after handling.
P280	Wear protective gloves/ protective clothing/ eye protection/ face protection.
Response	
P303 + P361 + P353	IF ON SKIN (or hair): Remove/ Take off immediately all contaminated clothing. Rinse skin with water/ shower.
P304 + P340 + P310	IF INHALED: Remove victim to fresh air and keep at rest in a position comfortable for breathing. Immediately call a POISON CENTER or doctor/ physician.
P305 + P351 + P338 + P310	IF IN EYES: Rinse cautiously with water for several minutes. Remove contact lenses, if present and easy to do. Continue rinsing. Immediately call a POISON CENTER/doctor.
Storage	
P403 + P233	Store in a well-ventilated place. Keep container tightly closed.

### 2.3 Other hazards - none

## 3. SECTION 3: Composition and information of the ingredients of the hazardous chemical

### 3.2 Mixtures

Formula	:	HCl
Molecular weight	:	36,46 g/mol
CAS-No.	:	7647-01-0

Component	Classification	Concentration
<b>Hydrochloric acid</b>		
CAS-No.	7647-01-0	Met. Corr. 1; 1B; 1; STOT SE 3; H290, H314, H335 >= 30 - < 60 %
EC-No.	231-595-7	
Index-No.	017-002-01-X	
Registration number	01-2119484862-27-XXXX	

For the full text of the H-Statements and R-Phrases mentioned in this Section, see Section 16

## 4. FIRST AID MEASURES

### 4.1 Description of first aid measures

#### General advice

Consult a physician. Show this safety data sheet to the doctor in attendance.

#### If inhaled

If breathed in, move person into fresh air. If not breathing, give artificial respiration. Consult a physician.

#### In case of skin contact

Take off contaminated clothing and shoes immediately. Wash off with soap and plenty of water. Consult a physician.

#### In case of eye contact

Rinse thoroughly with plenty of water for at least 15 minutes and consult a physician.

**If swallowed**

Do NOT induce vomiting. Never give anything by mouth to an unconscious person. Rinse mouth with water. Consult a physician.

**4.2 Most important symptoms and effects, both acute and delayed**

Inhalation of vapors may cause: burning sensation, Cough, wheezing, Shortness of breath, spasm, inflammation and edema of the larynx, spasm, inflammation and edema of the bronchi, pneumonitis, pulmonary edema (Hydrochloric acid)

**4.3 Indication of any immediate medical attention and special treatment needed**

No data available

---

**5. FIREFIGHTING MEASURES****5.1 Extinguishing media****Suitable extinguishing media**

Use water spray, alcohol-resistant foam, dry chemical or carbon dioxide.

**5.2 Special hazards arising from the substance or mixture**

No data available

**5.3 Advice for firefighters**

Wear self-contained breathing apparatus for firefighting if necessary.

**5.4 Further information**

No data available

---

**6. ACCIDENTAL RELEASE MEASURES****6.1 Personal precautions, protective equipment and emergency procedures**

Wear respiratory protection. Avoid breathing vapours, mist or gas. Ensure adequate ventilation. Evacuate personnel to safe areas.

**6.2 Environmental precautions**

Do not let product enter drains.

**6.3 Methods and materials for containment and cleaning up**

Soak up with inert absorbent material and dispose of as hazardous waste. Keep in suitable, closed containers for disposal. Soak up with inert absorbent material and dispose of as hazardous waste. Keep in suitable, closed containers for disposal.

**6.4 Reference to other sections**

For disposal see section 13.

---

**7. HANDLING AND STORAGE****7.1 Precautions for safe handling**

Avoid contact with skin and eyes. Avoid inhalation of vapour or mist.

**7.2 Conditions for safe storage, including any incompatibilities**

Store in cool place. Keep container tightly closed in a dry and well-ventilated place. Containers which are opened must be carefully resealed and kept upright to prevent leakage.

**7.3 Specific end use(s)**

No data available

---

**8. Exposure controls and personal protection****8.1 Control parameters****Permissible exposure limit**

Component	CAS-No.	Value	Control parameters	Basis
Hydrochloric acid	7647-01-0	CEIL	5 ppm 7,5 mg/m <sup>3</sup>	Malaysia. Occupational Safety and Health (Use and Standards of Exposure of Chemicals Hazardous to Health) Regulations 2000.

## 8.2 Exposure controls

### Appropriate engineering controls

Handle in accordance with good industrial hygiene and safety practice. Wash hands before breaks and at the end of workday.

### Personal protective equipment

#### Eye/face protection

Tightly fitting safety goggles. Faceshield (8-inch minimum). Use equipment for eye protection tested and approved under appropriate government standards such as NIOSH (US) or EN 166(EU).

#### Skin protection

Handle with gloves. Gloves must be inspected prior to use. Use proper glove removal technique (without touching glove's outer surface) to avoid skin contact with this product. Dispose of contaminated gloves after use in accordance with applicable laws and good laboratory practices. Wash and dry hands.

The selected protective gloves have to satisfy the specifications of EU Directive 89/686/EEC and the standard EN 374 derived from it.

#### Full contact

Material: Nitrile rubber

Minimum layer thickness: 0,4 mm

Break through time: 480 min

Material tested: Camatril® (KCL 730 / Aldrich Z677442, Size M)

#### Splash contact

Material: Nitrile rubber

Minimum layer thickness: 0,11 mm

Break through time: 69 min

Material tested: Dermatril® (KCL 740 / Aldrich Z677272, Size M)

data source: KCL GmbH, D-36124 Eichenzell, phone +49 (0)6659 87300, e-mail sales@kcl.de, test method: EN374

If used in solution, or mixed with other substances, and under conditions which differ from EN 374, contact the supplier of the CE approved gloves. This recommendation is advisory only and must be evaluated by an industrial hygienist and safety officer familiar with the specific situation of anticipated use by our customers. It should not be construed as offering an approval for any specific use scenario.

#### Body Protection

Complete suit protecting against chemicals, The type of protective equipment must be selected according to the concentration and amount of the dangerous substance at the specific workplace.

#### Respiratory protection

Where risk assessment shows air-purifying respirators are appropriate use a full-face respirator with multi-purpose combination (US) or type ABEK (EN 14387) respirator cartridges as a backup to engineering controls. If the respirator is the sole means of protection, use a full-face supplied air respirator. Use respirators and components tested and approved under appropriate government standards such as NIOSH (US) or CEN (EU).

#### Thermal hazards

No data available

## 9. PHYSICAL AND CHEMICAL PROPERTIES

### 9.1 Information on basic physical and chemical properties

a) Appearance	Form: liquid Colour: light yellow
b) Odour	pungent
c) Odour Threshold	No data available
d) pH	No data available
e) Melting point/freezing point	-30 °C
f) Initial boiling point and boiling range	> 100 °C
g) Flash point	Not applicable
h) Evaporation rate	No data available
i) Flammability (solid, gas)	No data available
j) Upper/lower flammability or explosive limits	No data available
k) Vapour pressure	226,636 hPa at 21,1 °C 546,596 hPa at 37,7 °C
l) Vapour density	No data available
m) Relative density	1,18 g/mL at 25 °C
n) Water solubility	soluble
o) Partition coefficient: n-octanol/water	No data available
p) Auto-ignition temperature	No data available
q) Decomposition temperature	No data available
r) Viscosity	No data available

---

## 10. STABILITY AND REACTIVITY

### 10.1 Reactivity

No data available

### 10.2 Chemical stability

No data available

### 10.3 Possibility of hazardous reactions

No data available

### 10.4 Conditions to avoid

No data available

### 10.5 Incompatible materials

Bases, Amines, Alkali metals, Metals, permanganates, e.g. potassium permanganate, Fluorine, metal acetylides, hexalithium disilicide

### 10.6 Hazardous decomposition products

Hazardous decomposition products formed under fire conditions. - Hydrogen chloride gas  
Other decomposition products - No data available

---

## 11. TOXICOLOGICAL INFORMATION

### 11.1 Information on toxicological effects

#### Acute toxicity

No data available (Hydrochloric acid)

Inhalation: Inhalation may provoke the following symptoms: Respiratory irritation Cough Difficulty in breathing  
Pneumonia (Hydrochloric acid)

#### Skin corrosion/irritation

Skin - Rabbit - Causes burns. (Hydrochloric acid)

#### Serious eye damage/eye irritation

Eyes - Rabbit - Corrosive to eyes (Hydrochloric acid)

#### Respiratory or skin sensitisation

Did not cause sensitisation on laboratory animals. (Hydrochloric acid)

#### Germ cell mutagenicity

No data available (Hydrochloric acid)

#### Carcinogenicity

This product is or contains a component that is not classifiable as to its carcinogenicity based on its IARC, ACGIH, NTP, or EPA classification. (Hydrochloric acid)

(Hydrochloric acid)

IARC: 3 - Group 3: Not classifiable as to its carcinogenicity to humans (Hydrochloric acid)

#### Reproductive toxicity

No data available (Hydrochloric acid)

#### Specific target organ toxicity - single exposure

The substance or mixture is classified as specific target organ toxicant, single exposure, category 3 with respiratory tract irritation. (Hydrochloric acid)

#### Specific target organ toxicity - repeated exposure

The substance or mixture is not classified as specific target organ toxicant, repeated exposure.

#### Aspiration hazard

No aspiration toxicity classification (Hydrochloric acid)

#### Potential health effects

<b>Inhalation</b>	May be harmful if inhaled. Material is extremely destructive to the tissue of the mucous membranes and upper respiratory tract. Causes respiratory tract irritation.
<b>Ingestion</b>	May be harmful if swallowed. Causes burns.
<b>Skin</b>	May be harmful if absorbed through skin. Causes skin burns.
<b>Eyes</b>	Causes eye burns.

#### Signs and Symptoms of Exposure

Inhalation of vapors may cause: burning sensation, Cough, wheezing, Shortness of breath, spasm, inflammation and edema of the larynx, spasm, inflammation and edema of the bronchi, pneumonitis, pulmonary edema (Hydrochloric acid)

#### Additional Information

RTECS: MW4025000

---

## 12. ECOLOGICAL INFORMATION

### 12.1 Ecotoxicity

Toxicity to fish LC50 - Lepomis macrochirus (Bluegill) - 24,6 mg/l - 96 h (Hydrochloric acid)

Toxicity to daphnia and other aquatic invertebrates EC50 - Daphnia magna (Water flea) - 4,91 mg/l - 48 h (Hydrochloric acid)

### 12.2 Persistence and degradability

No data available

### 12.3 Bioaccumulative potential

No data available

### 12.4 Mobility in soil

No data available (Hydrochloric acid)

### 12.5 Other adverse effects

May be harmful to aquatic organisms due to the shift of the pH. Do not empty into drains.

---

## 13. SECTION 13: Disposal information

### 13.1 Waste treatment methods

#### Product

Offer surplus and non-recyclable solutions to a licensed disposal company.

#### Contaminated packaging

Dispose of as unused product.

---

## 14. TRANSPORT INFORMATION

### 14.1 UN number

ADR/RID: 1789

IMDG: 1789

IATA-DGR: 1789

### 14.2 UN proper shipping name

ADR/RID:

HYDROCHLORIC ACID

IMDG

HYDROCHLORIC ACID

IATA-DGR:

Hydrochloric acid

### 14.3 Transport hazard class(es)

ADR/RID: 8

IMDG: 8

IATA-DGR: 8

### 14.4 Packaging group

ADR/RID: II

IMDG: II

IATA-DGR: II

### 14.5 Environmental hazards

ADR/RID: no

IMDG Marine pollutant: no

IATA-DGR: no

### 14.6 Transport in bulk according to Annex II of MARPOL 73/78 and the IBC Code

No data available

### 14.7 Special precautions for user

No data available

---

## 15. REGULATORY INFORMATION

### 15.1 Safety, health and environmental regulations/legislation specific for the substance or mixture

No data available

---

**16. OTHER INFORMATION****Text of H-code(s) and R-phrase(s) mentioned in Section 3**

	Skin corrosion/irritation
H290	May be corrosive to metals.
H314	Causes severe skin burns and eye damage.
H335	May cause respiratory irritation.
Met. Corr.	Corrosive to metals
STOT SE	Specific target organ toxicity - single exposure

**Further information**

Copyright 2016 Sigma-Aldrich Co. LLC. License granted to make unlimited paper copies for internal use only.

The above information is believed to be correct but does not purport to be all inclusive and shall be used only as a guide. The information in this document is based on the present state of our knowledge and is applicable to the product with regard to appropriate safety precautions. It does not represent any guarantee of the properties of the product. Sigma-Aldrich Corporation and its Affiliates shall not be held liable for any damage resulting from handling or from contact with the above product. See [www.sigma-aldrich.com](http://www.sigma-aldrich.com) and/or the reverse side of invoice or packing slip for additional terms and conditions of sale.

---

---

### 1. SECTION 1: Identification of the hazardous chemical and of the supplier

#### 1.1 Product identifiers

Product name : Sodium hydroxide

Product Number : 655104

Brand : Sigma-Aldrich

#### 1.2 Other means of identification

'Caustic soda'

#### 1.3 Recommended use of the chemical and restrictions on use

For R&D use only. Not for pharmaceutical, household or other uses.

#### 1.4 Details of the supplier of the safety data sheet

Company : Merck Sdn. Bhd. Malaysia  
Level 3, Menara Sunway Annexe Jalan  
Lagoon Timur (PJS9/1)  
Bandar Sunway  
Petaling Jaya  
46150 SELANGOR DARUL EHSAN  
MALAYSIA

Telephone : +60 3 7494 3688

Fax : +60 3 7491 0850

#### 1.5 Emergency telephone number

Emergency Phone # : +62 08001401253

---

### 2. HAZARDS IDENTIFICATION

#### 2.1 Classification of the hazardous chemical

##### Classification according to CLASS regulations 2013

Skin corrosion/irritation (Category 1A)

Serious eye damage/eye irritation (Category 1)

#### 2.2 Label elements

##### Labelling according to CLASS regulations 2013

Pictogram



Signal word : Danger

Hazard statement(s)

H314

Causes severe skin burns and eye damage.



## Precautionary statement(s)

### Prevention

P260 Do not breathe dust or mist.  
P264 Wash skin thoroughly after handling.  
P280 Wear protective gloves/ protective clothing/ eye protection/ face protection.

### Response

P303 + P361 + P353 IF ON SKIN (or hair): Remove/ Take off immediately all contaminated clothing. Rinse skin with water/ shower.  
P304 + P340 + P310 IF INHALED: Remove victim to fresh air and keep at rest in a position comfortable for breathing. Immediately call a POISON CENTER or doctor/ physician.  
P305 + P351 + P338 + P310 IF IN EYES: Rinse cautiously with water for several minutes. Remove contact lenses, if present and easy to do. Continue rinsing. Immediately call a POISON CENTER/doctor.

## 2.3 Other hazards - none

---

## 3. SECTION 3: Composition and information of the ingredients of the hazardous chemical

### 3.1 Substances

#### Chemical identity

Synonyms : 'Caustic soda'  
Formula : HNaO  
Molecular weight : 40,00 g/mol  
CAS-No. : 1310-73-2

Component	Concentration
<b>Sodium hydroxide</b>	
CAS-No.	1310-73-2
EC-No.	215-185-5
Index-No.	011-002-00-6
Registration number	01-2119457892-27-XXXX
	<= 100 %

---

## 4. FIRST AID MEASURES

### 4.1 Description of first aid measures

#### General advice

Consult a physician. Show this safety data sheet to the doctor in attendance.

#### If inhaled

If breathed in, move person into fresh air. If not breathing, give artificial respiration. Consult a physician.

#### In case of skin contact

Take off contaminated clothing and shoes immediately. Wash off with soap and plenty of water. Consult a physician.

#### In case of eye contact

Rinse thoroughly with plenty of water for at least 15 minutes and consult a physician.

#### If swallowed

Do NOT induce vomiting. Never give anything by mouth to an unconscious person. Rinse mouth with water. Consult a physician.

- 4.2 Most important symptoms and effects, both acute and delayed**  
Material is extremely destructive to tissue of the mucous membranes and upper respiratory tract, eyes, and skin.
- 4.3 Indication of any immediate medical attention and special treatment needed**  
No data available
- 

## **5. FIREFIGHTING MEASURES**

- 5.1 Extinguishing media**  
**Suitable extinguishing media**  
Use water spray, alcohol-resistant foam, dry chemical or carbon dioxide.
- 5.2 Special hazards arising from the substance or mixture**  
No data available
- 5.3 Advice for firefighters**  
Wear self-contained breathing apparatus for firefighting if necessary.
- 5.4 Further information**  
No data available
- 

## **6. ACCIDENTAL RELEASE MEASURES**

- 6.1 Personal precautions, protective equipment and emergency procedures**  
Wear respiratory protection. Avoid dust formation. Avoid breathing vapours, mist or gas. Ensure adequate ventilation. Evacuate personnel to safe areas. Avoid breathing dust.
- 6.2 Environmental precautions**  
Prevent further leakage or spillage if safe to do so. Do not let product enter drains. Discharge into the environment must be avoided.
- 6.3 Methods and materials for containment and cleaning up**  
Pick up and arrange disposal without creating dust. Sweep up and shovel. Keep in suitable, closed containers for disposal.
- 6.4 Reference to other sections**  
For disposal see section 13.
- 

## **7. HANDLING AND STORAGE**

- 7.1 Precautions for safe handling**  
Avoid formation of dust and aerosols.  
Provide appropriate exhaust ventilation at places where dust is formed.
- 7.2 Conditions for safe storage, including any incompatibilities**  
Store in cool place. Keep container tightly closed in a dry and well-ventilated place.
- 7.3 Specific end use(s)**  
No data available
- 

## **8. Exposure controls and personal protection**

- 8.1 Control parameters**  
**Permissible exposure limit**

Component	CAS-No.	Value	Control parameters	Basis
Sodium hydroxide	1310-73-2	CEIL	2 mg/m <sup>3</sup>	Malaysia. Occupational Safety and Health (Use and Standards of Exposure of Chemicals Hazardous to Health) Regulations 2000.

## 8.2 Exposure controls

### Appropriate engineering controls

Handle in accordance with good industrial hygiene and safety practice. Wash hands before breaks and at the end of workday.

### Personal protective equipment

#### Eye/face protection

Face shield and safety glasses Use equipment for eye protection tested and approved under appropriate government standards such as NIOSH (US) or EN 166(EU).

#### Skin protection

Handle with gloves. Gloves must be inspected prior to use. Use proper glove removal technique (without touching glove's outer surface) to avoid skin contact with this product. Dispose of contaminated gloves after use in accordance with applicable laws and good laboratory practices. Wash and dry hands.

The selected protective gloves have to satisfy the specifications of EU Directive 89/686/EEC and the standard EN 374 derived from it.

#### Full contact

Material: Nitrile rubber

Minimum layer thickness: 0,11 mm

Break through time: 480 min

Material tested: Dermatril® (KCL 740 / Aldrich Z677272, Size M)

#### Splash contact

Material: Nitrile rubber

Minimum layer thickness: 0,11 mm

Break through time: 480 min

Material tested: Dermatril® (KCL 740 / Aldrich Z677272, Size M)

data source: KCL GmbH, D-36124 Eichenzell, phone +49 (0)6659 87300, e-mail sales@kcl.de, test method: EN374

If used in solution, or mixed with other substances, and under conditions which differ from EN 374, contact the supplier of the CE approved gloves. This recommendation is advisory only and must be evaluated by an industrial hygienist and safety officer familiar with the specific situation of anticipated use by our customers. It should not be construed as offering an approval for any specific use scenario.

#### Body Protection

Complete suit protecting against chemicals, The type of protective equipment must be selected according to the concentration and amount of the dangerous substance at the specific workplace.

#### Respiratory protection

Where risk assessment shows air-purifying respirators are appropriate use a full-face particle respirator type N100 (US) or type P3 (EN 143) respirator cartridges as a backup to engineering controls. If the respirator is the sole means of protection, use a full-face supplied air respirator. Use respirators and components tested and approved under appropriate government standards such as NIOSH (US) or CEN (EU).

#### Thermal hazards

No data available

## 9. PHYSICAL AND CHEMICAL PROPERTIES

### 9.1 Information on basic physical and chemical properties

a) Appearance	Form: powder Colour: white
b) Odour	odourless
c) Odour Threshold	No data available
d) pH	14 at 50 g/l at 20 °C
e) Melting point/freezing point	Melting point/range: 318 °C - lit.
f) Initial boiling point and boiling range	1.390 °C
g) Flash point	Not applicable
h) Evaporation rate	No data available
i) Flammability (solid, gas)	No data available
j) Upper/lower flammability or explosive limits	No data available
k) Vapour pressure	< 24,00 hPa at 20 °C 4,00 hPa at 37 °C
l) Vapour density	1,38 - (Air = 1.0)
m) Relative density	2,1300 g/cm <sup>3</sup>
n) Water solubility	ca.1.260 g/l at 20 °C
o) Partition coefficient: n-octanol/water	No data available
p) Auto-ignition temperature	No data available
q) Decomposition temperature	No data available
r) Viscosity	No data available

---

## 10. STABILITY AND REACTIVITY

### 10.1 Reactivity

No data available

### 10.2 Chemical stability

No data available

### 10.3 Possibility of hazardous reactions

No data available

### 10.4 Conditions to avoid

No data available

### 10.5 Incompatible materials

Strong oxidizing agents, Strong acids, Organic materials

### 10.6 Hazardous decomposition products

Other decomposition products - No data available

Hazardous decomposition products formed under fire conditions. - Sodium oxides

---

## 11. TOXICOLOGICAL INFORMATION

### 11.1 Information on toxicological effects

#### Acute toxicity

No data available

#### Skin corrosion/irritation

Skin - Rabbit - Causes severe burns. - 24 h

#### Serious eye damage/eye irritation

Eyes - Rabbit - Corrosive - 24 h

#### Respiratory or skin sensitisation

Does not cause skin sensitisation.

Will not occur

#### Germ cell mutagenicity

No data available

#### Carcinogenicity

IARC: No component of this product present at levels greater than or equal to 0.1% is identified as probable, possible or confirmed human carcinogen by IARC.

#### Reproductive toxicity

No data available

#### Specific target organ toxicity - single exposure

No data available

#### Specific target organ toxicity - repeated exposure

No data available

#### Aspiration hazard

No data available

#### Potential health effects

##### Inhalation

May be harmful if inhaled. Material is extremely destructive to the tissue of the mucous membranes and upper respiratory tract.

##### Ingestion

May be harmful if swallowed. Causes burns.

##### Skin

May be harmful if absorbed through skin. Causes skin burns.

##### Eyes

Causes eye burns.

#### Signs and Symptoms of Exposure

Material is extremely destructive to tissue of the mucous membranes and upper respiratory tract, eyes, and skin.

#### Additional Information

RTECS: WB4900000

---

## 12. ECOLOGICAL INFORMATION

### 12.1 Ecotoxicity

Toxicity to fish

LC50 - Gambusia affinis (Mosquito fish) - 125 mg/l - 96 h

LC50 - Oncorhynchus mykiss (rainbow trout) - 45,4 mg/l - 96 h

Toxicity to daphnia and other aquatic invertebrates

Immobilization EC50 - Daphnia (water flea) - 40,38 mg/l - 48 h

## 12.2 Persistence and degradability

The methods for determining the biological degradability are not applicable to inorganic substances.

## 12.3 Bioaccumulative potential

No data available

## 12.4 Mobility in soil

No data available

## 12.5 Other adverse effects

Harmful to aquatic life.

---

## 13. SECTION 13: Disposal information

### 13.1 Waste treatment methods

#### Product

Offer surplus and non-recyclable solutions to a licensed disposal company. Dissolve or mix the material with a combustible solvent and burn in a chemical incinerator equipped with an afterburner and scrubber.

#### Contaminated packaging

Dispose of as unused product.

---

## 14. TRANSPORT INFORMATION

### 14.1 UN number

ADR/RID: 1823

IMDG: 1823

IATA-DGR: 1823

### 14.2 UN proper shipping name

ADR/RID:

IMDG

IATA-DGR:

SODIUM HYDROXIDE, SOLID

SODIUM HYDROXIDE, SOLID

Sodium hydroxide, solid

### 14.3 Transport hazard class(es)

ADR/RID: 8

IMDG: 8

IATA-DGR: 8

### 14.4 Packaging group

ADR/RID: II

IMDG: II

IATA-DGR: II

### 14.5 Environmental hazards

ADR/RID: no

IMDG Marine pollutant: no

IATA-DGR: no

### 14.6 Transport in bulk according to Annex II of MARPOL 73/78 and the IBC Code

No data available

### 14.7 Special precautions for user

No data available

---

## 15. REGULATORY INFORMATION

### 15.1 Safety, health and environmental regulations/legislation specific for the substance or mixture

No data available

---

## 16. OTHER INFORMATION

### Further information

Copyright 2016 Sigma-Aldrich Co. LLC. License granted to make unlimited paper copies for internal use only.

The above information is believed to be correct but does not purport to be all inclusive and shall be used only as a guide. The information in this document is based on the present state of our knowledge and is applicable to the product with regard to appropriate safety precautions. It does not represent any guarantee of the properties of the product. Sigma-Aldrich Corporation and its Affiliates shall not be held

liable for any damage resulting from handling or from contact with the above product. See [www.sigma-aldrich.com](http://www.sigma-aldrich.com) and/or the reverse side of invoice or packing slip for additional terms and conditions of sale.

---

## SAFETY DATA SHEET

according to Regulation (EC) No. 453/2010

Version 6.0 Revision Date 10.07.2015

Print Date 26.08.2018

GENERIC EU MSDS - NO COUNTRY SPECIFIC DATA - NO OEL DATA

### SECTION 1: Identification of the substance/mixture and of the company/undertaking

#### 1.1 Product identifiers

Product name : Potassium hydroxide

Product Number : P6310  
Brand : Sigma  
Index-No. : 019-002-00-8  
REACH No. : 01-2119487136-33-XXXX  
CAS-No. : 1310-58-3

#### 1.2 Relevant identified uses of the substance or mixture and uses advised against

Identified uses : Laboratory chemicals, Manufacture of substances

#### 1.3 Details of the supplier of the safety data sheet

Company : Merck Sdn. Bhd. Malaysia  
Level 3, Menara Sunway Annexe Jalan  
Lagoon Timur (PJS9/1)  
Bandar Sunway  
Petaling Jaya  
46150 SELANGOR DARUL EHSAN  
MALAYSIA

Telephone : +60 3 7494 3688  
Fax : +60 3 7491 0850

#### 1.4 Emergency telephone number

Emergency Phone # +62 08001401253

### SECTION 2: Hazards identification

#### 2.1 Classification of the substance or mixture

##### Classification according to Regulation (EC) No 1272/2008

Corrosive to metals (Category 1), H290

Acute toxicity, Oral (Category 4), H302

Skin corrosion (Category 1A), H314

For the full text of the H-Statements mentioned in this Section, see Section 16.

#### 2.2 Label elements

##### Labelling according Regulation (EC) No 1272/2008

Pictogram



Signal word : Danger

Hazard statement(s)

H290 : May be corrosive to metals.

H302 : Harmful if swallowed.

H314 : Causes severe skin burns and eye damage.



Precautionary statement(s) P280	Wear protective gloves/ protective clothing/ eye protection/ face protection.
P301 + P312 + P330	IF SWALLOWED: Call a POISON CENTER or doctor/ physician if you feel unwell. Rinse mouth.
P303 + P361 + P353	IF ON SKIN (or hair): Take off immediately all contaminated clothing. Rinse skin with water/shower.
P304 + P340 + P310	IF INHALED: Remove person to fresh air and keep comfortable for breathing. Immediately call a POISON CENTER or doctor/ physician.
P305 + P351 + P338	IF IN EYES: Rinse cautiously with water for several minutes. Remove contact lenses, if present and easy to do. Continue rinsing.
Supplemental Hazard Statements	none

### 2.3 Other hazards

This substance/mixture contains no components considered to be either persistent, bioaccumulative and toxic (PBT), or very persistent and very bioaccumulative (vPvB) at levels of 0.1% or higher.

---

## SECTION 3: Composition/information on ingredients

### 3.1 Substances

Synonyms	: Caustic potash
Formula	: KOH HKO
Molecular weight	: 56,11 g/mol
CAS-No.	: 1310-58-3
EC-No.	: 215-181-3
Index-No.	: 019-002-00-8
Registration number	: 01-2119487136-33-XXXX

#### Hazardous ingredients according to Regulation (EC) No 1272/2008

Component	Classification	Concentration
<b>Potassium hydroxide</b>		
CAS-No. 1310-58-3 EC-No. 215-181-3 Index-No. 019-002-00-8 Registration number 01-2119487136-33-XXXX	Met. Corr. 1; Acute Tox. 4; Skin Corr. 1A; H290, H302, H314 Concentration limits: >= 5 %: Skin Corr. 1A, H314; 2 - < 5 %: Skin Corr. 1B, H314; 0,5 - < 2 %: Skin Irrit. 2, H315; 0,5 - < 2 %: Eye Irrit. 2, H319;	<= 100 %

For the full text of the H-Statements mentioned in this Section, see Section 16.

---

## SECTION 4: First aid measures

### 4.1 Description of first aid measures

#### General advice

Consult a physician. Show this safety data sheet to the doctor in attendance.

#### If inhaled

If breathed in, move person into fresh air. If not breathing, give artificial respiration. Consult a physician.

#### In case of skin contact

Take off contaminated clothing and shoes immediately. Wash off with soap and plenty of water. Consult a physician.

**In case of eye contact**

Rinse thoroughly with plenty of water for at least 15 minutes and consult a physician.

**If swallowed**

Do NOT induce vomiting. Never give anything by mouth to an unconscious person. Rinse mouth with water. Consult a physician.

**4.2 Most important symptoms and effects, both acute and delayed**

The most important known symptoms and effects are described in the labelling (see section 2.2) and/or in section 11

**4.3 Indication of any immediate medical attention and special treatment needed**

No data available

---

**SECTION 5: Firefighting measures****5.1 Extinguishing media****Suitable extinguishing media**

Use water spray, alcohol-resistant foam, dry chemical or carbon dioxide.

**5.2 Special hazards arising from the substance or mixture**

Potassium oxides

**5.3 Advice for firefighters**

Wear self-contained breathing apparatus for firefighting if necessary.

**5.4 Further information**

Gives off hydrogen by reaction with metals.

---

**SECTION 6: Accidental release measures****6.1 Personal precautions, protective equipment and emergency procedures**

Wear respiratory protection. Avoid dust formation. Avoid breathing vapours, mist or gas. Ensure adequate ventilation. Evacuate personnel to safe areas. Avoid breathing dust. For personal protection see section 8.

**6.2 Environmental precautions**

Prevent further leakage or spillage if safe to do so. Do not let product enter drains. Discharge into the environment must be avoided.

**6.3 Methods and materials for containment and cleaning up**

Pick up and arrange disposal without creating dust. Sweep up and shovel. Keep in suitable, closed containers for disposal.

**6.4 Reference to other sections**

For disposal see section 13.

---

**SECTION 7: Handling and storage****7.1 Precautions for safe handling**

Avoid contact with skin and eyes. Avoid formation of dust and aerosols. Provide appropriate exhaust ventilation at places where dust is formed. For precautions see section 2.2.

**7.2 Conditions for safe storage, including any incompatibilities**

Store in cool place. Keep container tightly closed in a dry and well-ventilated place. Absorbs carbon dioxide (CO<sub>2</sub>) from air.

Air sensitive. strongly hygroscopic

Storage class (TRGS 510): Non-combustible, corrosive hazardous materials

**7.3 Specific end use(s)**

Apart from the uses mentioned in section 1.2 no other specific uses are stipulated

## SECTION 8: Exposure controls/personal protection

### 8.1 Control parameters

#### Components with workplace control parameters

##### Derived No Effect Level (DNEL)

Application Area	Exposure routes	Health effect	Value
Workers	Inhalation	Long-term local effects	1 mg/m <sup>3</sup>
Consumers	Inhalation	Long-term local effects	1 mg/m <sup>3</sup>

### 8.2 Exposure controls

#### Appropriate engineering controls

Handle in accordance with good industrial hygiene and safety practice. Wash hands before breaks and at the end of workday.

#### Personal protective equipment

##### Eye/face protection

Face shield and safety glasses Use equipment for eye protection tested and approved under appropriate government standards such as NIOSH (US) or EN 166(EU).

##### Skin protection

Handle with gloves. Gloves must be inspected prior to use. Use proper glove removal technique (without touching glove's outer surface) to avoid skin contact with this product. Dispose of contaminated gloves after use in accordance with applicable laws and good laboratory practices. Wash and dry hands.

The selected protective gloves have to satisfy the specifications of EU Directive 89/686/EEC and the standard EN 374 derived from it.

##### Full contact

Material: Nitrile rubber

Minimum layer thickness: 0,11 mm

Break through time: 480 min

Material tested: Dermatril® (KCL 740 / Aldrich Z677272, Size M)

##### Splash contact

Material: Nitrile rubber

Minimum layer thickness: 0,11 mm

Break through time: 480 min

Material tested: Dermatril® (KCL 740 / Aldrich Z677272, Size M)

data source: KCL GmbH, D-36124 Eichenzell, phone +49 (0)6659 87300, e-mail sales@kcl.de, test method: EN374

If used in solution, or mixed with other substances, and under conditions which differ from EN 374, contact the supplier of the CE approved gloves. This recommendation is advisory only and must be evaluated by an industrial hygienist and safety officer familiar with the specific situation of anticipated use by our customers. It should not be construed as offering an approval for any specific use scenario.

##### Body Protection

Complete suit protecting against chemicals, The type of protective equipment must be selected according to the concentration and amount of the dangerous substance at the specific workplace.

##### Respiratory protection

Where risk assessment shows air-purifying respirators are appropriate use a full-face particle respirator type N100 (US) or type P3 (EN 143) respirator cartridges as a backup to engineering controls. If the respirator is the sole means of protection, use a full-face supplied air respirator. Use respirators and components tested and approved under appropriate government standards such as NIOSH (US) or CEN (EU).

### Control of environmental exposure

Prevent further leakage or spillage if safe to do so. Do not let product enter drains. Discharge into the environment must be avoided.

---

## SECTION 9: Physical and chemical properties

### 9.1 Information on basic physical and chemical properties

a) Appearance	Form: solid
b) Odour	No data available
c) Odour Threshold	No data available
d) pH	13,5
e) Melting point/freezing point	Melting point/range: 361 °C - lit.
f) Initial boiling point and boiling range	1.320 °C
g) Flash point	No data available
h) Evaporation rate	No data available
i) Flammability (solid, gas)	No data available
j) Upper/lower flammability or explosive limits	No data available
k) Vapour pressure	1 hPa at 719 °C 1 hPa at 714 °C
l) Vapour density	No data available
m) Relative density	2,044 g/cm <sup>3</sup>
n) Water solubility	1.120 g/l - soluble
o) Partition coefficient: n-octanol/water	No data available
p) Auto-ignition temperature	No data available
q) Decomposition temperature	No data available
r) Viscosity	No data available
s) Explosive properties	No data available
t) Oxidizing properties	No data available

### 9.2 Other safety information

Bulk density	1.300 kg/m <sup>3</sup>
--------------	-------------------------

---

## SECTION 10: Stability and reactivity

### 10.1 Reactivity

No data available

### 10.2 Chemical stability

Heat of solution is very high, and with limited amounts of water, violent boiling may occur  
Stable under recommended storage conditions.

### 10.3 Possibility of hazardous reactions

No data available

#### 10.4 Conditions to avoid

Do not heat above melting point.

#### 10.5 Incompatible materials

Nitro compounds, Organic materials, Magnesium, Copper, Water, reacts violently with:, Metals, Light metals, Contact with aluminum, tin and zinc liberates hydrogen gas. Contact with nitromethane and other similar nitro compounds causes formation of shock-sensitive salts., vigorous reaction with:, Alkali metals, Halogens, Azides, Anhydrides

#### 10.6 Hazardous decomposition products

Other decomposition products - No data available  
In the event of fire: see section 5

---

### SECTION 11: Toxicological information

#### 11.1 Information on toxicological effects

##### Acute toxicity

LD50 Oral - Rat - 333 mg/kg

##### Skin corrosion/irritation

Skin - Rabbit

Result: Severe skin irritation - 24 h

##### Serious eye damage/eye irritation

Eyes - Rabbit

Result: Corrosive to eyes

(OECD Test Guideline 405)

##### Respiratory or skin sensitisation

No data available

##### Germ cell mutagenicity

No data available

In vitro mammalian cell gene mutation test

mouse lymphoma cells

Result: negative

##### Carcinogenicity

IARC: No component of this product present at levels greater than or equal to 0.1% is identified as probable, possible or confirmed human carcinogen by IARC.

##### Reproductive toxicity

No data available

##### Specific target organ toxicity - single exposure

No data available

##### Specific target organ toxicity - repeated exposure

No data available

##### Aspiration hazard

No data available

##### Additional Information

RTECS: TT2100000

To the best of our knowledge, the chemical, physical, and toxicological properties have not been thoroughly investigated.

---

### SECTION 12: Ecological information

#### 12.1 Toxicity

Toxicity to fish

LC50 - Gambusia affinis (Mosquito fish) - 80 mg/l - 96 h

## 12.2 Persistence and degradability

The methods for determining the biological degradability are not applicable to inorganic substances.

## 12.3 Bioaccumulative potential

No data available

## 12.4 Mobility in soil

No data available

## 12.5 Results of PBT and vPvB assessment

This substance/mixture contains no components considered to be either persistent, bioaccumulative and toxic (PBT), or very persistent and very bioaccumulative (vPvB) at levels of 0.1% or higher.

## 12.6 Other adverse effects

Harmful to aquatic life.

---

## SECTION 13: Disposal considerations

### 13.1 Waste treatment methods

#### Product

Offer surplus and non-recyclable solutions to a licensed disposal company. Dissolve or mix the material with a combustible solvent and burn in a chemical incinerator equipped with an afterburner and scrubber.

#### Contaminated packaging

Dispose of as unused product.

---

## SECTION 14: Transport information

### 14.1 UN number

ADR/RID: 1813

IMDG: 1813

IATA: 1813

### 14.2 UN proper shipping name

ADR/RID: POTASSIUM HYDROXIDE, SOLID

IMDG: POTASSIUM HYDROXIDE, SOLID

IATA: Potassium hydroxide, solid

### 14.3 Transport hazard class(es)

ADR/RID: 8

IMDG: 8

IATA: 8

### 14.4 Packaging group

ADR/RID: II

IMDG: II

IATA: II

### 14.5 Environmental hazards

ADR/RID: no

IMDG Marine pollutant: no

IATA: no

### 14.6 Special precautions for user

No data available

---

## SECTION 15: Regulatory information

This safety datasheet complies with the requirements of Regulation (EC) No. 453/2010.

### 15.1 Safety, health and environmental regulations/legislation specific for the substance or mixture

### 15.2 Chemical Safety Assessment

A Chemical Safety Assessment has been carried out for this substance.

---

## SECTION 16: Other information

### Full text of H-Statements referred to under sections 2 and 3.

H290

May be corrosive to metals.

H302

Harmful if swallowed.

H314

Causes severe skin burns and eye damage.

H315 Causes skin irritation.  
H319 Causes serious eye irritation.

**Further information**

Copyright 2015 Sigma-Aldrich Co. LLC. License granted to make unlimited paper copies for internal use only.

The above information is believed to be correct but does not purport to be all inclusive and shall be used only as a guide. The information in this document is based on the present state of our knowledge and is applicable to the product with regard to appropriate safety precautions. It does not represent any guarantee of the properties of the product. Sigma-Aldrich Corporation and its Affiliates shall not be held liable for any damage resulting from handling or from contact with the above product. See [www.sigma-aldrich.com](http://www.sigma-aldrich.com) and/or the reverse side of invoice or packing slip for additional terms and conditions of sale.